



universität  
wien

# MASTERARBEIT

Titel der Masterarbeit

Epigenetic regulation of microRNAs as biomarkers in malignant pleural mesothelioma

verfasst von

Mustafa Aslan, BSc

angestrebter akademischer Grad

Master of Science (MSc)

Wien, 2014

Studienkennzahl lt. Studienblatt:

A 066 877

Studienrichtung lt. Studienblatt:

Masterstudium Genetik und Entwicklungsbiologie

Betreut von:

ao. Univ.-Prof. Dr. Franz-Michael Jantsch

## Index

0.	Abstract.....	Page 03
1.	Introduction to Malignant Pleural Mesothelioma (MPM).....	Page 04
1.1.	Definition and epidemiology.....	Page 04
1.2.	Causes and carcinogenesis.....	Page 05
1.3.	Genetic alterations in MPM and genetic susceptibility.....	Page 09
1.4.	Diagnosis and treatment.....	Page 10
2.	Introduction to MicroRNAs.....	Page 13
2.1	Function and features of MicroRNAs and their role in cancer.....	Page 13
2.2	MicroRNAs in MPM and their diagnostic value.....	Page 15
2.3	Regulation of MiR-145 and its' cellular activities.....	Page 18
3	Aims of the thesis and hypothesis.....	Page 20
4	Materials and Methods.....	Page 22
4.1	Origin of the Samples.....	Page 22
4.2	DNA extraction.....	Page 24
4.3	DNA concentration measurement.....	Page 25
4.4	Bisulfite conversion of DNA.....	Page 26
4.5	Methylation Specific Polymerase Chain Reaction (MSP).....	Page 29
4.6	PCR of bisulfite treated DNA for Pyrosequencing.....	Page 31
4.7	Pyrosequencing.....	Page 34
5	Results.....	Page 41
5.1	Results of Methylation Specific PCR of DNA samples.....	Page 41
5.2	Results of Pyrosequencing from DNA samples.....	Page 70
5.3	Real time quantitative PCR (RT-qPCR) data.....	Page 111
6	Discussion.....	Page 112
7	Acknowledgments.....	Page 116
8	References.....	Page 117
9	Attachments.....	Page 122
9.1	Abstract in German.....	Page 122
9.2	Scientific CV in English.....	Page 124

## 0. Abstract

**Purpose:** Determination of epigenetic down-regulation mechanism of microRNA-145 in malignant pleural mesothelioma (MPM) and potential use of miR-145 as a diagnostic biomarker in MPM.

**Experimental Design:** Correlating the methylation-status and expression-pattern of the miR-145 and by investigating mechanisms of co-regulation with its' possible host-genes. Analysis of DNA methylation as possible epigenetic mechanism involved in down-regulation of miR-145, in MPM is performed by using methylation-specific PCR (MSP) on formalin-fixed paraffin-embedded (FFPE) surgical samples after bisulfite treatment. The methylation of miRs is further quantified by pyrosequencing and the methylation status correlated with miR expression levels detected by quantitative RT-PCR (qRT-PCR).

**Results:** Methylation specific PCR results as can be seen in table 12 gave the following results: In total there were 11 samples that were full methylated, 22 samples that were hemi-methylated and 1 sample that is unmethylated. On average tumour tissue samples from MPM patients (n=25) had 72,6% methylation for pri-miR-145 promoter region and NNP tissue samples from MPM patients had 74,6% (n=10) methylation. These results indicate that both non-neoplastic pleural tissue and tumour tissue has the same amount of methylation on their pri-miR-145 promoter region. Moreover there was no significant difference detected between MPM patients with epithelioid malignant mesothelioma (EMM) diagnosis and MPM patients with biphasic malignant mesothelioma (BMM) diagnosis between both tumour tissues – NNP tissues and EMM – BMM diagnosis.

QPCR data that I have received from the lab also shows downregulation of miR-145 in tumour tissue samples vs NNP tissue samples of MPM patients. On average miR-145 expression rate of tumour tissue samples from MPM patients (n=13) is 2,7 compared to NNP tissue samples from MPM patients (n=7) is 4,5 and control tissue sample from the patient with pneumothorax has 5,13. This indicates that a higher amount of downregulation takes place in EMM patients compared to BMM patients. Taken together even though there is a downregulation miR-145 in tumour tissue samples of MPM patients compared to NNP tissue samples from MPM patients, the mechanism of downregulation is not methylation as previously suspected.

# 1. Introduction to Malignant Pleural Mesothelioma (MPM)

## 1.1. Definition and epidemiology

The lungs are lined by a thin serous membrane, the pleura, which also covers the inner surface of the chest wall. The pleural tissue lining the lungs is called visceral pleura and the layer covering the chest wall names parietal pleura. In normal conditions a virtual pleural cavity containing a very thin layer of lubricating liquid separates the visceral from parietal pleura. The entire pleural tissue consists of a single layer of a specialized epithelium, called mesothelium resting on a basal membrane with underlying connective tissue. The latter is associated with many structures like lymphatic and blood vessels, immune cells and fibroblast-like cells. (Figure 1)

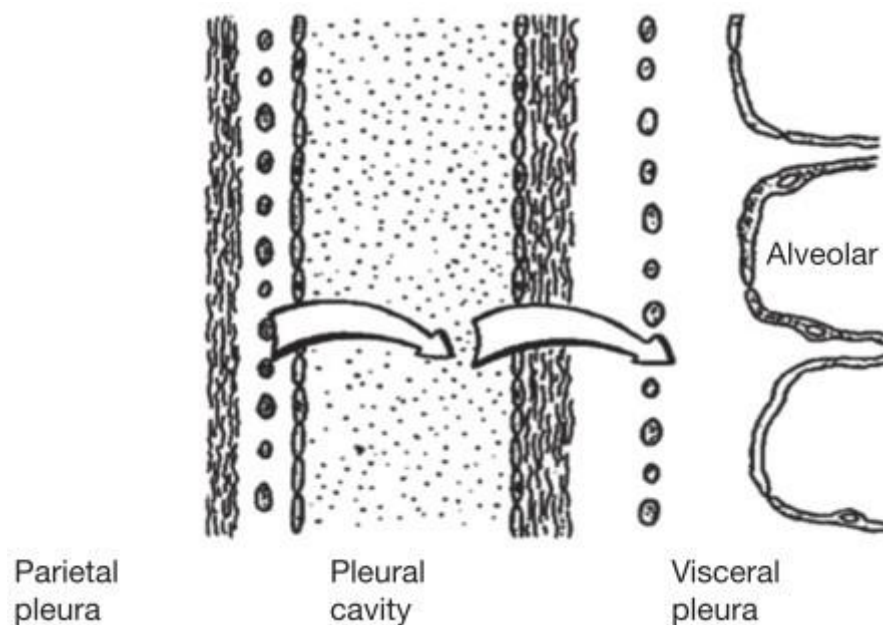


Figure 1: A diagram showing the structure of the pleura. Modified from the original source<sup>1</sup>

The most frequent malignancies of the pleura are metastases from cancers in other organs. Metastases to the pleura can cause pleural effusions with significant accumulation into the pleural cavity. There are approximately 200 000 pleural metastases in the USA each year.<sup>2</sup> Metastases can also cause pleural thickening and pleural based masses. Common metastases to the pleura include lymphoma, lung cancer and breast cancer; however, malignancies from any primary may metastasize to the pleura.<sup>2</sup>

Malignant Pleural Mesothelioma (MPM) is a relatively rare, mesothelium-derived, extremely lethal cancer that affects the pleura. MPM is associated with poor prognosis and median survival approximately 12 months.<sup>2-5</sup> Occupational and non-occupational exposure to asbestos, a set of naturally occurring silicate minerals, is the main risk factor for MPM. MPM incidence rate is still rising, even though its use was banned in a large part of the civilized world during the period from the 80's to 90's.<sup>6</sup>

Incidence rate vary across countries. Australia has the highest national incidence rate with 32 cases per million inhabitants, whereas in United States of America approximately 2000 – 2500 new cases are diagnosed every year that shows an incidence range of 12 per million inhabitants.<sup>7-9</sup>

In Italy the asbestos use was banned in 1992. The incidence range is at 24 cases per million inhabitants.<sup>9</sup> Approximately 100-120 new cases of MPM are diagnosed each year in Denmark (i.e., approx. 20-25 cases per million), most of them from the area of Aalborg, where the inhabitants for industrial reasons have had heavy exposure for decades in the 50's to 80's.<sup>10</sup> At the moment MPM causes approximately 3000 deaths per year in the USA and 5000 deaths per year in the Western Europe.

## **1.2. Causes and carcinogenesis**

Asbestos exposure is the main cause of MPM. Asbestos indicates a group of minerals, with a microcrystalline structure and a fibrous appearance; in fact they are chemical compounds containing magnesium, silicates, calcium and iron.<sup>11</sup>

First relation between MPM and asbestos was described in British Journal of Cancer by J. Christopher Wagner in 1960 even though the harmful effects of asbestos was already known in 1930's.<sup>12,13</sup> He found out that miners who were exposed to crocidolite had developed a tumour in their pleura called mesothelioma.<sup>13</sup> Asbestos fibers include the amphibole crocidolite, which is the most carcinogenic asbestos type, since these fibers being straight, thin, and

long can penetrate deep in the lung parenchyma and are not effectively eliminated by macrophages ("frustrated phagocytosis"). Thus, crocidolite can easily reach the pleura, either directly or transported by macrophages or lymphatic vessels. In contrast the other type of asbestos fibers, chrysotile is considered less dangerous, because they are convoluted, short and thick and therefore not so penetrating through the airways and more easily phagocytized once inhaled. Selikoff et al. inoculated asbestos to animals to show the carcinogenicity of it. Indeed, the animals treated with asbestos developed MPM conforming the causative link between asbestos exposure and cancer development.<sup>14</sup>

MPM can have a long latency period which refers to the length of time it takes from being exposed to asbestos until the time when the disease becomes apparent in a clinical examination, for this reason the latency can be longer than 20 years, not uncommonly up to 40 years or longer.<sup>3,11,15</sup>

In 2001 Suzuki Y. et al. published a large statistics about the occurrence of malignant mesothelioma from 1,517 human mesothelioma cases and find out that 85.8% were between 50 and 79 years in age and 92.3% of these patients were males. Males are much higher risks of MPM due to occupational exposure.<sup>3,16</sup>

Asbestos was used between 1930 and 1960 in a massive scale for commercial purposes, especially during the Second World War in American shipyards for building different parts of ships due to its ability to withstand high temperatures and corrosion. The American fleet grew from 394 ships in 1939 to 6,768 in 1945. More than 4 million men and women joined the workforce to build and repair that vast fleet.<sup>6,17,18</sup> For every thousand workers about fourteen died of mesothelioma and an unknown number died from asbestosis, a type of asbestos-induced lung fibrosis. In comparison combat date rate was 18 per thousand soldiers.<sup>18</sup>

Currently asbestos is banned or intensely restricted in many countries of Western Europe, the bans took place between 1985 and 1995.<sup>6</sup> However many countries in Eastern Europe, Latin America and Asia import and consume Asbestos even today.<sup>6,11,19</sup>

The mechanisms of asbestos carcinogenicity are not fully understood. <sup>16</sup> Published work demonstrates that tumour necrosis factor alpha (TNF- $\alpha$ ) and nuclear factor kappa-light-chain-enhancer of activated B cells pathway (NF- $\kappa$ B pathway) play a crucial role for the survival of mesothelial cells by activating pro-survival genes that protect these cells from cell death due to asbestos exposure. (Figure 2)

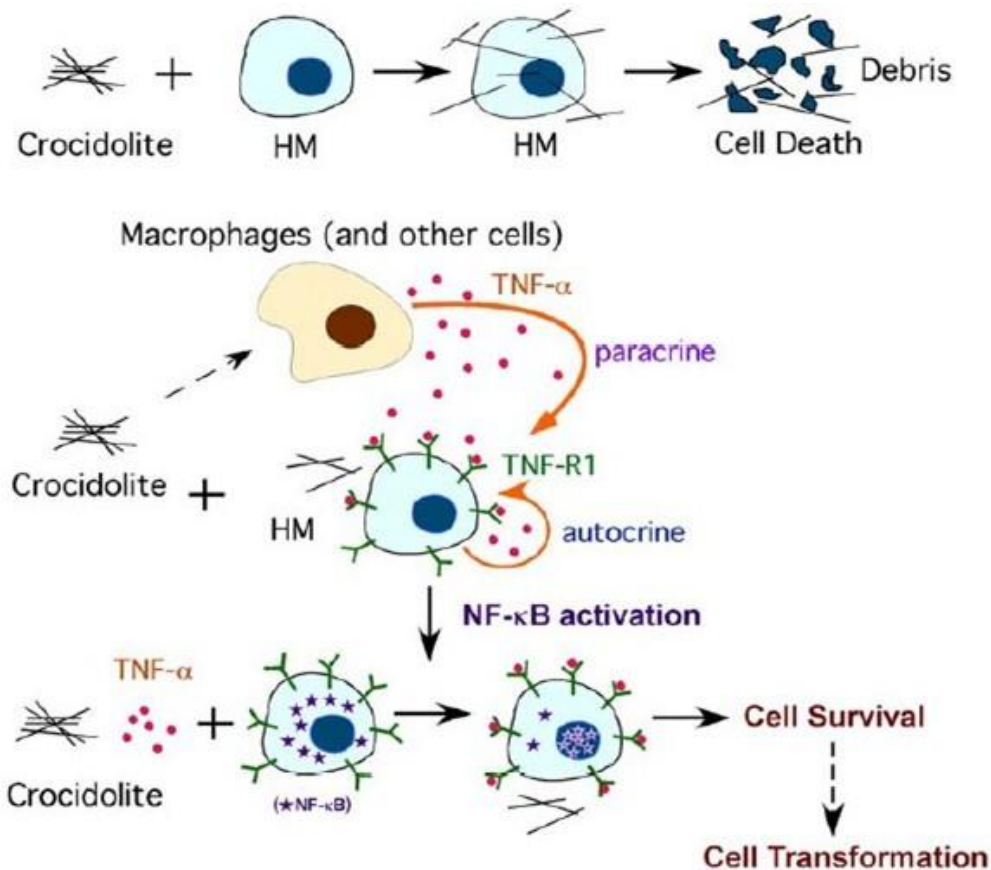


Figure 2: One of the proposed mechanism of asbestos carcinogenicity: Asbestos induces secretion of TNF- $\alpha$  by macrophages and mesothelial cells resulting in activation of NF- $\kappa$ B-dependent anti-apoptotic pathway. This allows mesothelial cells with asbestos-induced DNA alterations to survive increasing the risk of developing MPM. Crocidolite is a type of Asbestos. HM: Human mesothelioma cells. Modified from original source.<sup>16</sup>

Alternative mechanisms of asbestos-induced carcinogenicity are: A) the production of genotoxic reactive oxygen and nitrogen species in macrophages and mesothelial cells catalysed by the iron contained in the asbestos fibers; B) The direct and prolonged physical interaction

between asbestos fibers and the epidermal growth factor receptor (EGFR) on the surface of mesothelial cells, which induces continuous auto-phosphorylation and activation of EGFR and its downstream signalling cascades (MAPK and PI3K/Akt pathways)<sup>20</sup>

It was postulated that Simian virus 40, a DNA monkey virus known to produce the small t antigen (tag) and the large T antigen (TAG) that inhibit the tumour suppressor genes p53 and Rb, is also associated with MPM. However the results are conflicting since some of the publications showed a positive and some of them showed a negative association. For instance, initial analysis of human MPMs revealed that SV40 DNA-sequences were present in tumour cells of approximately 60% of investigated MPM samples and not present in the adjacent tissue. Animal experiments also demonstrated that %100 of hamsters injected intrapleurally with SV40 and %60 of those injected intracardially developed malignant mesothelioma (MM) within 6 months.<sup>16</sup>

It was also shown that SV40 Virus and asbestos can be co-carcinogens. The most likely transmission from monkey to human was through the SV40 contaminated polio vaccines that were produced between 1955 and 1978.<sup>16,21</sup> Asbestos and a modified version of SV40 (that does not express the necessary small t antigen (tag) to cause MM in animals) cause in combination in %90 of all hamsters MM, whereas modified SV40 Virus alone did not cause MM in any hamsters and asbestos alone only caused MM in %20 of the hamsters.<sup>16,22</sup> However, other studies did not confirm, the presence of SV40 sequences in MPM and ascribed previous results to SV40-contamination of plasmids used for PCR-reactions or cross-reactivity with other viruses.<sup>23</sup> Additional studies reported that SV40 DNA was present in only 6% of the previously identified positive cases.<sup>24</sup> Furthermore, SV40 associated microRNAs were not identified in MPM.<sup>25</sup> Thus, the involvement of SV40, if any, in the development of MPM remains widely debated.

Erionite is also another type of mineral fibers that can induce MPM. Animal experiments showed that it is even more potent than Asbestos in inducing MPM. For instance, MPM was observed in 19 rats out of 40 that were injected with asbestos, whereas 40 rats out of 40 developed MPM when injected with erionite.<sup>16</sup> In three small towns in Cappadocia, Turkey, the presence of erionite in the soil, rocks, and houses combined with genetic susceptibility of

the population to MPM, has caused more than 50% of all deaths due to MPM in this geographic area.<sup>26</sup>

### **1.3. Genetic Alterations in MPM and genetic susceptibility**

Cytogenetic and loss of heterozygosity analyses of MPMs have detected frequent deletions of specific regions within chromosome arms 1p, 3p, 4p, 4q, 6q, 9p, 13q, 14q, 15q, and 22q.<sup>16,26</sup> Recent research from 2015 with whole-exome sequencing revealed that frequent genetic alterations in BRCA1 associated protein-1 (*BAP1*), Neurofibromin 2 (*NF2*), cyclin-dependent kinase Inhibitor 2A (*CDKN2A*) and Cullin 1 (*CUL1*) in MPM.<sup>27</sup>

The tumour-suppressor *BAP1*, one of several classes of deubiquitinating enzymes, may be involved in regulation of chromatin dynamics, histone structure, transcription, cell cycle and growth, and response to DNA damage. Frequent somatic mutations in *BAP1* gene have been reported in many types of cancer including mesothelioma. Reportedly, about 23% of sporadic MPMs carry somatic *BAP1* mutations and germline *BAP1* mutations have been implicated in familial predisposition to the development of MPM and other cancers including uveal melanoma, breast cancer, and skin cancer.<sup>28-30</sup> In their recent study, Guo et al. analysed somatic mutations in 22 sporadic MPMs compared with matched normal samples using whole-exome sequencing and showed that 9 tumours harboured somatic mutations or somatic copy number alterations (SCNAs) in *BAP1*, suggesting that the frequency of somatic *BAP1* mutations is even higher than expected.<sup>27</sup>

Guo et al. found genetic alterations in the tumour suppressor gene *NF2*,<sup>27</sup> which encodes Merlin, a component of the Hippo signalling pathway that inhibits cell proliferation and apoptosis in correlation to previous studies.<sup>31,32</sup> A previous study reported the occurrence of inactivating homozygous deletions or mutations of *LATS2*, another member of the Hippo pathway, among 45 MPM tumour tissues or cancer cell lines,<sup>33</sup> although no mutations in *LATS2* was found in by Guo et al. These studies suggest that the Hippo signalling pathway may be implicated in MPM tumorigenesis. However, no somatic mutations in genes of the Hippo pathway other than *NF2* and *LATS1* were found in their study.<sup>27</sup>

Guo et al. also found mutations in *CUL1* as previously reported. *CUL1* gene encodes a core component of SCF E3 ubiquitin–protein ligase complexes that mediate the ubiquitination of proteins involved in cell-cycle progression, signal transduction, and transcription.<sup>27</sup>

The deletion of 9p21 containing the tumour suppressor gene *CDKN2A* was the most common event occurring in 10 of 22 MPMs.<sup>27</sup> Moreover, seven of *CDKN2A*-deleted tumours also harboured genetic alterations in *NF2*. No somatic substitutions and coding insertions-deletions (indels) were found in *CDKN2A* in their cohort. *CDKN2A/ARF* encodes the tumour suppressors p16 (INK4a), a cyclin-dependent kinase inhibitor suppressing cyclin D-CDK4/6 activities, and p14 (ARF), a component of the p53 cell cycle checkpoint. Therefore, homozygous deletions of the *CDKN2A/ARF* locus in MM might simultaneously impair both the retinoblastoma (Rb) and p53 pathways.<sup>16,34</sup>

As mentioned above, genetic susceptibility to MPM was observed as an epidemic, with the result of half of the population dying from MPM. in three small villages in Turkey in Cappadocia. Although there was no difference in the amount of erionite that was present in houses, MPM occurred in only certain families. Studies in this villages showed that MPM seemed to be inherited in an autosomal dominant pattern. When high risk MPM family members married into families with no history of the disease, MPM developed in the descendants. Genetically predisposed family members born and raised outside the MPM villages did not seem to develop MPM, which indicated that in combination of genetics and erionite exposure was the cause of deaths.<sup>16,26</sup>

## 1.4 Diagnosis and treatment

MPM is usually diagnosed late, since many of its symptoms are unspecific and common to other types of respiratory diseases. Symptoms appear at advanced stage and MPM is particularly difficult to diagnose for clinicians and pathologists, which very often results in delayed diagnosis and poor response to chemo-radiotherapy not least because only 20% of patients are operable at the time of diagnosis. The mean survival for patients with MPM is 12 months after diagnosis, though radically operated patients can almost double their survival, according

to the statistics of international specialized MPM centres, such as Rigshospitalet in Copenhagen.

Breathlessness and chest pain are common symptoms that are present in MPM. The reason for these is the accumulation of fluid in the pleural cavity located between the visceral pleura lining the lung and the parietal pleura lining the chest cavity, known as pleural effusion that constricts the underlying lung parenchyma.<sup>5,10</sup> (Figure 3)

For the diagnostic of MPM the most widely used methods are chest radiography, computed tomography, magnetic resonance imaging or positron emission tomography scan and histological examinations of pleural biopsies. During these procedures occurrence of pleural thickening and the possible presence of an effusion is investigated. The accumulated fluid can be removed and analysed for abnormal mesothelial cells but it is not a conclusive analysis, since reactive mesothelial proliferation due to severe inflammation can be the reason for presence of these cells too.<sup>11</sup> Moreover, it is quite difficult to distinguish cytologically these reactive noncancerous mesothelial cells from their malignant counterparts. The ultimate diagnosis of MPM, therefore, requires a biopsy in which unequivocal deep invasion of tumour cells into the pleura or subpleural fat tissue can be detected.

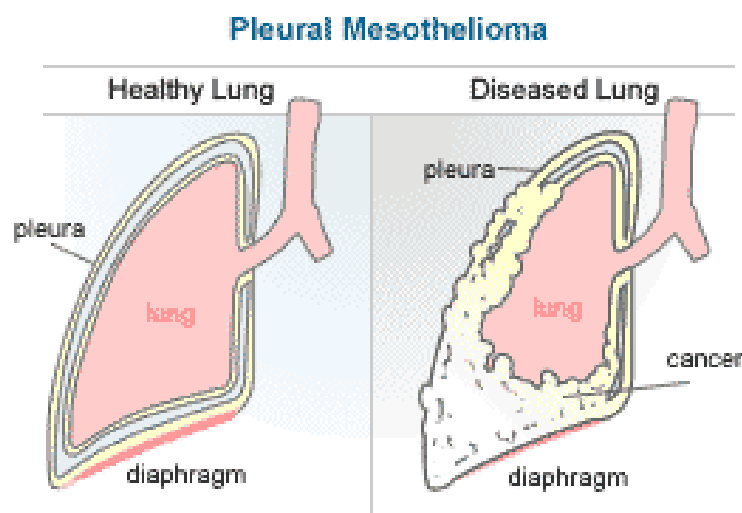


*Figure 3: Normal conditions of Pleura (left) and in MPM (right), where pleural space can be filled with fluid and/or tumour tissue.<sup>11</sup>*

There are 3 subtypes of MPM, epithelioid (similar to mesothelium, thus with the character of an epithelial cancer), sarcomatoid (similar to a sarcoma), and biphasic (mixed epithelioid and sarcomatoid), representing approx. 60%, 30%, and 10% of MPM cases, respectively which are known to have better, worse and intermediate prognosis.<sup>35</sup>

The main histopathological diagnostic criterion for MPM is deep invasion into the pleura and underlying thoracic fat tissue, but this is often difficult to demonstrate in small pleural biopsy samples. Thus, MPM may be challenging to distinguish from non-malignant pleural changes, such as reactive mesothelial hyperplasia (resembles epithelioid MPM) or organizing pleuritis with fibrosis (resembles sarcomatoid MPM). Currently, there are no generally accepted immunohistochemical tissue biomarkers for distinguishing MPM from these noncancerous reactive conditions and the diagnostic immunomarkers that have been proposed by the research group that I joined in Rigshospitalet and others need to be further validated.<sup>36</sup> Thus, new reliable biomarkers for this difficult differential diagnosis are urgently required.

Metastatic pulmonary adenocarcinomas, the most common type of lung cancer is a frequent differential diagnosis with MPM. Since no antibody shows absolute specificity or sensitivity to either tumour type immunohistochemistry, a combination of different antibodies are used to give best diagnosis.<sup>37-39</sup>

A trimodal therapy, which consists of preoperative chemotherapy, cytoreductive surgery and postoperative radiotherapy has been attempted in recent years as treatment of choice when feasible. However only 25% of patients are eligible by the time of diagnosis due to advanced stage of MPM.<sup>10,40</sup> Surgical procedures utilized against MPM are pleurectomy/decortication (P/D) and extrapleural pneumonectomy (EPP). EPP implies a complete en bloc removal of the involved parietal and visceral pleura including the whole ipsilateral lung. If required, the diaphragm and pericardium can also be resected. P/D refers to removal of all gross tumour, without resection of the diaphragm or the pericardium. The mortality rates differ between both procedures (7%) for EPP compared with P/D (4%) and higher survival rates of 16 months were observed for P/D versus 12 months for EPP.<sup>41</sup>

For patients who are not eligible for this therapy model, chemotherapy with a combination of pemetrexed and cisplatin therapy is used, though with limited efficacy.<sup>42</sup>

Currently 192 (Phase 1-3) registered clinical trials are ongoing to develop new therapy methods for MPM. These therapies focus on the following broad mechanisms of Tyrosine kinase inhibitors, antibody-conjugated toxins, immune checkpoint inhibitors, cytokine gene therapy and dendritic cell vaccines. Most promising of these methods are cytokine gene therapy with a survival rate of up to 22 months and dendritic cell vaccines with a survival rate of up to 15 months are observed. Though it is yet too early to make conclusions since these trials are still ongoing and there is no published evidence of randomized Phase 3 trials.<sup>43</sup>

## **2. Introduction to MicroRNAs**

### **2.1. Function and Features of MicroRNAs and their role in cancer**

MicroRNAs (miRNAs) are small noncoding RNAs that are 22 - 25 nucleotides in length have many important functions as regulators of fundamental cellular processes such as cell cycle, differentiation, development and metabolism along with different roles in cancer and other human diseases<sup>44</sup> Maturation of miRNAs occurs through different steps: First of all the long primary miRNAs transcripts (pri-miRNA) are transcribed from DNA by RNA Polymerase II (Pol II) or RNA Polymerase III (Pol III). Drosha, a nuclear RNase, processes the long pri-miRNAs to create pre-miRNAs that have a stemloop hairpin secondary structure. Afterwards pre-miRNA are exported from the nucleus into the cytoplasm, where Dicer, a cytoplasmatic RNase III, turns them into mature miRNAs by trimming them.<sup>45</sup>

Mature miRNAs bind to the 3' untranslated regions (3' UTRs) of their target genes, after they become a part of the RNA-induced silencing complex (RISC). Mature miRNAs can degrade their target mRNA by a perfect match or they block the translation of the target mRNA by a binding that is only partially complementary. Thanks to this imperfect pairing, miRNAs can regulate multiple genes.<sup>45</sup>

Since miRNAs are involved in many pathways and functions their aberrant expression is common in a wide spectrum of cancer types including MPM. <sup>46,47</sup> Studies with mouse models where microRNAs were under- or overexpressed also showed the link between cancer and miRNAs. <sup>46</sup>

The loss of function of miRNAs can contribute to the malignant transformation of a cell since some of the miRNAs have tumour suppressor functions such as miR-15a and miR-16-1 in 13q14.2 region. In a subset of chronic lymphocytic leukaemia (CLL), the miR-15a/16-1 cluster is observed to be deleted or downregulated and their target, the antiapoptotic gene BCL2 is widely overexpressed. It has been shown by Cimmino et al. that miR-15a/miR-16-1 expression levels are inversely correlated to BCL-2 expression in CLL patients and miR15a/miR-16-1 induce apoptosis by targeting BCL-2. <sup>48</sup>

MiRNAs can also act as oncogenes (“oncomiRs”), such as for instance miR-21 which has been showed to be upregulated in a wide variety of haematological malignancies and solid tumours, including acute myeloid leukaemia (AML), CLL, lung- breast- and liver cancers. It has been also showed that when overexpressed mir-21 block cell apoptosis, whereas silencing its gene promotes cell apoptosis in cultured cells. <sup>44</sup>

Epigenetic alterations, mutations, genomic deletions and miRNA processing alterations are among mechanisms that causes loss of function of miRNAs. <sup>44,47</sup> (Figure 4)

MiRNAs are interesting biomarkers in tissue samples processed for routine pathology, since by being short nucleotide-sequences they remain stable and can be quantified in formalin-fixed paraffin-embedded (FFPE) material by polymerase-chain-reaction (PCR) and in situ hybridization (ISH) techniques. <sup>49</sup>

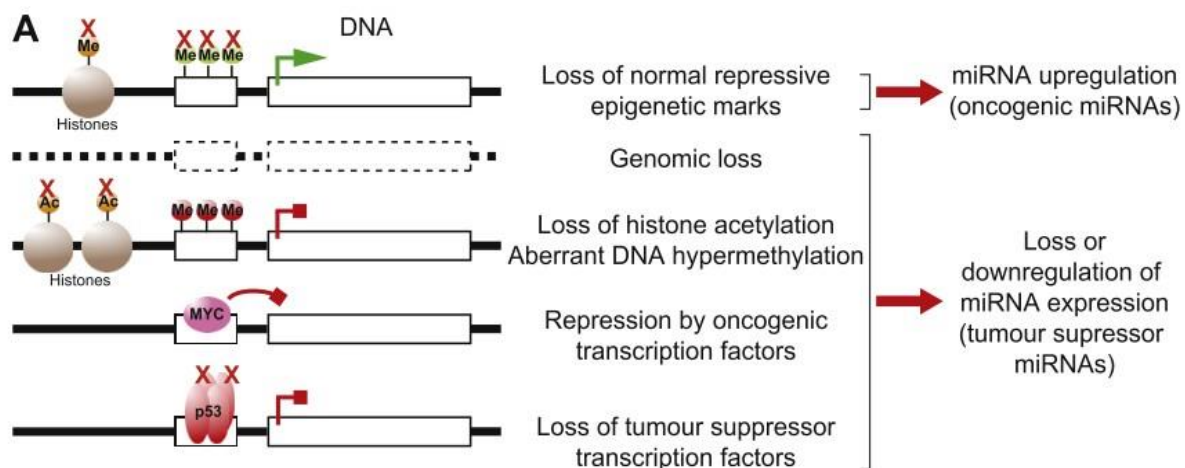


Figure 4: Mechanisms that cause deregulation of miRNAs. Me, methylation; Ac, acetylation. Modified from original source.<sup>46</sup>

## 2.2. MicroRNAs in MPM and their diagnostic value

Different studies have provided us with insights about the expression levels of miRNAs in MPM. In some of these studies, miRNA expression levels in compared in MPM cell lines and normal mesothelial cells, others assessed whether miR expression levels could differentiate MPM from lung adenocarcinoma. Only few studies compared the miRNA profiling of MPM and non-neoplastic pleura in vivo. A short summary of the most relevant data published in the literature on these issues follows.

Guled et al. were the first group to show deregulated miRNA-expression in MPM and they demonstrated that 12 miRs were highly expressed in a small cohort of 16 MPMs as compared to normal tissue samples, whereas 9 other miRs were downregulated or not expressed. Moreover they identified the exclusive expression of certain miRNAs in the 3 different histological subtypes of MPM.<sup>50</sup>

Using a microarray-based miRNA profiling followed by validation with quantitative PCR (RT-qPCR), Busacca et al. showed that MPM cell lines consistently overexpressed miR-17-5p and miR-30c and underexpressed miR-221 and miR-222 as compared to immortalized human mesothelial cells.<sup>51</sup>

By comparing the expression of 470 human and 63 viral miRNAs in primary human normal mesothelial cell cultures and commercially available MPM cell lines, Balatti et al. showed that 23 miRs were differentially expressed. They confirmed the miR-17-5p upregulation observed by Busacca et al. in MPM cell lines and, in addition to this miR, also observed deregulation of other members of the miR-17-92 cluster, which are linked to the oncogenesis of MPM.<sup>52</sup>

Other studies performed *in vivo* focused instead on miR-signatures that could discriminate MPM from lung adenocarcinoma. Benjamin et al. compared miR expression levels of MPM to those in lung adenocarcinomas and found out that the miR-200 family and miR-192 were expressed highly in adenocarcinoma but very low in MPM. By combining the overexpression of miR-200 and miR-192 in lung adenocarcinomas and the overexpression of miR-193a-3p in MPM, they developed an assay that could distinguish MPM from lung adenocarcinoma with 100% sensitivity and 94% specificity.<sup>53</sup>

Gee et al. confirmed the potential value of miR-200 family members in the differential diagnosis between MPM and pulmonary adenocarcinoma, finding that miR-141, miR200a, miR200b, miR200c, miR-203, miR205 and miR-429 are downregulated in MPM. They concluded that a combination of these microRNAs can be used to discriminate MPM from lung adenocarcinoma when pathological findings are inconclusive.<sup>54</sup>

However, apart from the miR-17-5p and miR-106a upregulation observed in MPM cell lines, the studies named above were difficult to compare, since they described deregulated expression of different miRNAs in MPM cells. This is probably caused by differences in experimental setups, reference specimens, number and types of samples investigated (cell lines vs. tissue samples) and goals of the studies. Some of the miRNA signatures obtained in these studies could distinguish the different histotypes of MPM or discriminate between MPM cell lines and normal mesothelial cultured cells or between MPM and pulmonary adenocarcinoma. Nevertheless, it remained unclear whether the identified deregulated miRNAs could be used as biomarkers for the difficult distinction between MPM and non-malignant reactive mesothelial proliferations (RMP) *in vivo*.

This issue was investigated by the group at Rigshospitalet in Copenhagen where I have performed the studies of my Master thesis. They assessed whether the deregulated miR-17-5p, -30c, -221, and -222 observed in cell lines may be suitable for this purpose. However, as opposed to the findings *in vitro*,<sup>51</sup> Andersen et al. found significant downregulation of miR-17-5p, upregulation of miR-221, and no differential expression of miR-30c and miR-222 in MPM as compared to patient-matched non-neoplastic pleura (NNP).<sup>55</sup> This indicates, that these 4 miRNAs are differently regulated in MPM cells *in vivo* and *in vitro*. Furthermore, regression analysis showed that despite having been reported as specific for MPM subtypes or differentially expressed in MPM cell-lines, miR-17-5p, miR-30c, and miR-221/222 were not suitable biomarkers for accurately discriminating MPM from non-neoplastic RMP.<sup>55</sup>

Therefore, to detect more specific miRNAs that could accomplish this task, the group at Rigshospitalet in Copenhagen recently screened by RT-qPCR the expression of 742 miRNAs in resected MPM tissue samples.<sup>10</sup> They then validated the 14 identified differentially expressed miRNAs with diagnostic potential in different cohorts of preoperative FFPE tumour-biopsies, surgically removed MPM specimens and corresponding patient-matched NNP samples as well as independent pleural specimens with pneumothorax-induced reactive mesothelial proliferation. The authors discovered that miR-126, -143, -145 and -652 were consistently downregulated in resected MPM resections and tumour-biopsies and could significantly differentiate MPM from NNP/RMP samples. Furthermore, when combined in a 4-miR-classifier with enhanced diagnostic performance these 4 miRs could correctly diagnose MPM with high sensitivity, specificity and overall accuracy (all three > 93%) and were associated with poor prognosis.<sup>10</sup>

Reduced levels of miR-126 in MPM were first reported by Santarelli et al in surgically removed tissue samples and also in the patients' serum.<sup>56</sup> The possibility of using low levels of circulating miR-126 for diagnosing MPM patients was also published by others.<sup>57</sup>

Other miRNAs that have been reported to be differentially expressed and potentially able to discriminate between MPM and RMP are miR-16<sup>58</sup> and miR-34a/b/c.<sup>59</sup> The 3 miR-34s are transcriptionally regulated by p53 and mediate some of its tumour-suppressive functions<sup>60</sup> and in MPM they appear to be epigenetically repressed by methylation of their promoter region.

Ak et al. discovered that miR-484, miR-230, let-7a and miR-125a-5p were significantly upregulated in MPM as compared to asbestos-related benign pleural effusion (BAPE). They concluded that a combination of these microRNAs can be used to discriminate MPM from BAPE, however the diagnostic value of these results should be validated in larger, more homogeneous, and patient-matched cohorts of MPM/NNP specimens.<sup>61</sup>

### 2.3. Regulation of Mir-145 and its' cellular activities

MiR-145 is in a bicistronic cluster with miR-143 in 5q33.1 (Figure 5) and they are co-expressed. Various studies have shown that they are tumour suppressors and they are downregulated or the cluster is deleted<sup>62-64</sup> in various cancer types.<sup>65</sup>

The sequence of miR-145 was predicted by Lagos-Quintana et al. based on the homology of verified miRNA from mouse.<sup>66</sup> Later on, the sequence was based on large scale cloning studies.<sup>67</sup> (Figure 6)

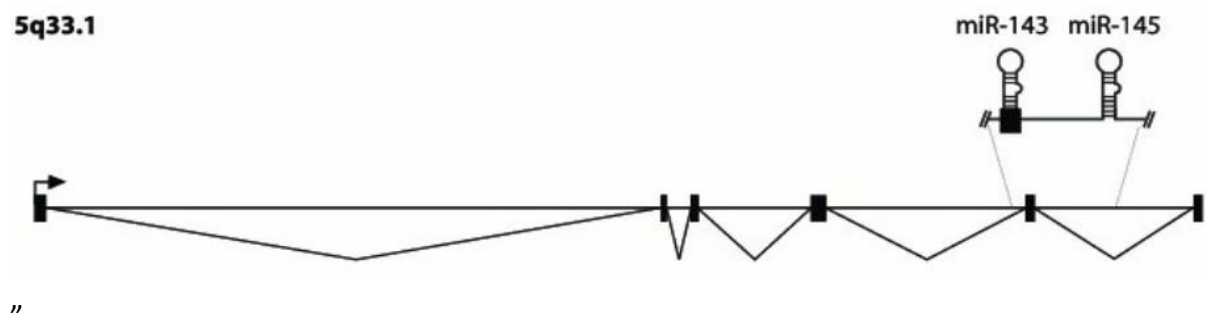


Figure 5: The genomic organisation of the miR – 143/ 145 cluster on the chromosome 5. Major primary transcript structure of miR-143/145 can be also seen. Modified from original source.<sup>65</sup>

The expression of the miR - 143/miR – 145 cluster is regulated by p53, whereas the oncogene the murine double minute 2 (MDM2) is directly targeted by miR-143/miR-145. Therefore, any deletions or deregulations of miR-143/miR-145 cluster impairs the cancer cells MDM2 – p53 feedback loop.<sup>68</sup>

In MPM the acquired resistance to chemotherapy is associated with the transcription factor OCT4, which regulates the epithelial-to-mesenchymal transition (EMT). MiR – 145 targets this transcription factors, therefore reducing the ability of MPM cells to resist to chemotherapy. The expression of OCT 4 and miR-145 was inversely correlated in MPM samples as assessed by Cioce et al,<sup>47</sup> suggesting that miR-145 acts as tumour suppressor partly by targeting OCT4. MiR-143 and miR-145 are considered tumour suppressors in part because they mediate p53 function, but also because they target oncogenes, such as v-myc avian myelocytomatosis viral oncogene homolog (MYC), Kirsten rat sarcoma viral oncogene homolog (KRAS) and Ras responsive element binding protein 1 (RREB1).<sup>69,70</sup>

In their recent study, Cioce et al. also observed significant differential expression of this miR in MPMs vs. benign mesothelium, consistent with similar findings by Andersen et al<sup>10,47</sup>. Moreover, they found miR-145 down-regulation in the MPM cell lines MSTO-211H, NCI-H2052 and NCI-H28 when compared to untransformed mesothelial cells, whereas forced expression of miR-145 agonists in MPM cell lines suppressed their proliferation and the ability to resist chemotherapy and lead to replicative senescence. Moreover, these miR-145-transfected MPM cell lines showed reduced ability to form tumours after transplantation into SCID-mice.<sup>47</sup>

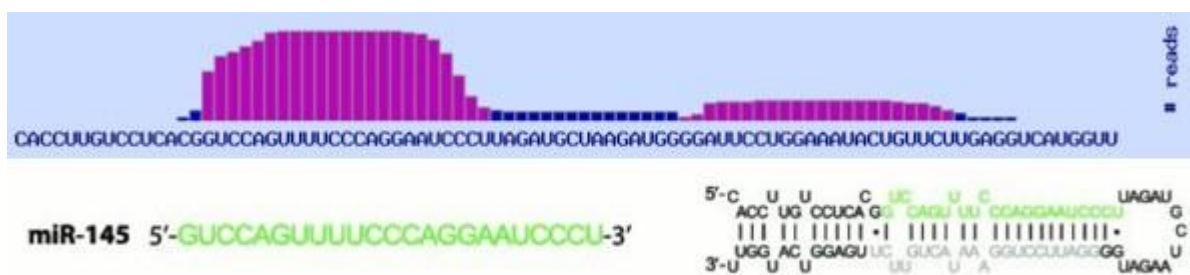


Figure 6: Sequence of miR-145 gene based on 48543 reads by 63 experiments with deep sequencing on the top side. On the bottom pre-miR-145 stem loop and mature miRNA sequences can be seen. Modified from original sources.<sup>65,71</sup>

### 3. Aims of the thesis and hypothesis

Having Rigshospitalet in Copenhagen been in the last 10 years the centre for surgical treatment of Scandinavian MPM patients, the samples archived at the Department of Pathology represent useful material for research projects aimed at improving diagnostics and therapy of this disease. Indeed, the research group that I have joined at the end of August 2014 has previously reported the predictive value of certain biomarkers for potential selection of MPM patients to chemotherapy.<sup>72,73</sup>

During the last 4 years, the research group has particularly focused on assessing whether miRs may provide new opportunities for making the differential diagnosis between MPM and the above-mentioned noncancerous reactive mesothelial proliferations (RMPs) more accurate.<sup>74</sup> As mentioned above, the group<sup>55</sup> and others recently reported miR signatures in tissue specimens or serum that seem to discriminate between MPM and pleural spreading from other cancer types or among different histological subtypes of MPM. In addition, the group recently published the results of an RT-PCR screening and validation of 742 miRs in different cohorts of formalin-fixed paraffin-embedded (FFPE) operation samples as well as preoperative diagnostic biopsies. This work has led to the identification of miR-126, miR-143, miR-145, and miR-652 as consistently down-regulated in MPM and helpful in the difficult differential diagnosis between MPM and RMPs<sup>10</sup>. Both alone and even more when combined by logistic regression analysis in a 4-miR-classifier with enhanced performance, these miRs were able to differentiate MPM with high sensitivity, specificity, and accuracy (area under the curve, AUC, for all > 0.93). Inverse correlation with their targets and correlation with poor overall survival of these miRs were also found<sup>10</sup>.

Aiming at confirming the diagnostic utility of miR-126, miR-143, miR-145, and miR-652 in MPM and better establishing their mechanistic impact on mesothelial oncogenesis as well as their potential therapeutic relevance, the group wishes now to explore the possible molecular mechanisms causing down-regulation of these miRs in MPM (including, epigenetic modifications, altered gene sequence and changes in abundance/function of the enzymes Drosha and Dicer involved in microRNA-genesis).

With respect to this, one of the main approaches is achieved by correlating the methylation-status and expression-pattern of the 4 miRs and by investigating mechanisms of co-regulation with their possible host-genes. In this regard, the group has recently obtained the first results showing that in MPM: a) the putative tumour suppressor miR-126 is located in the alternative S2-transcript of the pro-angiogenic epidermal growth factor-like domain multiple 7 (*EGFL7*) gene; b) miR-126 and its host gene *EGFL7* are concomitantly down-regulated by methylation of the S2 CpG island promoter in *EGFL7*; c) the methylation-induced co-silencing of *EGFL7* and miR-126 is associated with poor clinical outcome and published.<sup>75</sup>

This master thesis project aims to analyse the methylation-status of miR-145, one of these four miRs, quantify methylation of the miR-145 promoters, correlate methylation data with the expression of miR-145 and possible host gene's transcripts, correlate methylation data with clinic-pathological data, when possible. Our hypothesis is that miR-145 is regulated through promoter methylation like miR-126 in MPM as described above.

## 4. Materials and Methods

### 4.1. Origin of the samples

Sam. Nu.	Patient Matched pair?	Type	Sex	Age	Patient diagnosis	Notes/stage	Type of opera.
#03	Yes	N	M	63	EMM	pT3N0	EPP
#04	Yes	T	"	"	"	"	"
#05	No	T	M	58	BMM	pT3N0	EPP
#06	Yes	T	M	70	EMM	pT3N0	EPP
#07	Yes	N	"	"	"	"	"
#08	No	T	F	76	EMM	pT4N0	P/D
#09	No	T	M	55	BMM	pT3N0	EPP
#10	No	N	M	36	PNEU.	C	S.R.
#11	Yes	T	M	70	BMM	pT3N2	EPP
#12	Yes	N	"	"	"	"	"
#13	No	T	M	74	EMM	pT4N0	P/D
#14	No	T	F	71	EMM	pT2N0	P/D
#15	No	T	M	65	EMM	pT3N2	EPP
#16	No	T	M	81	EMM	pT3N0	P/D
#17	No	T	M	63	EMM	pT3N0	P/D
#18	Yes	T	M	76	BMM	pT4N0	P/D
#19	Yes	N	"	"	"	"	"
#20	No	T	M	52	BMM	pT4N0	P/D
#21	No	T	M	67	EMM	pT3N0	P/D
#22	Yes	T	M	70	EMM	pT1bN0	P/D
#23	Yes	N	"	"	"	"	"
#24	No	N	M	78	EMM	pT2N0	P/D
#25	Same sample as above	N	"	"	"	"	"
#26	Yes	T	F	70	BMM	pT3N0	P/D
#27	Yes	N	"	"	"	"	"
#28	Yes	T	M	75	EMM	pT3N2	P/D
#29	Yes	N	"	"	"	"	"
#30	No	T	F	57	EMM	pT3N1	P/D
#31	Yes	N	M	74	EMM	pT3N0	P/D
#32	Yes	T	"	"	"	"	"
#33	No	T	M	70	EMM	pT3N0	P/D
#34	No	T	M	64	BMM	pT4N2	P/D
#35	No	T	M	57	EMM	pT3N0	P/D
#36	No	T	M	"	"	"	"
#37	Yes	N	F	47	BMM	pT4N2	P/D
#38	Yes	T	"	"	"	"	"
#39	No	T	M	80	BMM	pT4N0	P/D
#40	No	T	F	64	BMM	p/2N0	P/D

**Table 1:** Table showing details of each sample from MPM patients. Please note sample 10 is not from an MPM patient and was used as a control (C). The tissue was taken from a patient with non neo-plastic mesothelial proliferation due to Pneumothorax. Following abbreviations

*apply: Sam. Nu. = Sample Number, Type of Opera. = Type of operation. There are 2 types of tissue: N= non-neoplastic pleura, T=tumour tissue and 2 types of gender: M=Male and F=Female. Age of the MPM patients vary between 47-81 years old. Patient diagnosis is provided according to MPM subtype either EMM= epithelioid or BMM=biphasic. The pTNM Stage provides following information: T: tumour extension in pleura and surrounding thoracic/mediastinal structures; N: lymph node metastases or not (which for the majority of the patients is NO, i.e. no lymph node metastases); M: metastases in distant organs, which for our cohort is irrelevant, since all the patients were without distant metastases in order to be operable. The letter "p" means established by pathological examination of the samples. Type of the operation: EPP= extrapleural pneumonectomy, P/D= pleurectomy/decortication as described in introduction. Non-neoplastic tissue samples are marked in green, control is marked in blue and tumour tissues are marked in red, patient-matched samples are marked in purple.*

Additional issues with Table 1: Sample #20 had a component of desmoplastic mesothelioma (DM) which is very collagenized and with just few cells, which could affect the methylation/expression results, while sample #24 contained mostly non-neoplastic fibrotic tissue. Sample #26 - #27 have mostly non-neoplastic fibrotic tissue with few cells, so that they are poorly representative for T and N, because of the too few and too many tumour cells present in them respectively ( Sample #26 should have had more tumour cells and sample #27 none for being representative). The problem with MPM sampling is that macroscopically tumour tissue and fibrotic tissue (w/ or w/o tumor cells) can often resemble each other. Due to these reasons, the results obtained from sample #26 and #27 should be taken with caution.

As described in Table 1 they were in total 37 samples from 26 different MPM patients. 20 of the patients were male and 6 of the patients were female.

9 MPM patients have matching tissue: non neoplastic pleura along with tumour tissue. These are sample: #03 - #04, #06 - #07, #11 - #12, #18 - #19, #22 - #23, #26 - #27, #28 - #29, #31 - #32, #37 - #38.

17 MPM patients have only tumour samples. These are: #5, #8, #9, #13, #14, #15, #16, #17, #20, #21, #30, #33, #34, #35, #36, #39, and #40. 1 MPM patient has only non-neoplastic pleura samples. These are sample #24 – #25.

## 4.2. DNA extraction

Paraffin-embedded tissue samples were cut into 4x10 µm thick slices on a microtome by technicians at the department. The tissue sections were put in 1.5 ml sterile Eppendorf tubes. As DNA purification kit the QIAamp DNA minikit from Qiagen was used to extract DNA out of the tissue sections. DNA purification takes 2 days including removal of paraffin, an overnight incubation with proteinase K and two different washing to purify the DNA from any contamination.

The whole protocol is as follows:

Day 1:

1. Switch on the heating block at 37°C.
2. Add 1000 (1200) µl xylene to the tissue and vortex (deparaffinization step).
3. Centrifuge at 20000x g (14000 rpm) for 5 min.
4. Gently remove supernatant by pipetting.
5. Add 1000 (1200) µl 96 - 100% ethanol to remove residual xylene and vortex.
6. Centrifuge at 20000x g (14000 rpm) for 5 min.
7. Carefully remove supernatant (ethanol) by pipetting.
8. Repeat steps 5 - 7.
9. Incubate in the heating block for 15 min. and check whether it is evaporated.
10. Resuspend the tissue pellet in 180 µl Buffer ATL.
11. Add 20 µl of proteinase K and vortex. (Proteinase K is for degradation of the cell membranes).
12. Incubate in the heating block and shake over night at 56°C. Day 2: can be done manually or using the QuiaCube system.

Day 2:

1. Briefly centrifuge to remove drops from the inside of the lid.
2. Add 200 µl AL Buffer and vortex for 15 sec. to get a homogeneous solution.
3. Incubate at 70°C for 10 min.

4. Briefly centrifuge.
5. Add 200  $\mu$ l 96---100% ethanol and vortex for 15 sec.
6. Briefly centrifuge.
7. Carefully apply the mixture from step 6 to the column without touching the rim.
8. Centrifuge at 6000x g (8000 rpm) for 2 min.
9. Discard the excess of liquid.
10. Add 500  $\mu$ l AW1 Buffer (washing buffer) without wetting the rim.
11. Centrifuge at 6000x g (8000 rpm) for 2 min.
12. Discard the excess of liquid.
13. Add 500  $\mu$ l AW2 Buffer without wetting the rim.
14. Centrifuge at 20000x g (14000 rpm) for 4 min.
15. Discard the excess of liquid.
16. Centrifuge at 20000x g (14000 rpm) for 2 min.
17. Place the column in a new collection tube.
18. Add 50  $\mu$ l AE Elution Buffer without touching the rim. This step increase the DNA yield with 15%.
19. Incubate for 5 min. at room temperature to increase the DNA yield.
20. Centrifuge at 6000x g (8000 rpm) for 2 min.
21. Repeat steps 18 to-20.
22. Place the DNA at -80°C for longterm storage.

### **4.3. DNA concentration measurement**

The concentration and the quality of nucleic acids was determined with the spectrophotometer UV-visible NanoDrop 2000. Samples are exposed to ultraviolet light at 260 nm, and a photo-detector measures the light that passes through them to determine the concentration of samples. Amount of light absorbed by the samples correlates with the concentration of the samples. High absorption indicates high concentration. Following protocol was used:

0. Load 2  $\mu$ l of DNase/RNase free to get a blank measurement.
1. Measure 2  $\mu$ l of the sample.

2. Wipe the instrument.
3. Repeat the step above for the new sample.

Following this protocol it is possible to obtain the absorbance from which the DNA concentration can be estimated. The purity is the ratio of A260/A280 absorbance, since 280 nm is the wavelength at which proteins absorb. This ratio should optimally lie between 1.8 and 2 for samples if it is free of contamination with proteins or other organic compounds. This method only measures the amount of nucleic acids, but doesn't give information about the quality.

#### **4.4. Bisulfite conversion of DNA**

Sodium bisulfite converts unmethylated cytosines in the DNA into uracils but it does not convert methylated cytosines. Because of this the treatment gives rise to different DNA sequences for methylated and unmethylated DNA. The conversion occurs in three steps: First sulphonation of cytosine creates cytosin-sulphonat. Afterwards cytosin-sulphonat will be hydrolytic deaminated to create uracil-sulphonat. Finally uracil-sulphonat will be converted to uracil through alkali-desulphonation (see Fig. 7). The nucleotide differences can be detected by pyrosequencing, restriction enzyme analysis, PCR and with other methods.

Complete conversion of unmethylated cytosines are achieved by incubating the DNA in high bisulfite salt concentrations, with high temperature and low pH. These harsh conditions mostly can cause a high degree of DNA fragmentation. Therefore, a part of the DNA will be lost during purification. Purification is done so that bisulfite salts and chemicals used in the conversion can be removed, to avoid inhibiting DNA polymerases used in the PCR and sequencing procedures. In this work, EZ DNA Methylation-Gold Kit by Zymo Research was used for bisulfite conversion.

DNA Protect Buffer protects the DNA against fragmentation during the bisulfite conversion reaction. This buffer contains a pH-indicator dye which allows to confirm if the pH is correct for cytosine conversion.

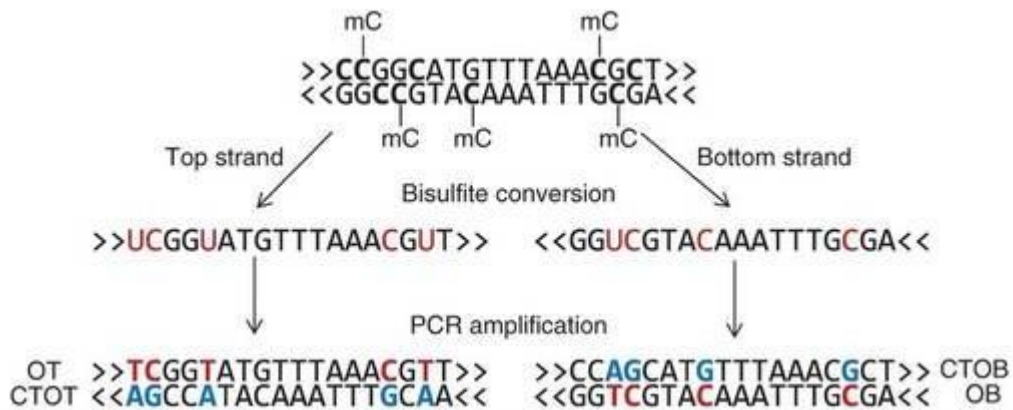


Figure 7: Schematic representative of Bisulfite conversion of a methylated DNA. Modified from the original source.<sup>76</sup>

Thermal cycling program for bisulfite conversion provides series of incubation steps so that thermal DNA denaturation, subsequent sulphonation and cytosine deamination can work with high efficiency. This enables cytosine conversion rates of over 99%. The last step of chemical conversion, desulphonation, is done with on-column step included in the purification procedure.

Following protocol was used for the bisulfite conversion according to the manufacturers protocol for the kit:<sup>77</sup>

DNA Input: Samples containing 500 pg. - 2 µg. of DNA. For optimal results, the amount of input DNA should be from 200 to 500 ng.

Normally same amount of DNA should be calculated to use in the experiments, however due to rather low concentration of the samples used in this work, negative value of concentrations were received partly during concentration measurement with UV spectrometer. Therefore, 25 µl of DNA from each sample was used for bisulfite conversion. However if the concentration was measured correctly, the amount of DNA used for conversation did not exceed 500 ng. Following protocol was used for preparation of CT conversion reagent:<sup>77</sup>

1. Add 900 µl water, 300 µl of M-Dilution Buffer, and 50 µl M-Dissolving Buffer to a tube of CT Conversion Reagent.

2. Mix at room temperature with frequent vortexing or shaking for 10 minutes.

Following protocol was used for preparation of M-Wash Buffer:<sup>77</sup>

1. Add 24 ml of 100% ethanol to the 6 ml M-Wash Buffer concentrate or 96 ml of 100% ethanol to the 24 ml M-Wash Buffer concentrate before use.

Following protocol was used for Bisulfite conversion:<sup>77</sup>

1. Add 130  $\mu$ l of the CT Conversion Reagent to 20  $\mu$ l of your DNA sample in a PCR tube. If the volume of the DNA sample is less than 20  $\mu$ l, make up the difference with water. Mix the sample by flicking the tube or pipetting the sample up and down, then centrifuge the liquid to the bottom of the tube.
2. Place the sample tube in a thermal cycler and perform the following steps:
  - 98°C for 10 min.
  - 64°C for 2.5 hrs.
  - 4°C storage up to 20 hrs.
3. Add 600  $\mu$ l of M-Binding Buffer to a Zymo-Spin™ IC Column and place the column into a provided collection tube.
4. Load the sample (from Step 2) into the Zymo-Spin™ IC Column containing the M-Binding Buffer. Close the cap and mix by inverting the column several times.
5. Centrifuge at full speed (>10,000 x g) for 30 secs. Discard the flow-through.
6. Add 100  $\mu$ l of M-Wash Buffer to the column. Centrifuge at full speed for 30 secs.
7. Add 200  $\mu$ l of M-Desulphonation Buffer to the column and let stand at room temperature (20-30°C) for 15-20 minutes. After the incubation, centrifuge at full speed for 30 secs.
8. Add 200  $\mu$ l of M-Wash Buffer to the column. Centrifuge at full speed for 30 sec. Add another 200  $\mu$ l of M-Wash Buffer and centrifuge for an additional 30 secs.
9. Place the column into a 1.5 ml microcentrifuge tube. Add 10  $\mu$ l of M-Elution Buffer directly to the column matrix. Centrifuge for 30 secs at full speed to elute the DNA.

The DNA is ready for immediate analysis or can be stored at or below -20°C for later use. For long term storage, store at or below -70°C. 1-4  $\mu$ l of eluted DNA for each PCR is recommended,

however, up to 10 µl can be used if necessary. The elution volume can be > 10 µl depending on the requirements of your experiments, but small elution volumes will yield more concentrated DNA.<sup>77</sup>

#### **4.5. Methylation specific Polymerase Chain Reaction (MSP)**

MSP is a PCR, which can discriminate between methylated and unmethylated DNA in bisulfite converted DNA. (Fig. 21). Two sets of primers can be used in two separate reactions: One primer set is complementary to methylated DNA (M-MSP reaction) while the other primer set is specific and complementary to unmethylated DNA (U-MSP reaction). MSP is a semi-quantitative method. This method cannot distinguish between samples with high and low levels of methylation for a positive M-MSP reaction, therefore it is only semiquantitative. MSP of the specific promoter region of pri-miR-145 after bisulfite conversion was performed using the primers published by Cioce et al.<sup>47</sup> Following Primers were used for the MSP:

- 1) 5' GGGTTTTCGGTATTTTTTAGGGTAATTGAAGTTTC 3' – Methylated forward primer (793- assigned number for ordering according to the hospital protocol)
- 2) 5' TAAAATACCACACGTCGCCG 3' – Methylated reverse primer ( 794- assigned number for ordering according to the hospital protocol)
- 3) 5' GGGTTTTGGTATTTTTTAGGGTAATTGAAGTTTT 3' – Unmethylated forward primer (791- assigned number for ordering according to the hospital protocol)
- 4) 5' AACCAAATAAAAATACCACACATCACCA 3' – Unmethylated reverse primer (792- assigned number for ordering according to the hospital protocol)

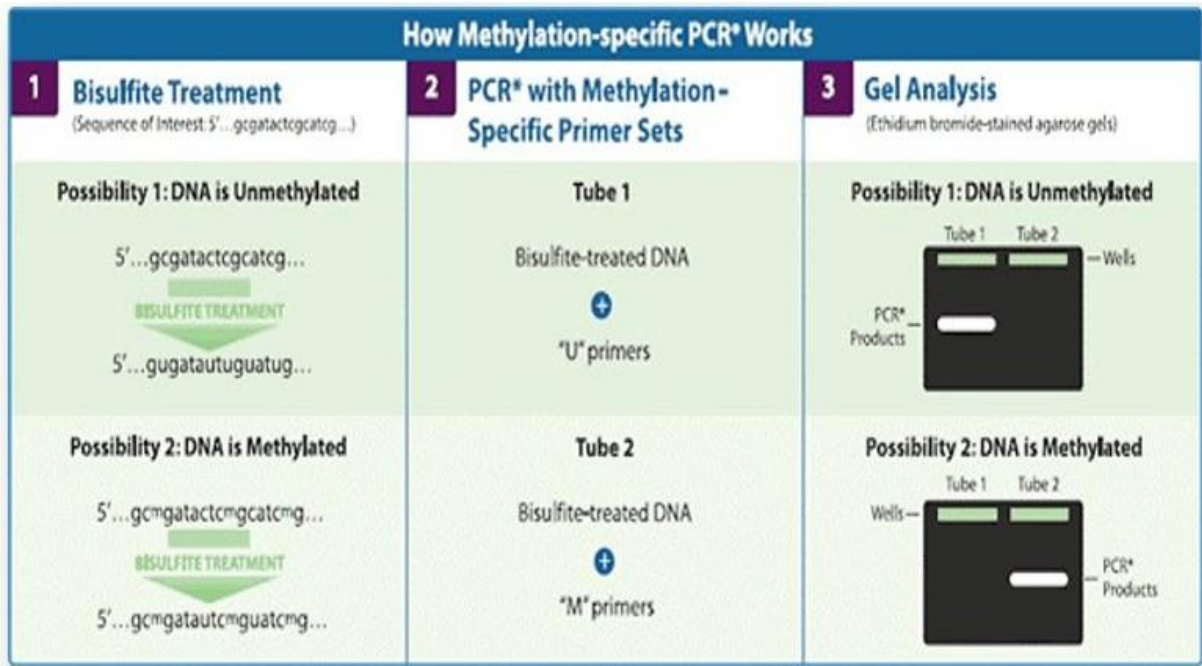


Figure 8: Schematic representative of bisulfite treatment, MSP and gel analysis of MSP products. Modified from original source.<sup>11</sup>

Following protocol was used for MSP for both M-MSP and U-MSP reactions:

- 1) Mix the components by vortexing and pipet into each PCR tube according to the Table 2.

Component	Volume per reaction (µl)
RedEx	5
Forward Primer	1
Reverse Primer	1
Template DNA	2
Distilled Water	1
Total volume	10

Table 2: Reaction composition of MSP – RedEx: REExtract-N-Amp from Sigma Aldrich.

- 2) Program the thermal cycler according to Table 3 depending on if it is a M-MSP reaction or U-MSP reaction.

Step	Time	Temperature
Initial activation step:	5 min.	95°C
3-step cycling:		
Denaturing:	30 sec.	94°C
Annealing:	30 sec.	56 ( U-MSP) or 64 (M- MSP)
Extension:	30 sec.	72°C
Number of cycles:	40	
Final extension	10 min.	72°C

*Table 3: Thermal cycler settings for M-MSP and U-MSP.*

These products were analysed using high-resolution capillary-electrophoresis from QIAxcel with the use of QIAxcel Screengel software version 1.4.0. As control Epitect PCR control DNA set was used. For M-MSP reactions positive control was bisulfite converted fully methylated human DNA and as negative control fully unmethylated human DNA was used. For U-MSP reaction it was vice versa. Both control DNA's gave a band at 100bp.

#### **4.6. PCR of Bisulfite Treated DNA for Pyrosequencing**

In order to analyse methylation of the CpG islands of pri-miR-145 promoter region, bisulfite-treated DNA samples were amplified by PCR with specific primers for island 1 and island 2 of specific promoter region of pri-miR-145. Following primers were used during the PCR:

- 1) 5' GGAGATTGGGGAATATATATGAGT 3' – Forward Primer for PCR region of island 1 (808- assigned number for ordering according to the hospital protocol)
- 2) 5' TTCTACATCCAACCCCATCTATAACA 3' – Reverse Primer for PCR region of island 1 (809- assigned number for ordering according to the hospital protocol)
- 3) 5' TGGGGTTGGATGTAGAAGAGAATT 3' – Forward Primer for PCR region of island 2 (811- assigned number for ordering according to the hospital protocol)
- 4) 5' TATTTCCAAAATCCCATCTTAACAT 3' – Reverse Primer for PCR region of island 2 (812- assigned number for ordering according to the hospital protocol)

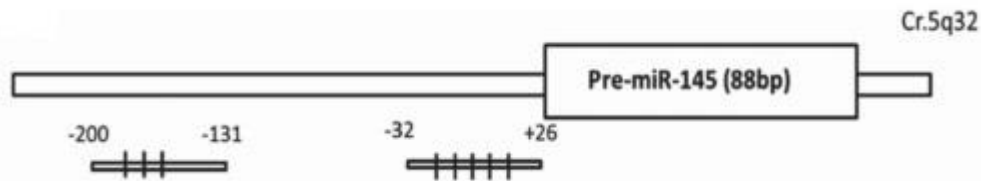


Figure 9: MiR-145 promotor regions containing CpG Islands. Island 1(left) and Island 2(right) are marked respectively. Modified from original source.<sup>47</sup>

At first PCR reaction was prepared using the following setup:

Component	Volume per reaction (µl)
RedEx	5
Forward Primer	1
Reverse Primer	1
Template DNA	2
Distilled Water	1
Total volume	10

Table 4: PCR Setup of PCR Region from island 1 & 2 of pri-miR-145

Step	Time	Temperature
Initial activation step:	5 min.	95°C
3-step cycling:		
Denaturing:	30 sec.	94°C
Annealing:	30 sec.	55°C
Extension:	1min 30 sec.	72°C
Number of cycles:	34	
Final extension	5 min.	72°C

Table 5: Thermo cycler setup of PCR region from island 1 & 2 of pri-miR-145

However, due to low efficiency of this setup different PCR setups were tested as seen in table 6 – 9 with the thermos cycler setup in table 5. After checking intensity of all the PCR products, PCR test setup no 2 was determined as the most efficient one as seen in Table 7.

Component	Volume per reaction (µl)
RedEx	12,5
Forward Primer	1
Reverse Primer	1
Template DNA	2
Distilled Water	8,5
Total volume	25

Table 6: PCR test setup no 1

Component	Volume per reaction ( $\mu$ l)
RedEx	12,5
Forward Primer	1
Reverse Primer	1
Template DNA	3
Distilled Water	7,5
Total volume	25

*Table 7: PCR test setup no 2*

Component	Volume per reaction ( $\mu$ l)
RedEx	12,5
Forward Primer	1
Reverse Primer	1
Template DNA	4
Distilled Water	6,5
Total volume	25

*Table 8: PCR test setup no 3*

Component	Volume per reaction ( $\mu$ l)
RedEx	12,5
Forward Primer	1
Reverse Primer	1
Template DNA	5
Distilled Water	5,5
Total volume	25

*Table 9: PCR test setup no 4*

Even though a better PCR product had a higher intensity than the previous setup with the PCR test setup no 2, these amount of PCR still was not enough to get clear results with Pyrosequencing. Therefore, PCR thermo cycler setup was also optimized using the setup as seen in table 10 with lower annealing temperature and increased number of cycles.

Step	Time	Temperature
Initial activation step:	5 min.	95°C
3-step cycling:		
Denaturing:	30 sec.	94°C
Annealing:	30 sec.	50°C
Extension:	1min 30 sec.	72°C
Number of cycles:	40	
Final extension	5 min.	72°C

*Table 10: Modified thermo cycler setup of PCR Region from island 1 & 2 of pri-miR-145.*

These PCR products were used for Pyrosequencing as described above.

## 4.7. Pyrosequencing

Pyrosequencing is a DNA sequencing technique that relies on detection of pyrophosphate release upon nucleotide incorporation rather than chain termination with dideoxynucleotides.<sup>78</sup>

Biochemical reactions are used by pyrosequencing to determine DNA nucleotide sequence. It is based on the balanced mixture of four enzymes and incorporation is monitored bioluminometrically. Each of the four nucleotides – adenine, guanine, cytosine and thymine are released during the reaction in a pre-determined order. The correct nucleotide binds to the template strand by the Klenow fragment of the *Escherichia coli* DNA polymerase I, which in return releases pyrophosphate. This pyrophosphate is used by ATP sulfurylase to produce ATP from adenosine-5'-phosphosulfate. The necessary energy to oxidize D-luciferin, which is done by luciferase, is provided by this ATP molecule. Oxyluciferin which is in an excited state after this reaction, returns to its ground state after emission of a photon. This photon can be detected by a charge-coupled device camera. (Figure 10) An apyrase degrades the nucleotides which are not used during this reaction along with the excess ATP before the addition of the next nucleotide.

The intensity of the bioluminometric and of the peaks is directly proportional with the number of the same nucleotides that are incorporated after each other. If two identical nucleotides are inserted after each other that peak will have double amount of the height of a peak, which had a single nucleotide incorporation. A pyrogram is created for further use.

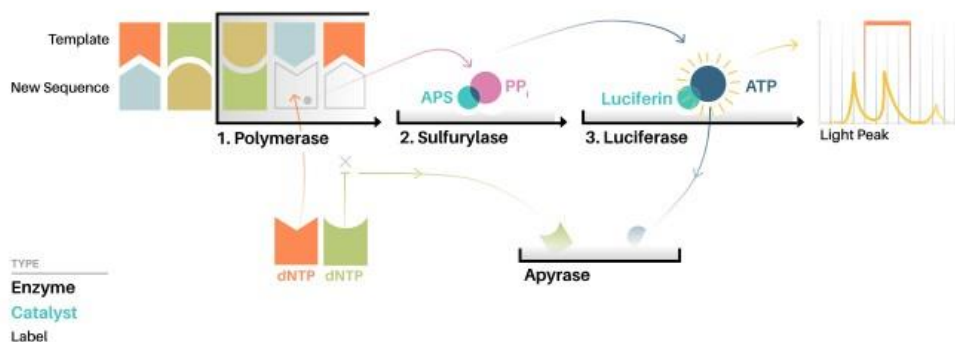


Figure 10: Schematic overview of pyrosequencing. Modified from original source.<sup>79</sup>

Sanger sequencing works with a mixture of four fluorescently labelled terminating dideoxy-nucleotides- (ddNTPs) and strand-elongating deoxy-nucleotides (dNTPs), whereas in pyrosequencing only one dNTP is dispensed at a given time by the cartridge that is an inkjet type. For the known DNA sequences, a previously defined order of the nucleotides can be used whereas for unknown DNA sequencing a cyclic ACGT dispensation is used. This enables to make de novo sequencing. Pyrosequencing with PyroMark instrument gives the ability to sequence up to 24 samples in parallel, therefore it is a cost-efficient and fast method.

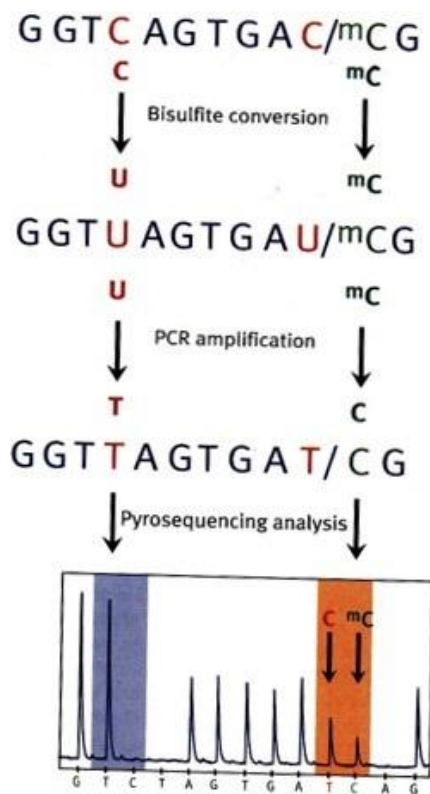


Figure 11: An example of pyrosequencing analysis, which is done to analyse a methylation site. Unmethylated cytosine (C) is measured as the relative content of T at the CpG site, and methylated cytosine (mC) is measured as relative content of C at the CpG site during pyrosequencing. The figure was tilted in its' original source. Modified from original source.<sup>11</sup>

Pyrosequencing protocol consists of 2 parts:

- 1) Preparing to run the assay that will be used during the pyrosequencing.
- 2) Lab work for preparing samples for the pyrosequencing.

Following protocol was used for the preparing of run assay that was used during the pyrosequencing:

- 1) Open programme: Pyromark Q24 - Version 2.0.6.
- 2) Choose new run.
- 3) Choose Instrument Method and marker Pyromark q24 method 11 – Which is modified instrument method as seen in Figure 12.

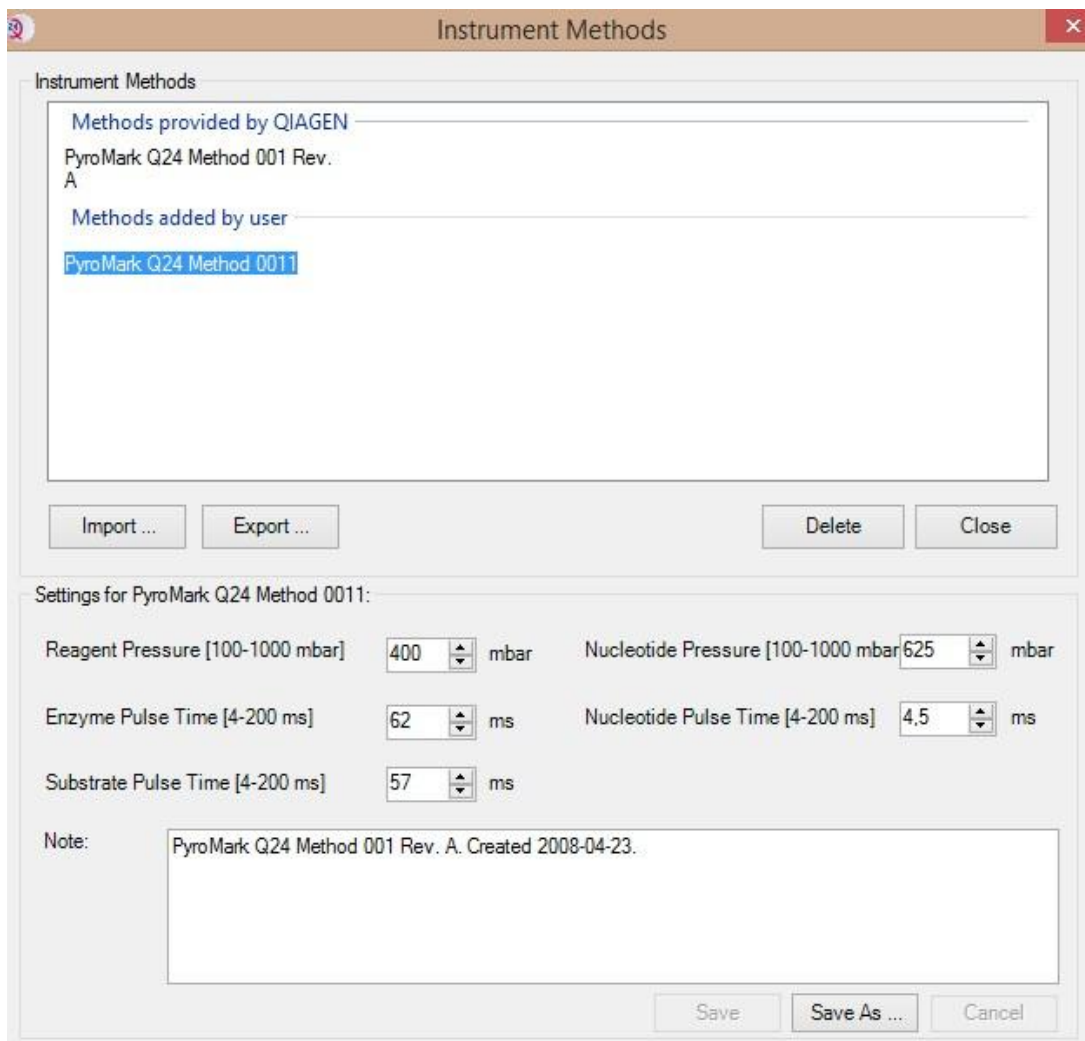


Figure 12: Modified settings for Pyromark Q24 Method 0011- Methods settings depends on the method number that is written on the cartridge.

- 4) Choose a plate at the plate setup window.

- 5) Load the assay depending on which samples you have - Load assay from the USB stick F:\Master thesis\Pyroassay mir145 gene island 1 (Figure 13) or mir 145 gene island 2 (Figure 15) or Control Oligo. ( Figure 17)
- 6) Name the plates and save them to the USB stick.
- 7) Choose tools and print pre run information.

Assay Name: mir145 gene island1

Sequence to Analyze

```
GGTGGGGYGTTAGAGGGTTTTYGGTATTTTTAGGGTAATTGAAGTTYGGTTATTATTTTTTTTA
```

Dispensation Order

```
AGTGGTCGTAGATGTTTCGTCATTAGTATGATGTTTCGTA
```

Figure 13: Assay setup for island 1 of pri-miR-145 gene promotor region for Pyrosequencing. Expected Histogram is given in Figure 14.

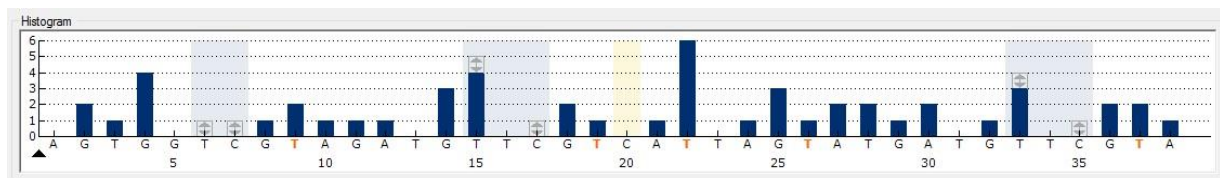


Figure 14: Expected Histogram for Assay setup in Figure 13.

Assay Name: mir145 gene island2

Sequence to Analyze

```
YGGYGGTTTTGGYGTTGAAGGTTATTYGTTTTATTTGTTTTAYGGTTTAGTTTTTAGGAATTTTTAGATGTTAAGAT
```

Dispensation Order

```
ATCTGTCGTTAGTCGTGAGTGATCGCTTATTGTTGATCGTA
```

Figure 15: Assay setup for island 2 of pri-miR-145 gene for Pyrosequencing. Expected Histogram is given in Figure 16.

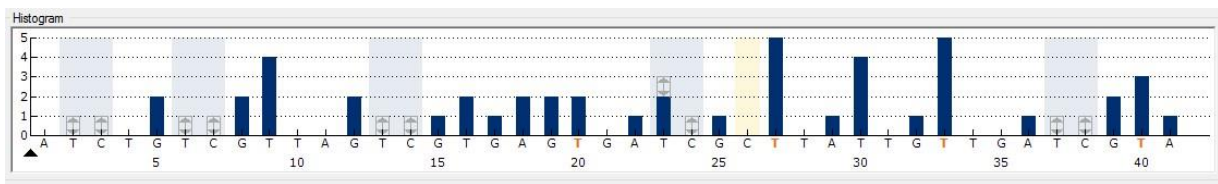


Figure 16: Expected Histogram for Assay setup in Figure 15.

Assay Name: Kontrol Oligo

Sequence to Analyze

Dispensation Order

Figure 17: Assay setup for the control oligos for Pyrosequencing. Expected Histogram is given in Figure 18.

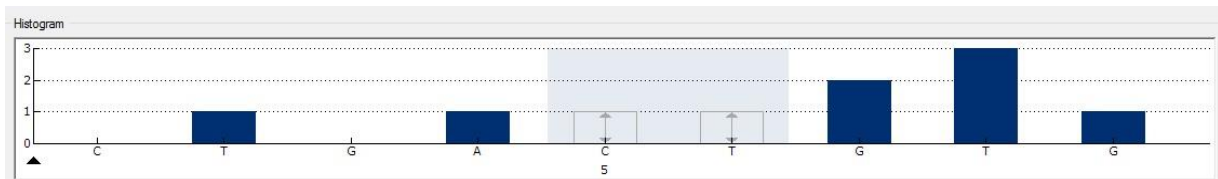


Figure 18: Expected Histogram for Assay setup in Figure 17.

Protocol for Lab Work. This protocol was used for daily routine work of pyrosequencing of patient samples. The sequencing primers are specially designed for PCR region of *pri-miR-145* gene from island 1 and island 2:

- 1) Take sepharose beads, denaturation solution, binding, annealing and wash buffers out of fridge and put them to room temperature 20-30 min prior to use.
- 2) Turn the heat block on and set it to 80°C.
- 3) Prepare the sepharose beads by mixing - 1 µl sepharose balls (vortex before pipetting) + 40 µl binding buffer + 14 µl distilled water for each sample.
- 4) Add sepharose balls mix to the PCR product that is obtained for the Pyrosequencing
- 5) Seal the PCR plate using strip caps.
- 6) Turn on the thermomixer, set it to 1400 rpm for 10 min and put samples there.

- 7) Prepare sequencing reaction mix - 1  $\mu$ l sequencing primer (7.5  $\mu$ M) + 24  $\mu$ l annealing buffer. Following sequencing primers were used during the experiments:

5' GAGGGTAGTTTTGGG 3' – Sequencing primer for PCR Region of island 1 of *pri-miR-145* gene (810- assigned number for ordering according to the hospital protocol)

5' TATTTCCAAAATCCCCATCTTAACAT 3' – Sequencing primer for PCR Region of island 2 of *pri-miR-145* gene (812- assigned number for ordering according to the hospital protocol)

- 8) Add the mix in point 7 to each well on the PyroMark Q24 Plate.
- 9) Place the PCR plate and PyroMark Q24 Plate in the workstation.
- 10) Apply vacuum to the tool by opening the vacuum switch.
- 11) Carefully lower the filter probes into the PCR plate (or strips) to capture the beads containing immobilized template. Hold the probes in place for 15 sec. Take care when picking up the tool.
- 12) Transfer the tool to the part of PyroMark Q24 Vacuum Workstation containing 70 % ethanol. Flush the filter probes for 10 sec.
- 13) Transfer the tool to the next part containing Denaturation solution. Flush the filter probes for 5 sec.
- 14) Transfer the tool to the trough containing Wash Buffer (trough 3). Flush the filter probes for 10 sec.
- 15) Raise the tool to beyond 90° vertical for 5 sec. to drain liquid from the filter probes.
- 16) While holding the tool over the PyroMark Q24 Plate, turn the vacuum switch off.
- 17) Release the beads into the PyroMark Q24 Plate by gently shaking the tool in the wells.
- 18) Transfer the tool to the trough containing water and agitate the tool for 10 sec.
- 19) Wash the filter probes by lowering the probes into and applying vacuum. Flush the probes with 70 ml water.
- 20) Raise the tool to beyond 90° vertical for 5 sec., to drain liquid from the filter probes.
- 21) Close the vacuum switch on the tool (Off) and place the tool in the Parking (P) position.
- 22) Turn off the vacuum pump.

- 23) Heat the PyroMark Q24 Plate containing the samples at 80°C for 2 min. using the PyroMark Q24 plate holder.
- 24) Allow the samples to cool to room temperature (15–25°C) for at least 5 min.
- 25) Place the reagent cartridge with the label facing you and load the cartridge with the appropriate volumes (as given in pre run information by the software) of nucleotides, enzyme and substrate mixtures.
- 26) Open the instrument lid and insert the reagent filled cartridge.
- 27) Open the plate---holding frame and place the PyroMark Q24 Plate on the heating block. Close the plate---holding frame and the instrument lid.
- 28) Insert the USB stick with the run file into the USB port at the front of the instrument and choose the necessary run assay.
- 29) When the run is finished and the instrument confirms that the run file has been saved to the USB stick open and analyse the processed run file in the CpG mode in PyroMark Q24 Software. The quantification of CpG methylation and quality assessment are displayed above each CpG site in the Pyrogram® trace.
- 30) Remove the cartridge and wash it. Throw away PyroMark Q24 Plate that was used during the experiment.

Note: Control oligos were used during the pyrosequencing procedures. Two wells were pipetted with control oligos - with one of them treated same as all samples, while the other one is treated only with step 23 onwards. These control samples enables to see any malfunction of reagents that are used during the experiments, cartridge problems and sequencing problems.

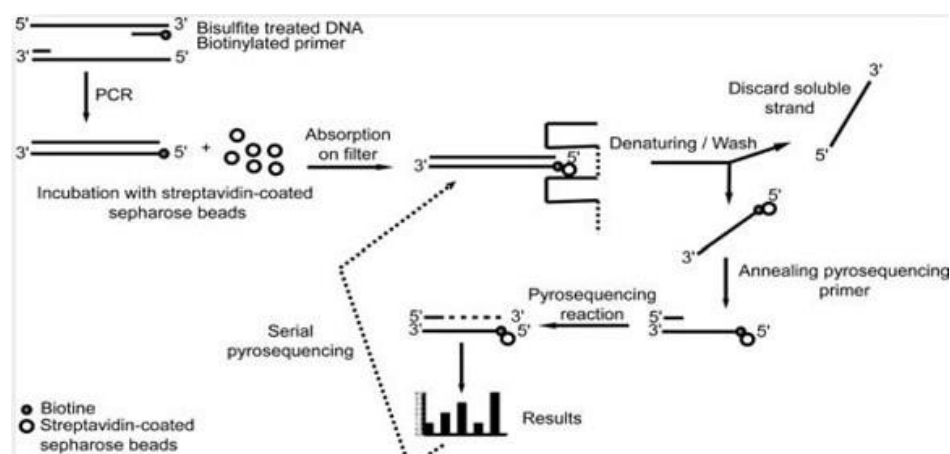


Figure 19: Overview of the major steps of Pyrosequencing protocol. Modified from original source.<sup>11</sup>

## 5. Results

The table 11 shows the successful and failed attempts of making MSP and Pyrosequencing of *pri-miR-145* gene island 1 and 2 for the patient samples. The missing experimental procedures and the DNA amount that is left after the experiments is also indicated.

Sample Number	Patient matched pair?	Type	MSP	Pyro. island 1	Pyro. island 2	What is missing
#03	Yes	N	done	done	done	all done
#04	Yes	T	done	done	done	all done
#05	No	T	done	done	done	all done
#06	Yes	T	done	missing	missing	pyro both islands
#07	Yes	N	done	done	done	all done
#08	No	T	done	done	done	all done
#09	No	T	done	done	done	all done
#10	No	N	done	done	done	all done
#11	Yes	T	done	done	done	all done
#12	Yes	N	done	done	done	all done
#13	No	T	done	done	done	all done
#14	No	T	done	done	done	all done
#15	No	T	done	done	done	all done
#16	No	T	done	done	done	all done
#17	No	T	done	done	done	all done
#18	Yes	T	done	done	done	all done
#19	Yes	N	done	done	done	all done
#20	No	T	done	failed	done	pyro island 1
#21	No	T	done	done	done	all done
#22	Yes	T	done	done	done	all done
#23	Yes	N	done	done	done	all done
#24	No	N	failed	done	done	MSPCR
#25	Same sample as above	N	failed	failed	failed	Mspcr+pyro both
#26	Yes	T	failed	done	done	MSPCR
#27	Yes	N	done	done	done	all done
#28	Yes	T	done	done	done	all done
#29	Yes	N	done	done	done	all done
#30	No	T	done	done	done	all done
#31	Yes	N	done	done	done	all done
#32	Yes	T	done	done	done	all done
#33	No	T	done	done	done	all done
#34	No	T	done	done	done	all done
#35	No	T	done	done	done	all done
#36	No	T	done	done	done	all done
#37	Yes	N	done	done	done	all done
#38	Yes	T	done	done	done	all done
#39	No	T	done	done	done	all done
#40	No	T	done	done	done	all done

Table 11: The procedures that are marked as "failed" did not work because of different reasons possibly partial degradation or bad quality DNA. Even though it was repeated 3-5 times. "Missing" indicates that there was not enough DNA to complete procedures due to missing blocks of FFPE tissue. Pyro. = Pyrosequencing

## 5.1. Results of Methylation Specific PCR of DNA samples

Sample Number	Patient matched pair?	Type	UMSP	MSP	Overall
#03	Yes	N	Negative	Positive	Methylated
#04	Yes	T	Positive	Positive	Hemimethylated
#05	No	T	Negative	Positive	Methylated
#06	Yes	T	Positive	Positive	Hemimethylated
#07	Yes	N	Failed	Failed	
#08	No	T	Negative	Positive	Methylated
#09	No	T	Positive	Positive	Hemimethylated
#10	No	N	Positive	Positive	Hemimethylated
#11	Yes	T	Positive	Positive	Hemimethylated
#12	Yes	N	Negative	Positive	Methylated
#13	No	T	Positive	Positive	Hemimethylated
#14	No	T	Positive	Positive	Hemimethylated
#15	No	T	Negative	Positive	Methylated
#16	No	T	Negative	Positive	Methylated
#17	No	T	Negative	Positive	Methylated
#18	Yes	T	Negative	Positive	Methylated
#19	Yes	N	Negative	Positive	Methylated
#20	No	T	Positive	Positive	Hemimethylated
#21	No	T	Negative	Positive	Methylated
#22	Yes	T	Positive	Positive	Hemimethylated
#23	Yes	N	Positive	Positive	Hemimethylated
#24	No	N	Failed	Failed	
#25	Same sample as above	N	Failed	Failed	
#26	Yes	T	Failed	Failed	
#27	Yes	N	Failed	Failed	
#28	Yes	T	Positive	Positive	Hemimethylated
#29	Yes	N	Positive	Positive	Hemimethylated
#30	No	T	Negative	Positive	Methylated
#31	Yes	N	Negative	Positive	Methylated
#32	Yes	T	Positive	Positive	Hemimethylated
#33	No	T	Positive	Positive	Hemimethylated
#34	No	T	Positive	Positive	Hemimethylated
#35	No	T	Positive	Positive	Hemimethylated
#36	No	T	Positive	Positive	Hemimethylated
#37	Yes	N	Positive	Positive	Hemimethylated
#38	Yes	T	Positive	Positive	Hemimethylated
#39	No	T	Positive	Positive	Hemimethylated
#40	No	T	Positive	Positive	Hemimethylated

Table 12: MSP and UMSP results of patient samples. This table shows the summary of all the gel pictures. In total there were 12 samples that were fully methylated, 21 samples that were hemimethylated. Five samples did not give any clear results even though the experiments were repeated 3 times.

Gel pictures of the samples that are listed in table 12 will be shown in the upcoming figures. The pictures are modified using the QIAxcel ScreenGel 1.4.0 to manually adjust alignment markers.

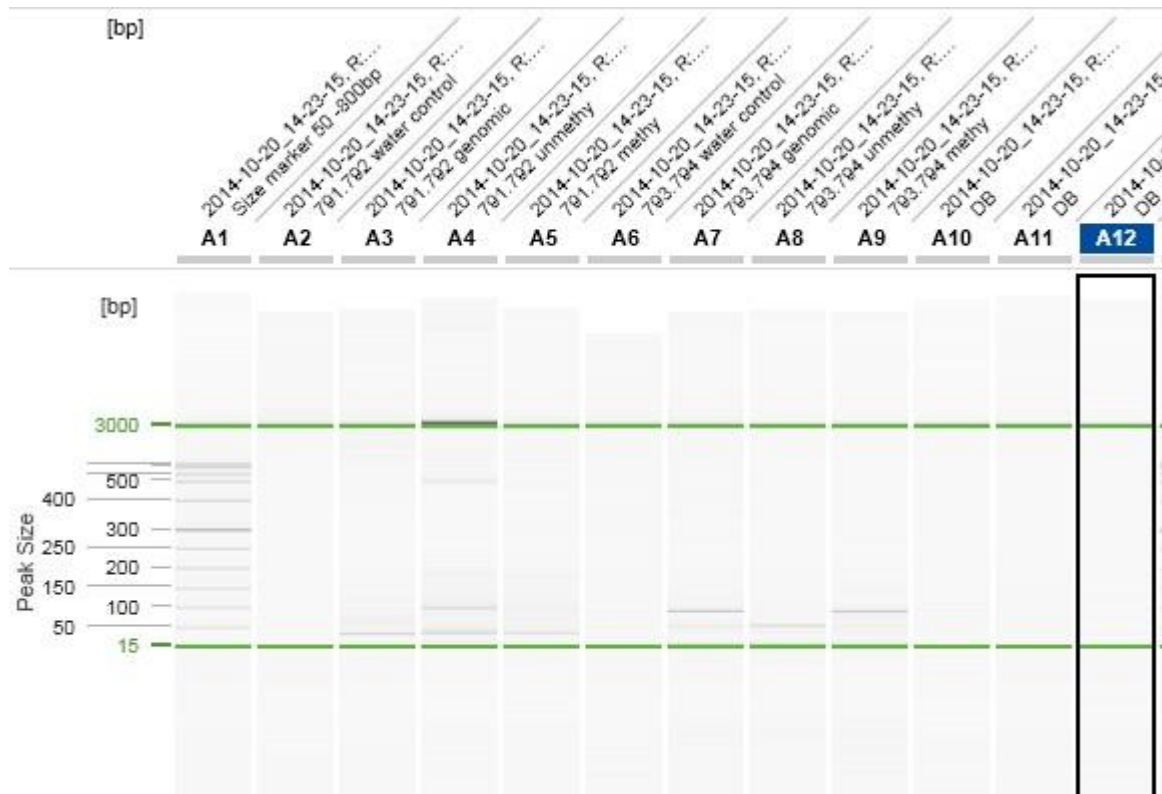


*Figure 20: PCR product length of MSP and UMSP primers - 791: Unmethylated forward Primer, 792: Unmethylated reverse primer, 793: Methylated forward primer, 794: Methylated reverse primer, DB: Dilution buffer, A6: IVS-003 clonal control DNA from InvivoScribe. As it can be seen in well A4 the primers 791+792 have given a PCR product at 100 bp length with fully unmethylated human DNA and a band at 500bp which is possibly a contamination. No PCR product in well A5 with bisulfite converted fully methylated human DNA. Whereas primers 793+794 gave a PCR Product of 100 bp with bisulfite converted fully methylated human DNA and no product with fully unmethylated human DNA. A6 water control shows no contamination and A7 clonal control DNA shows a band around 100 bp and no band at A3.*

The gel picture results of the patient samples will be given in the following figures. Throughout the figures the same abbreviations as in figure 20 are used. Unless otherwise indicated the controls are as follows: Positive control for MSP: bisulfite converted fully methylated human DNA, Positive control for UMSP: fully unmethylated human DNA, DB: Dilution buffer, water control for contamination check. The used primers will be indicated in each figure. The size

marker is the same for all the samples: 50 – 800 bp size marker. Patient samples are numbered throughout the pictures.

If a sample gives a band at 100 bp in MSP, it indicates that the sample is methylated if it shows a band at 100 bp in UMSP, this indicates that the sample is unmethylated. If the samples has in MSP and UMSP at 100 bp a band this indicates that the sample is hemimethylated. If a sample does not give a band in UMSP as well as MSP that means the reactions did not work possibly due to bad quality DNA or low amount of DNA. The bands below shows the primer cloud. The figures below are listed in the chronological order and abbreviations “BT methy.” and “BT unmethy.” show which primers were used during MSP. Please note if the unmethylated primers are used for the UMSP the samples are not bisulfite treated beforehand except the negative control even though they are labelled as BT in the figures. Some of the figures are modified using QIAxcel ScreenGel 1.4.0 to manually adjust alignment markers. An unmodified version of these figures is added after the modified ones. The bands that are listed as unspecific band can be due to failed bisulfite conversion of the samples, however the exact reason is unknown. Pyrosequencing results of the same samples will be shown in the next part of the thesis.

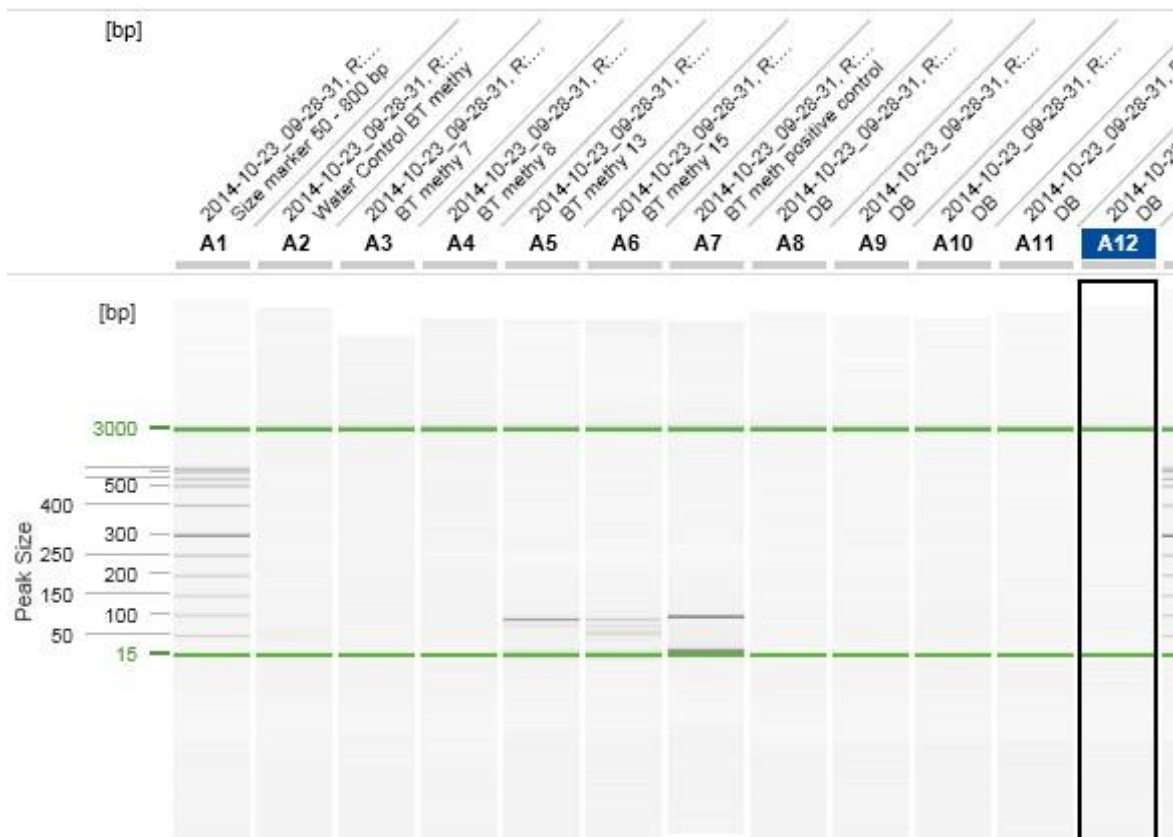


Figure 21: MSP results of MPM samples using the primers 793 and 794. As can be seen in the gel picture positive control in A7 gave a band at 100 bp as expected. Sample number 15 in A6 well and sample number 13 in A5 well gave a band at 100 bp as well. However, in A5 other bands can be seen in between 50 bp – 100 bp along with several bands between 50 – 100bp in A6, which indicates that the DNA was fragmented. Sample 7 in A3 and Sample 8 in A4 did not work. Possible reasons for this can be low concentration of DNA or pipetting mistakes. Water control in A2 is clean, which indicates that there is no contamination. Modified using QIAxcel ScreenGel 1.4.0 to manually adjust alignment markers.



Figure 22: Unmodified version of the figure 21. Wells from left to right A1-A12.

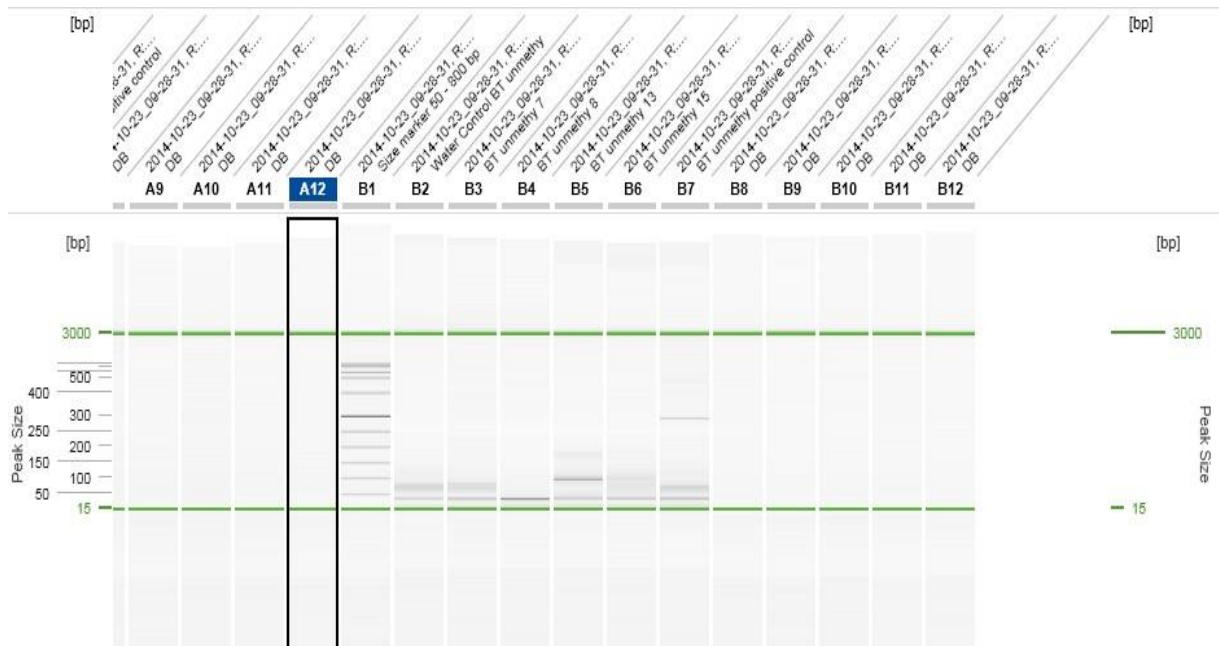


Figure 23: UMSF results of MPM samples using primers 791 and 792. Positive control in well B7 did not work as expected and gave bands at 300 bp and 75 bp. The reason for this can be that the DNA lost its integrity and degraded. Sample 13 in well B5 gave a band at 100 bp as expected. Positive control in B7 has a weak band, which can be seen in figure 24 more clearly. Sample 7 in B3 and sample 8 in B4 do not show any bands at 100 bp. Water control in B2 has the same problem as the samples in B3 and B4.



Figure 24: Close up of figure 23. From left to right wells from B1-B12.

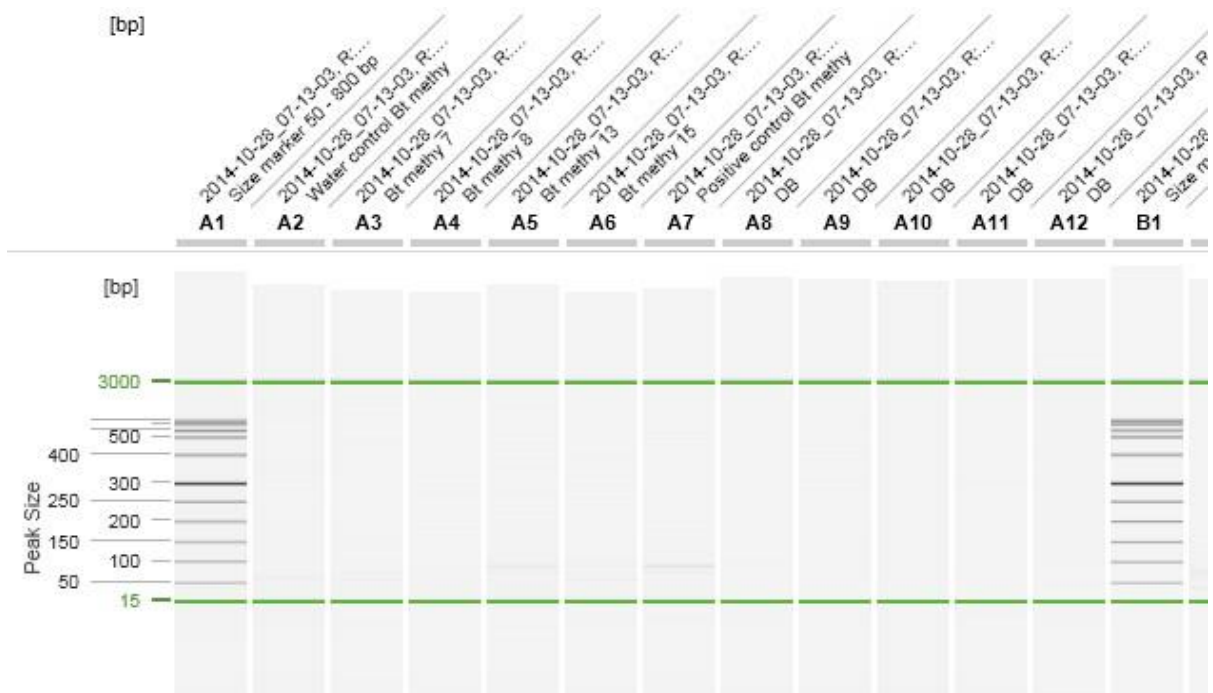


Figure 25: MSP results of MPM samples using primers 793 and 794. Positive control in A7 have a band at 100 bp as expected along with Sample 13 in well A5. Water control in A2 shows no contamination. Sample 7 in well A3, sample 8 in well A4, and sample 15 in A6 does not do not show any bands. Though repeated MSP experiment of sample 8 in Figure 56 showed a band at 100b. Also a band at 100 bp for Figure 15 in a repeated MSP experiment in figure 48 was observed.

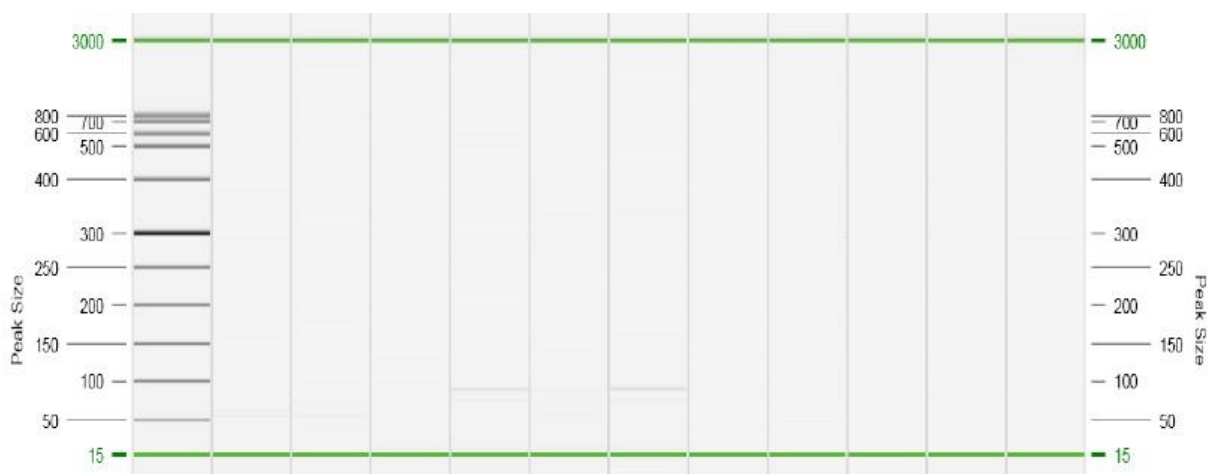


Figure 26: Close up of figure 25. From left to right wells A1-A12.

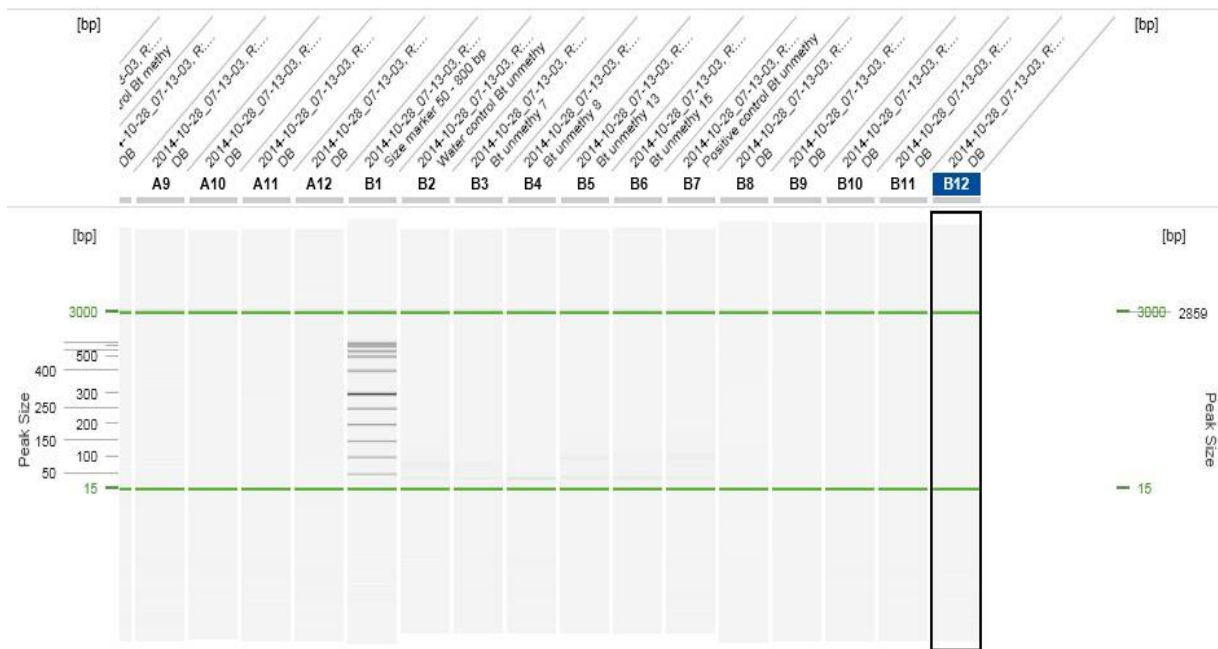


Figure 27: UMSF results of MPM samples using primers 791 and 792. Positive control in B7 and sample 13 in B5 shows a band at 100 bp, which can be more clearly seen in figure 28. Water shows no contamination. Sample 7 in B3, sample 8 in B4 and sample 15 in B6 does not show any bands. Though a band at 100 bp in repeated MSP experiment for figure 15 was observed in Figure 48.



Figure 28: Close up of figure 27. From left to right wells B1-B12.

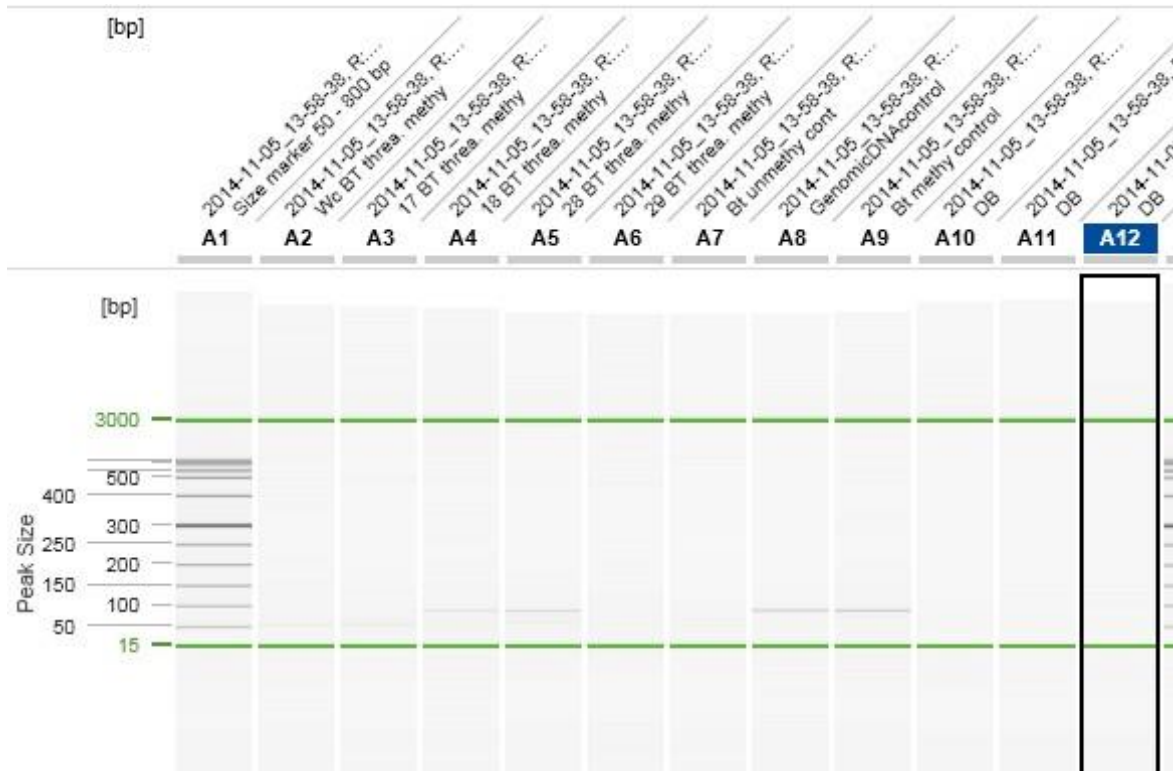


Figure 29: MSP of MPM samples using primers 793 and 794. Positive control in A9, IVS genomic DNA in A8, sample 28 in A5 and sample 18 in A4 shows a band at 100 bp. Water control in A2 does not show any contamination, whereas sample 17 in A3, sample 29 in A6, Negative control in A7 does not show any bands. However a repeated MSP experiment for sample 17 showed a band at 100 bp in figure 48. Modified using QIAxcel ScreenGel 1.4.0 to manually adjust alignment markers.



Figure 30: Close up of figure 29. From left to right wells A1-A12

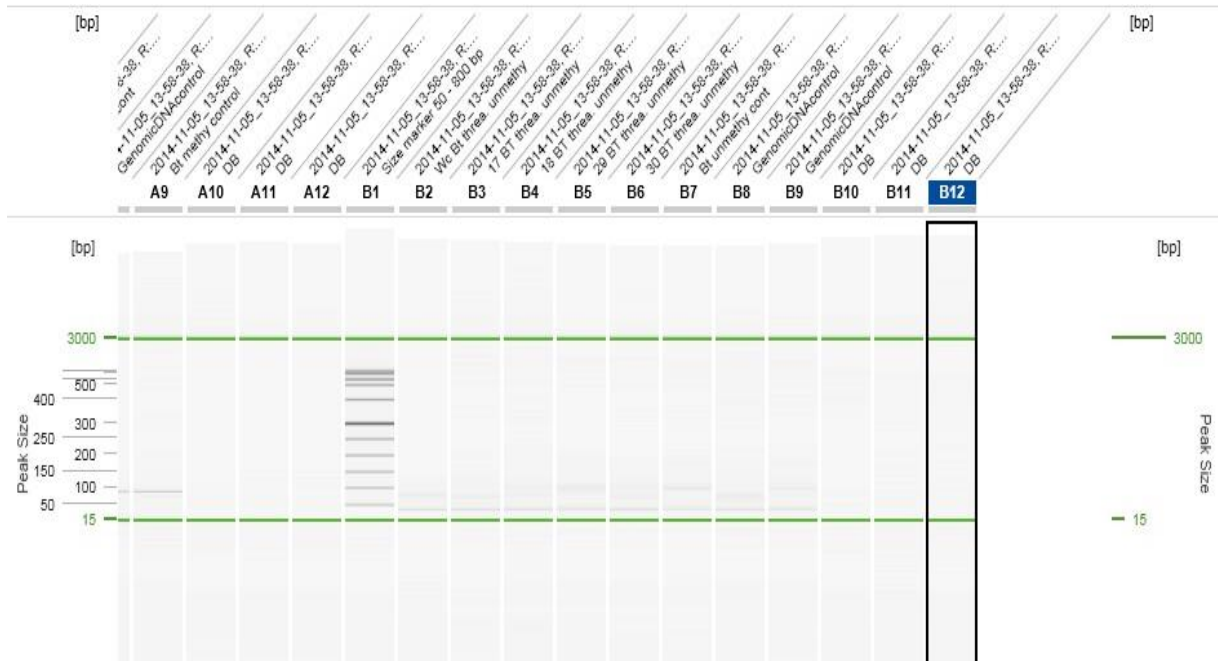


Figure 31: UMSF results of MPM samples using primers 791 and 792. Control sample in B7, sample 30 in B6, sample 29 in B5. Water control in B2 shows no contamination. Sample 17 in B3 and sample 18 in B4 show no bands. Interestingly, IVS Genomic control in B8 shows no band at 100 bp, although there is a band at 100 bp in B9. The reason for this can be failed reaction at the B8.



Figure 32: Close up of figure 31. From left to right wells B1-B12.

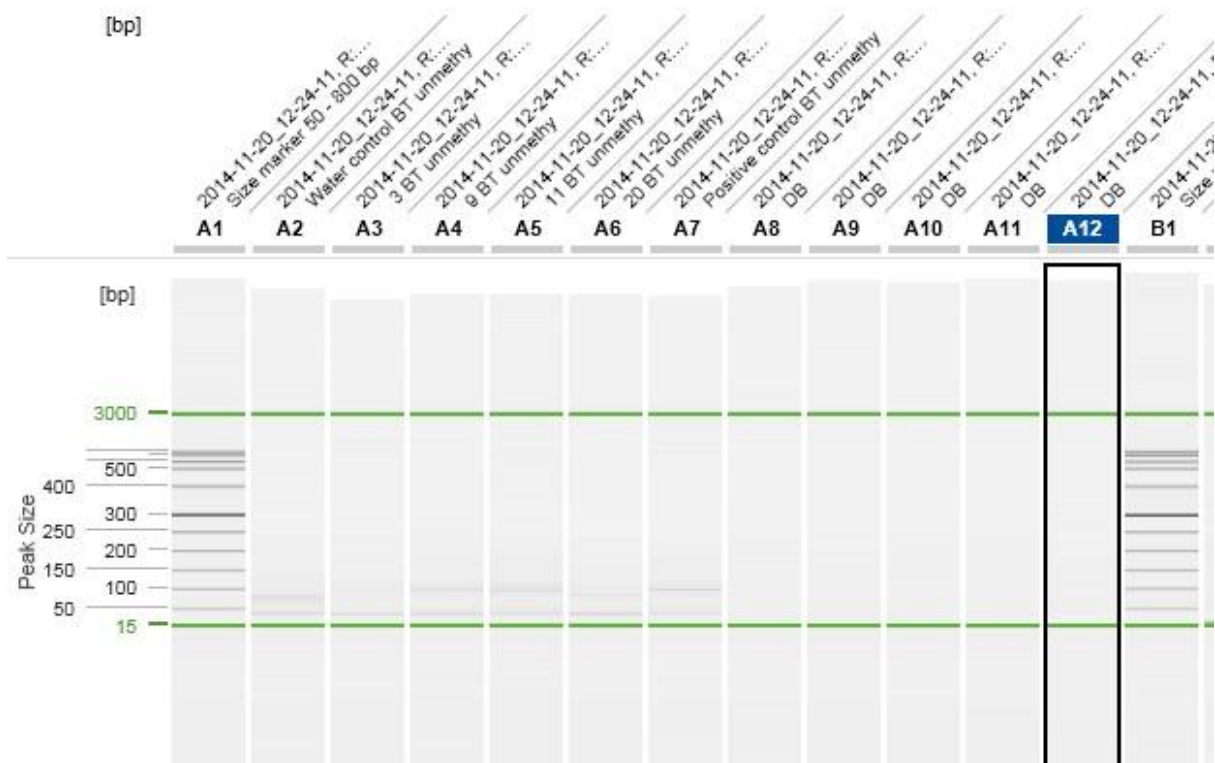


Figure 33: UMSP of MPM samples using primers 791 and 792. Positive Control in A7 shows a band at 100 bp. Sample 9 in A4 and sample 11 in A5 show a band at 100 bp. There is a light contamination in the water and sample 20 in A6 shows a band that is lower than 100 bp around 80 bp – which is an unspecific band possibly due to gel impurities or partial degradation. Sample 3 in A2 shows no bands.



Figure 34: Close up of figure 33. From left to right wells from A1-A12.

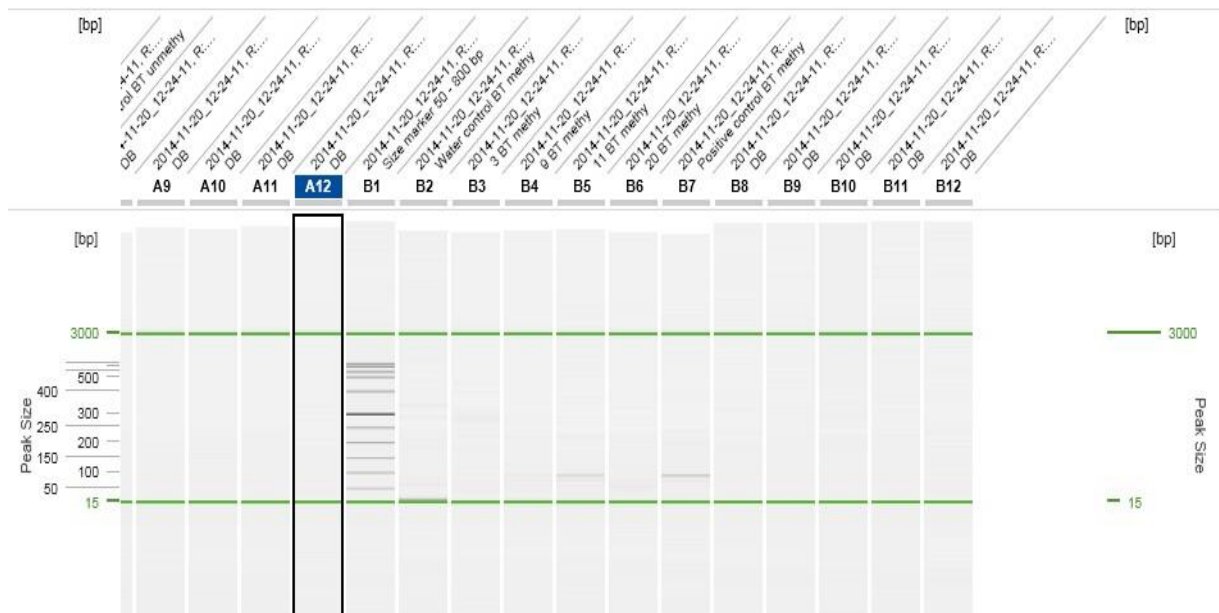


Figure 35: MSP of MPM samples using primers 793 and 794. Positive control in B7, sample 11 in B5 shows a band at 100 bp. Water control shows an unspecific band around 50 bp. Sample 3 in B3, sample 9 in B4 and sample 20 in B6 do not show any bands. Though sample 3 and sample 9 showed a band at 100bp in a repeated MSP experiment in figure 38. Also sample 20 shows a band at 100bp in a repeated MSP experiment in figure 42.



Figure 36: Close up of Figure 35. From left to right wells B1-B12. An unspecific second band can be seen for the sample number 11 in B5 and in positive control in B7.

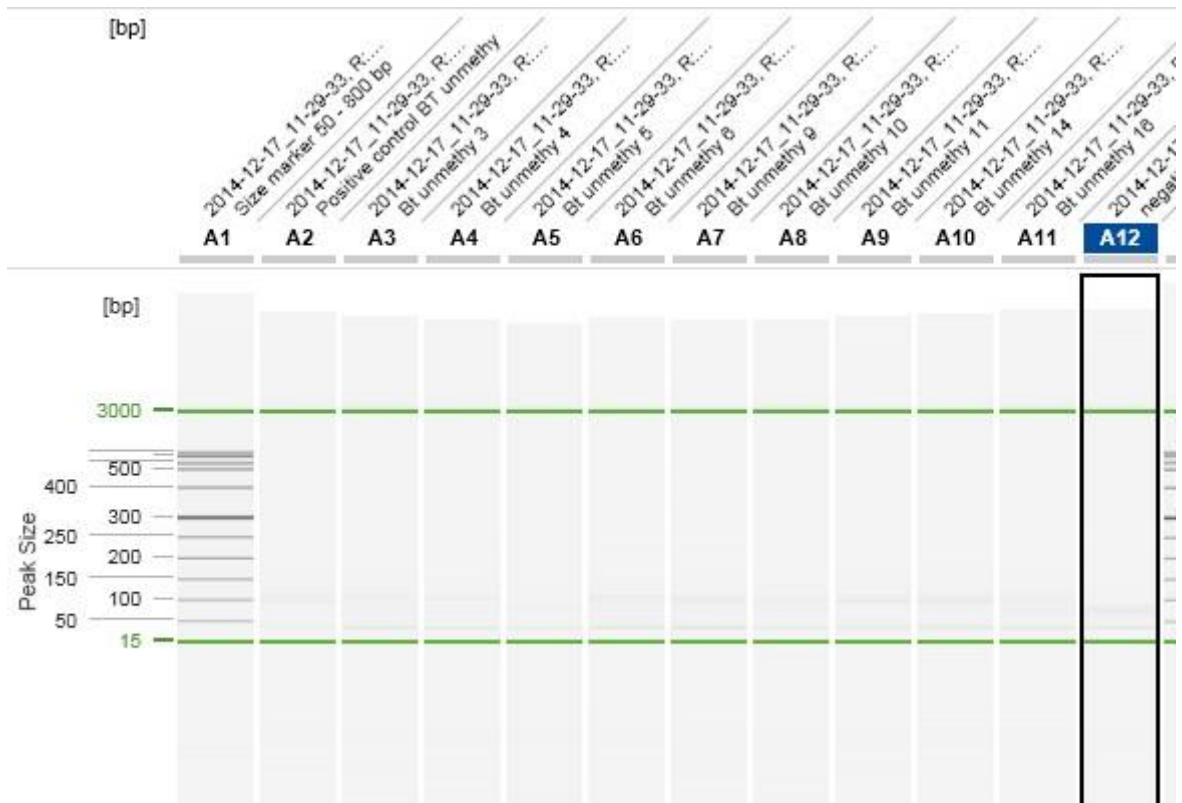


Figure 37: UMSP results of different MPM samples using primers 791 and 792. Positive control in A2, sample 4 in A4, sample 6 in A6, sample 9 in A7, sample 11 in A9, sample 14 in A10 show band at 100bp. Water control shows a contamination around 80 bp.



Figure 38: Close up of the figure 37. From left to right wells A1-A12.



Figure 39: MSP results of MPM samples using primers 793 and 794. Positive control in B2 shows a band around 100 bp as expected. Though the band is a bit lower than 100 bp, it is possible this was due to impurities in gel. Sample 3 in B3, sample 4 in B4, sample 5 in B5, sample 6 in B6, sample 9 in B7, sample 10 in B8, sample 11 in B9, sample 14 in B10 and sample 16 in B11 show a band at the same height as the positive control. Additionally sample 5 in B5 and sample 10 in B8 show an unspecific band at 50 bp along with negative control-fully unmethylated human DNA in B12.



Figure 40: Close up of figure 39. From left to right wells B1-B12.

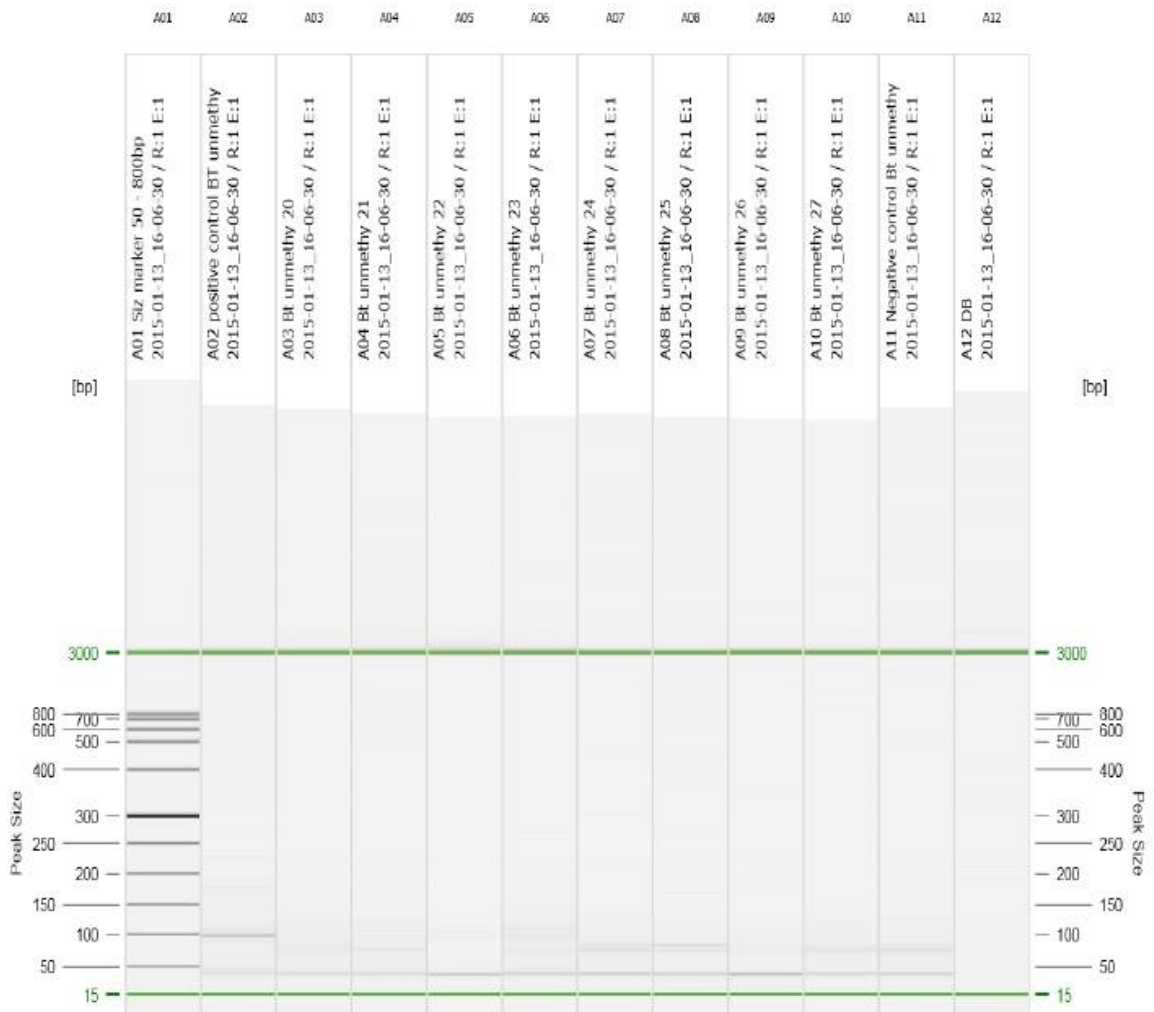


Figure 41: UMSP results of different samples using primers 791 and 792. Positive control in A2 has a band at 100 bp. Sample 23 in A6 shows a band at the same height along with a contamination at 80 bp. All other samples shows no clear bands at 100 bp. Except sample 22 in A5 all other samples shows a contamination around 80 bp including negative control in A11.

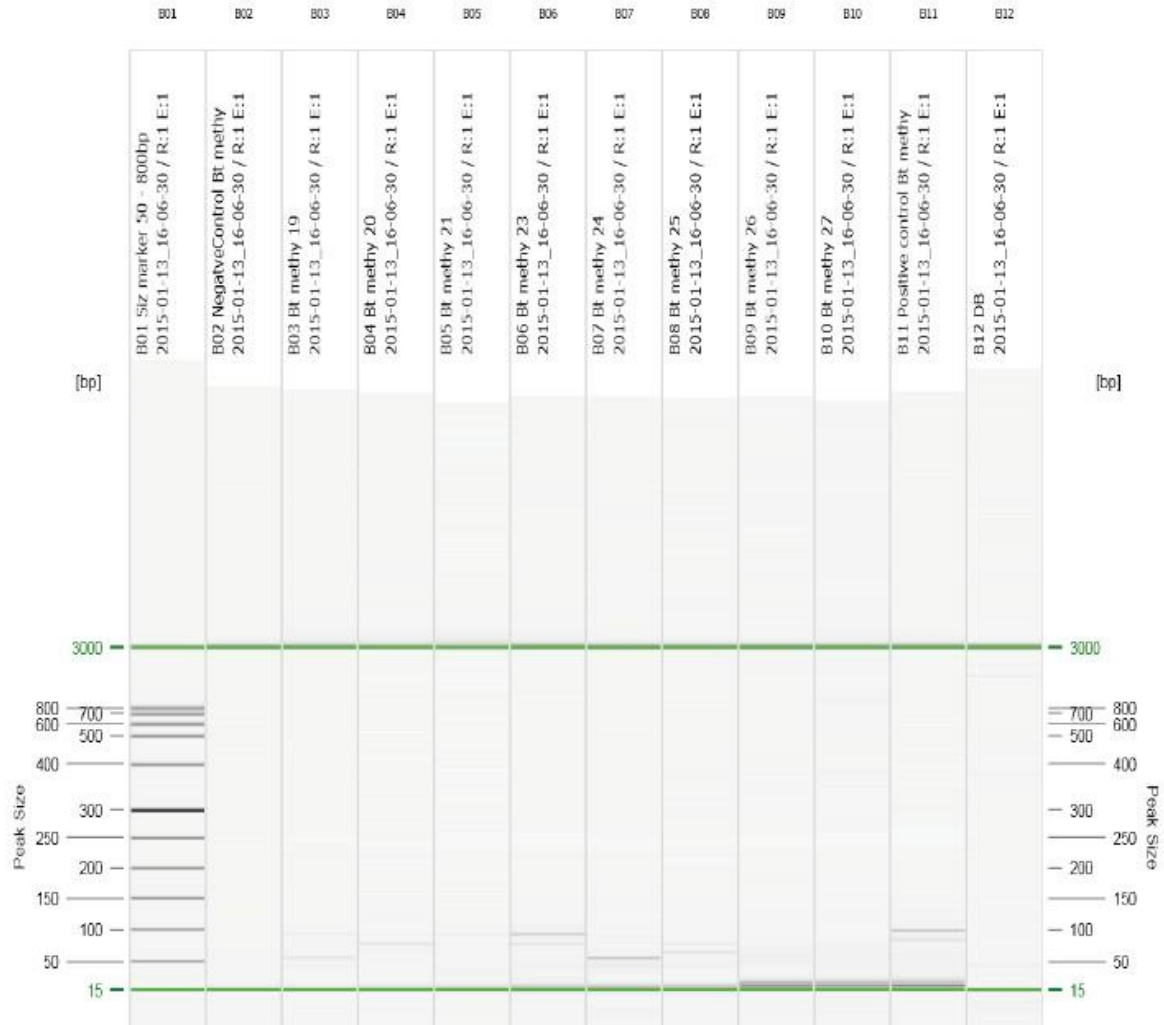


Figure 42: MSP samples of different samples using 793 and 794. Positive control in B11 shows a band at 100 bp along with an unspecific sec band at 90 bp. Sample 20 in B4 shows a weak band with the same size as the control sample. Other samples shows bands at different heights. This can be due to degraded or damaged DNA or unsuccessful BT conversion.

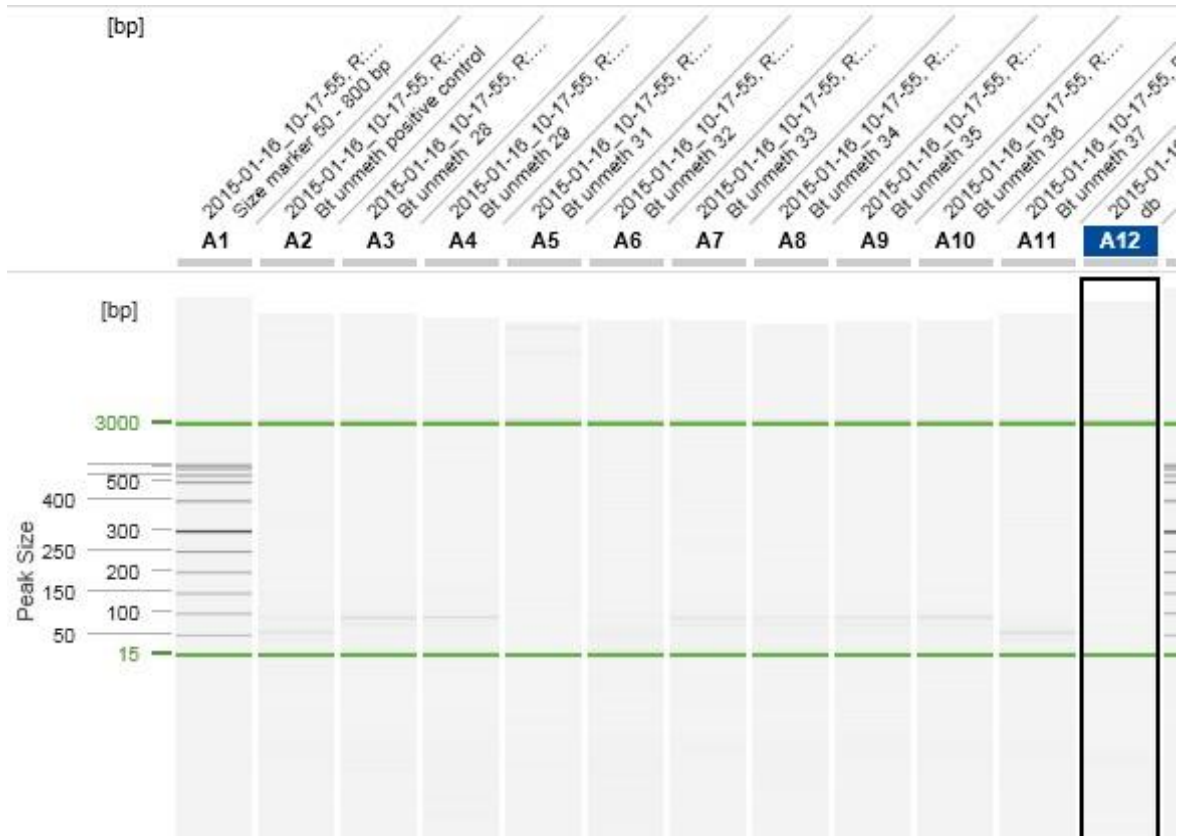


Figure 43: UMSP results of MPM samples using primers 791 and 792. Positive control in A2 has a band at 100 bp along with an unspecific band at 50bp. Sample 28 in A3, sample 29 in A4, sample 33 in A7, sample 34 in A8, sample 35 in A9, and sample 36 in A10 show a band at 100 bp as well. Whereas sample 31 in A5, sample 32 in A6 and sample 37 in A11 do not show any bands at 100 bp. Sample 37 also has an unspecific band at 50bp just like the positive control. Modified using QIAxcel ScreenGel 1.4.0 to manually adjust alignment markers.

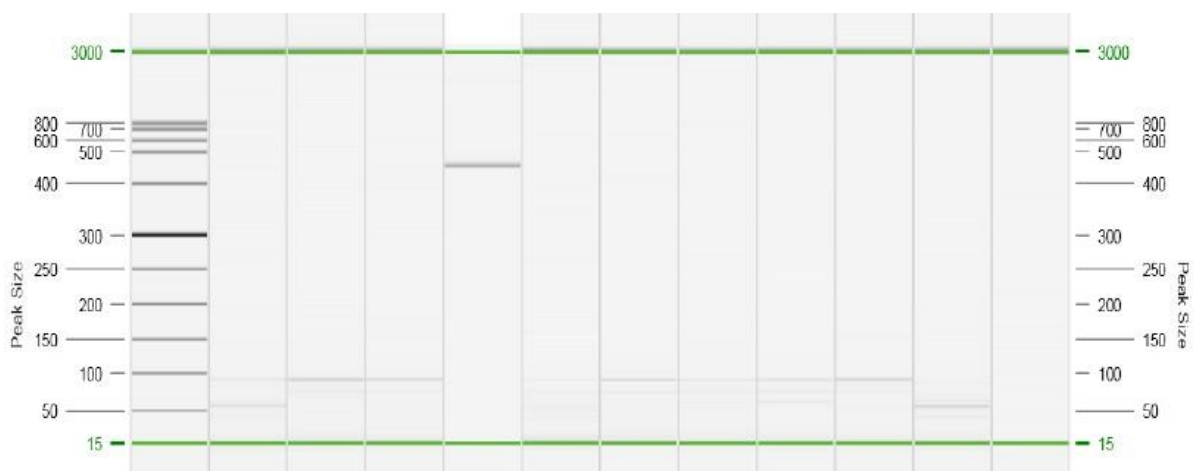


Figure 44: Unmodified and close up version of the figure 43. From left to right wells A1-A12.

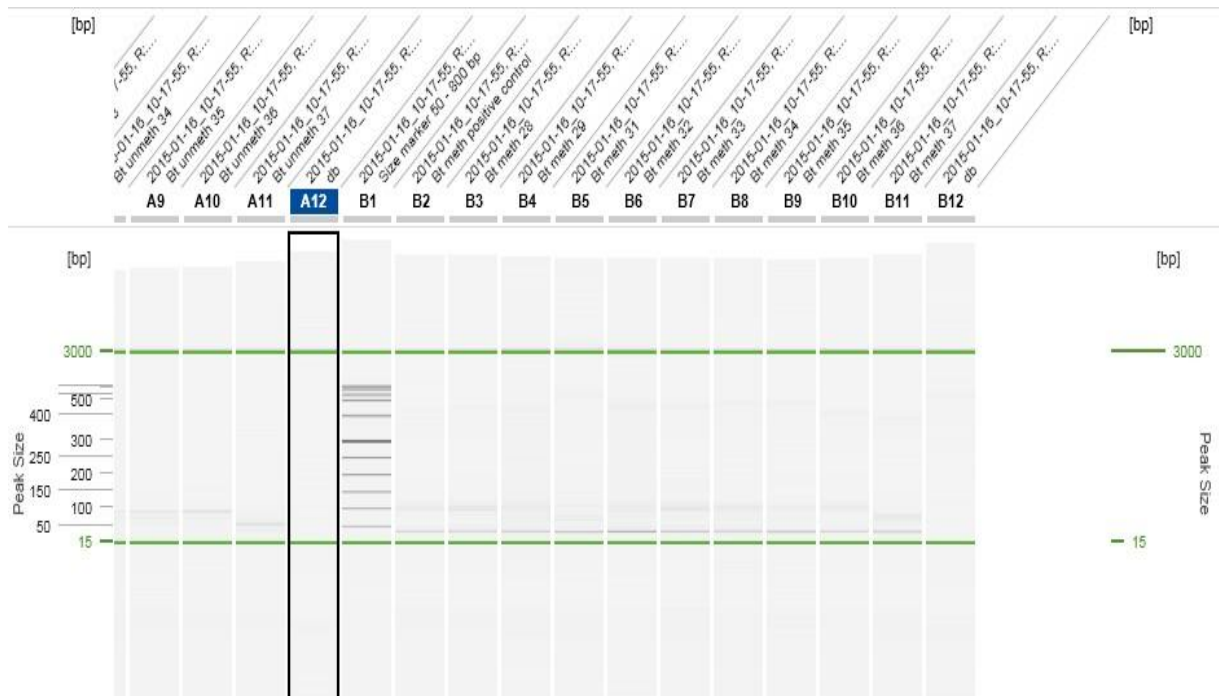


Figure 45: MSP results of MPM samples using primers 793 and 794. Positive control in B2 shows a band at 100 bp. Sample 28 in B3, sample 29 in B4, sample 32 in B6, sample 33 in B7, sample 34 in B8, sample 35 in B9, and sample 36 in B10 show a band 100 bp as well. Whereas sample 31 shows 2 bands one at 100 bp and the other one at 80bp, which indicates that the DNA was probably fragmented. Sample 37 shows also several bands which indicates that the DNA was fragmented. These can be more clearly seen in figure 46.



Figure 46: Close up of figure 45. From left to right wells B1-B12.

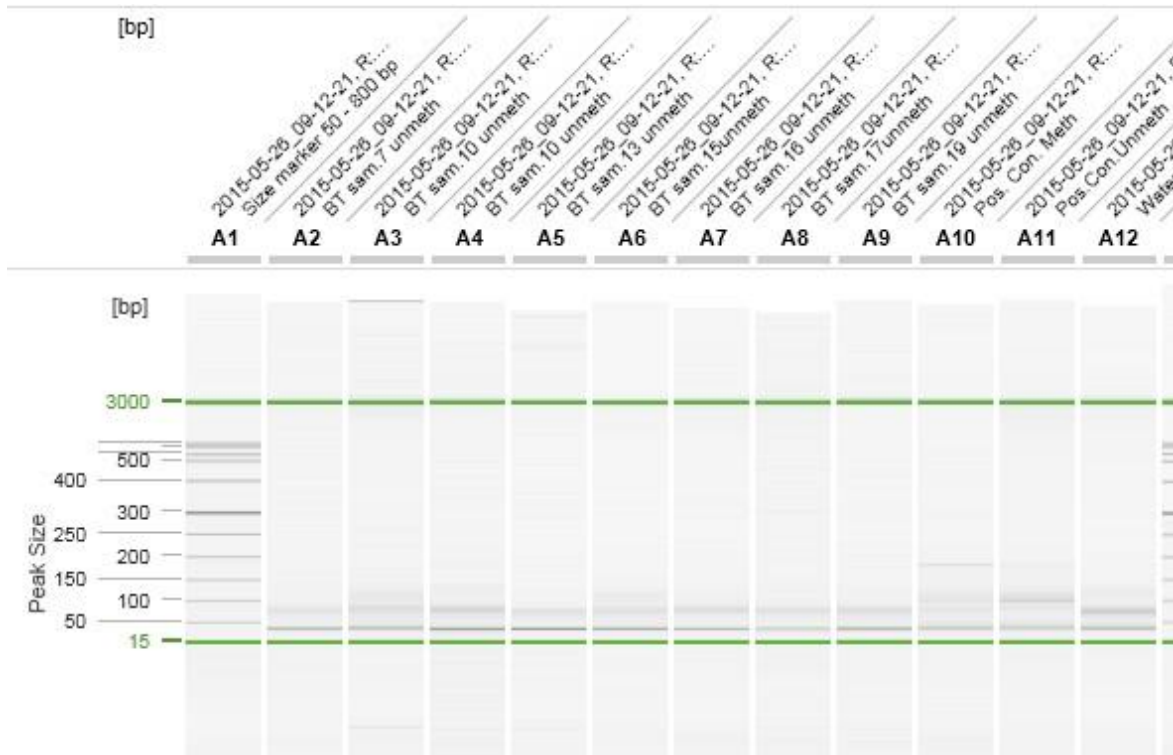


Figure 47: UMSP of MPM samples using primers 791 and 792. Positive control in A11 shows a band at 100 bp. However a severe contamination is detected in the water control A12 which affected all samples therefore the results are unreliable here and will not be discussed. Modified using QIAXcel ScreenGel 1.4.0 to manually adjust alignment markers.

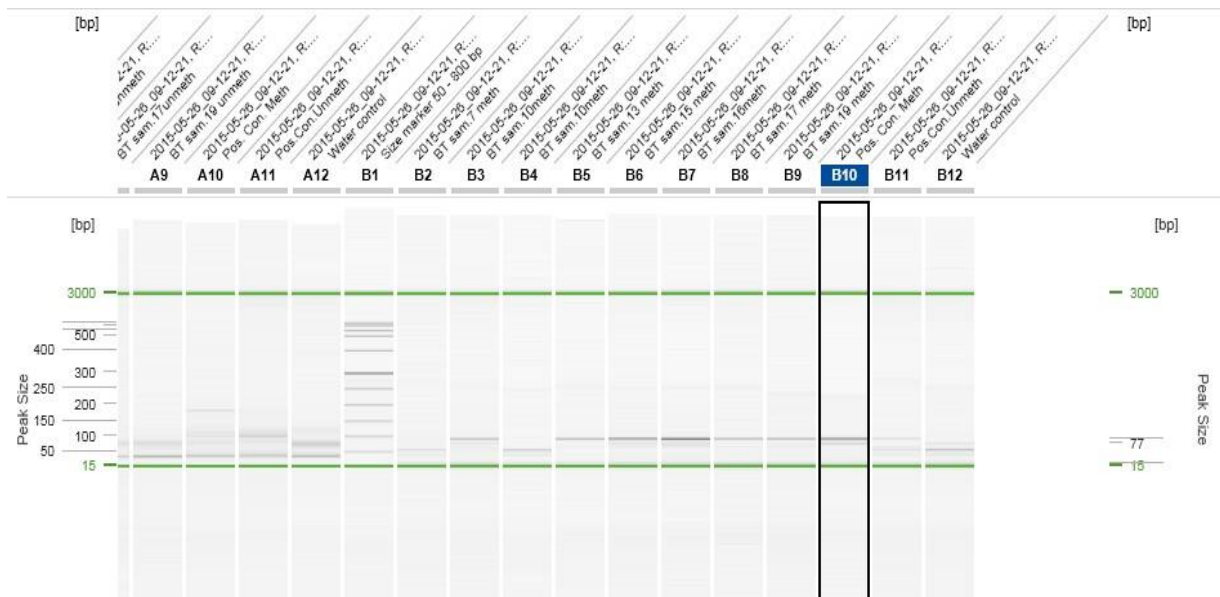


Figure 48: MSP results of MPM samples using primers 793 and 794. Positive control in B10 shows a band at 100 bp along with an unspecific band at 90 bp. Sample 10 in B3, sample 13 in

B5, sample 15 in B6, sample 16 in B7, sample 17 in B8, and sample 19 in B9 also have a band at 100 bp. Sample 7 in B2 and sample 10 in B4 show no bands at 100 bp and only an unspecific band at 50 bp. Negative control in B11 (named pos. con. unmeth. in the figure) shows also contamination from the well B10 as well as B12 and have 2 bands one at 100 bp and one at 50 bp. Water control in B12 shows also contamination in 2 bands one at 75 bp another one 50 bp. Interestingly, water control has the same band size as sample 7 and sample 10. The reason for this is unknown. Modified using QIAxcel ScreenGel 1.4.0 to manually adjust alignment markers.



Figure 49: Unmodified and close up gel picture of figure 48. From left to right wells B1-B12. Different band sizes can be more clearly seen here.

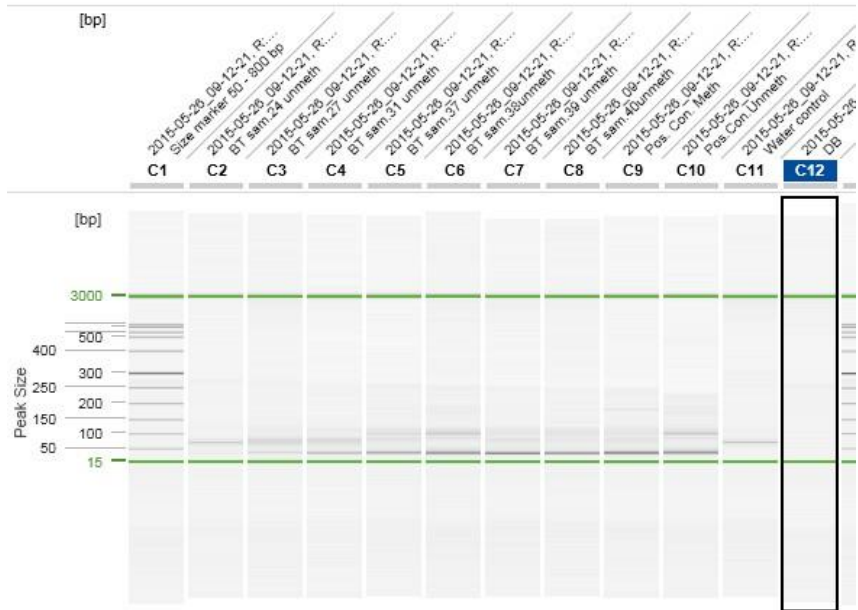


Figure 50: UMSP results of MPM samples using primers 791 and 792. Positive control in C10, sample 37 in C5 and sample 38 in C6 show a strong band at 100 bp. Sample 39 in C7 and sample 40 in C8 show a weak band at 100 bp. Negative control (named pos. con. meth.) at C9 shows also a weak band at 100bp, which could indicate contamination. It also has an unspecific band at 150 bp. whereas sample 24 in C2 show contamination at 75 bp along with other samples.



Figure 51: Close up of figure 50. From left to right wells C1-C12.

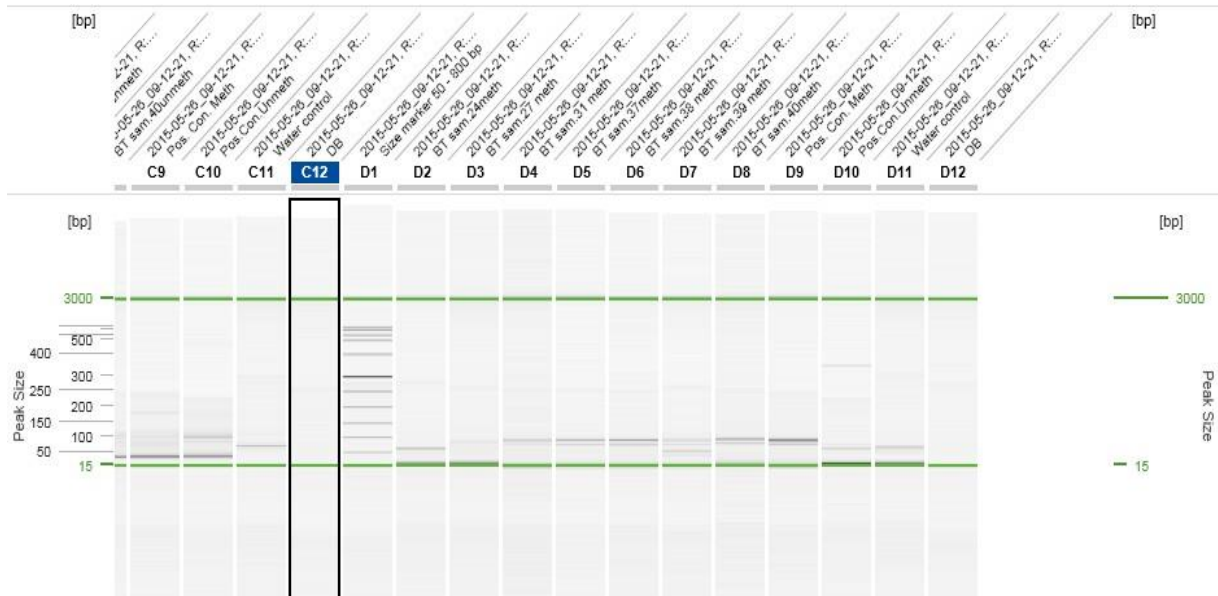


Figure 52: MSP results of MPM samples using primers 793 and 794. Positive control in D9 has a band at 100 bp size along with an unspecific band at 80bp. Sample 31 in D4, sample 37 in D5, sample 38 in D6, and sample 40 in D8 have also bands at the same sizes. Sample 24 in D2 has a band at 80 bp. Sample 27 in D3, Negative control (named pos. con. unmeth. in D10) and water control have unspecific bands at 60 bp Whereas sample 39 in D7 has 4 bands- one at 100bp, one at 80 bp, one at 60 bp and one at 40 bp- which show that the DNA was fragmented. Modified using QIAxcel ScreenGel 1.4.0 to manually adjust alignment markers.

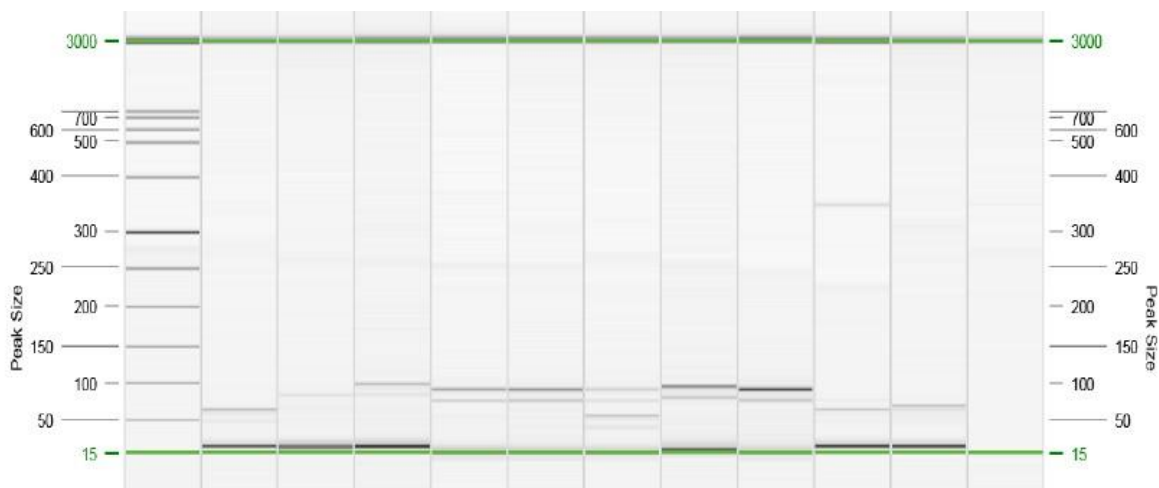


Figure 53: Unmodified version of figure 52 in close up. From left to right wells D1-D12.

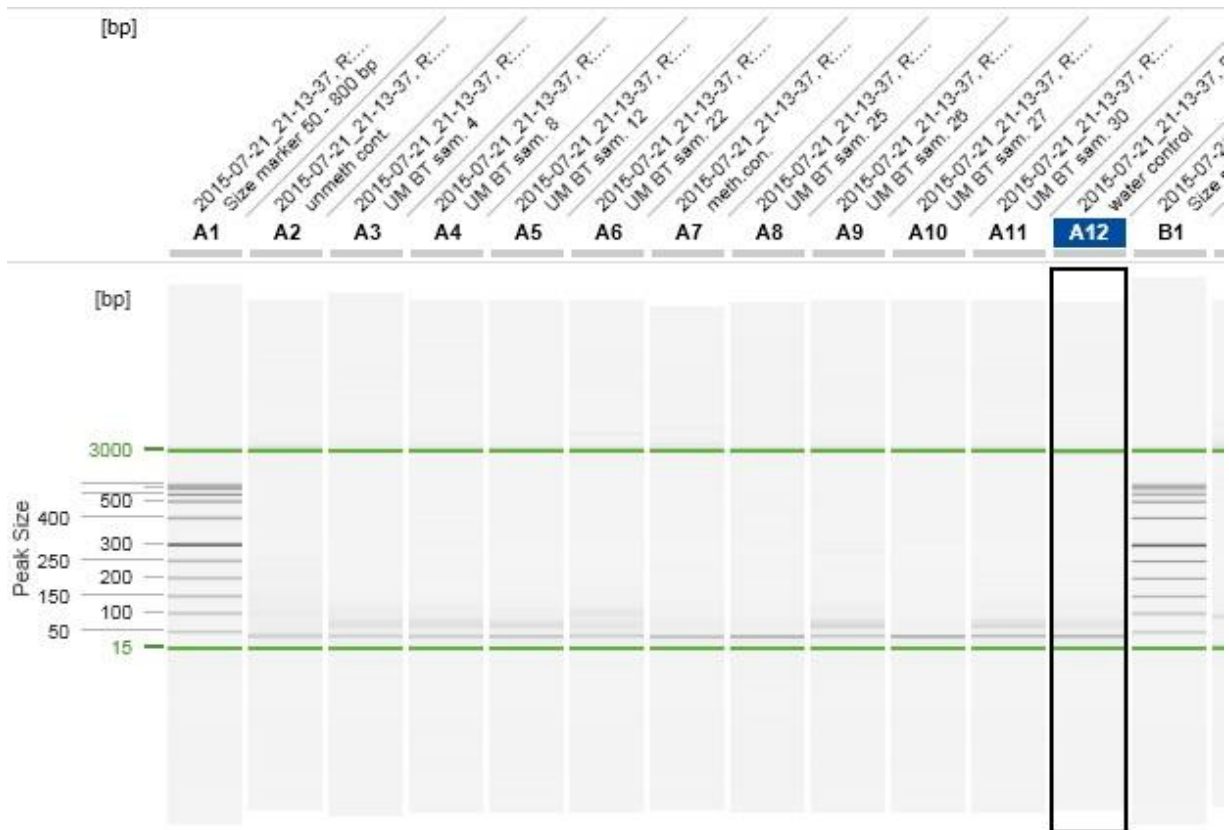


Figure 54: UMSF results of MPM samples using primers 791 and 792.. Positive control in A2 shows a weak band at 100bp. Sample 22 in A6 also shows a weak band at 100bp. All samples excluding sample 27 in A10, positive control in A2, Negative control in A7, sample 25 in A8 shows an unspecific band at 70 bp along with water control. Negative control in A7 does not show any bands except the primer cloud. Modified using QIAxcel ScreenGel 1.4.0 to manually adjust alignment markers.



Figure 55: Unmodified version of figure 54 in close up. From left to right wells A1-A12.

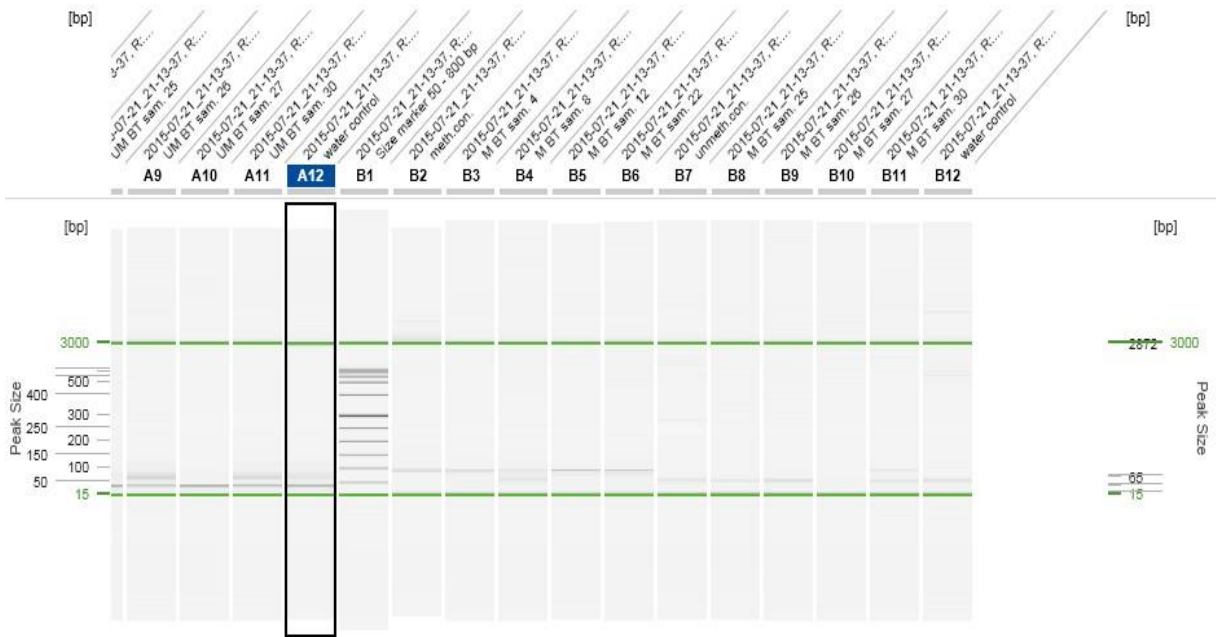


Figure 56: MSP results of MPM samples using primers 793 and 794. Positive control in B, sample 4 in B3, sample 8 in B4, sample 12 in B5, sample 22 in B6 show a band at 100 bp. An unspecific band around 70 bp can be seen in sample 8 in B4, negative control (named unmeth. con.) in B7, sample 25 in B8, sample 26 in B9, sample 27 in B10, sample 30 in B11 and water control in B12. Modified using QIAxcel ScreenGel 1.4.0 to manually adjust alignment markers.



Figure 57: Unmodified version of figure 56 in close up. From left to right wells B1-B12.

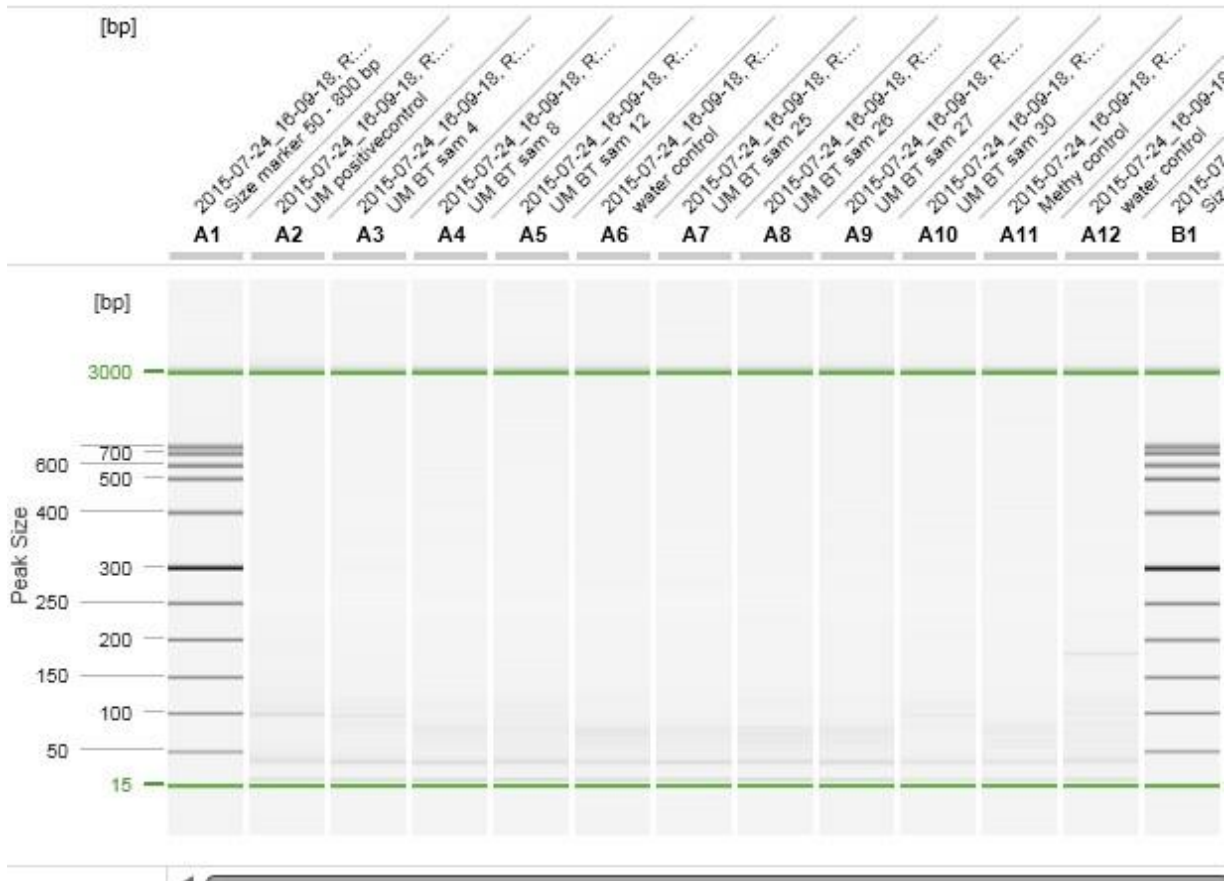


Figure 58: UMSP results of MPM samples using 791 and 792. Positive control in A2 shows a band at 100 bp. There is contamination in the water control at 100 bp as well. Therefore, the bands of sample 4 in A3 and sample 30 in A10 at 100 bp can be due to contamination. So it does not give conclusive results. Modified using QIAxcel ScreenGel 1.4.0 to manually adjust alignment markers.



Figure 59: Unmodified version of figure 58 in close up. From left to right wells A1-A12. Shifted bands can be seen in the figure.

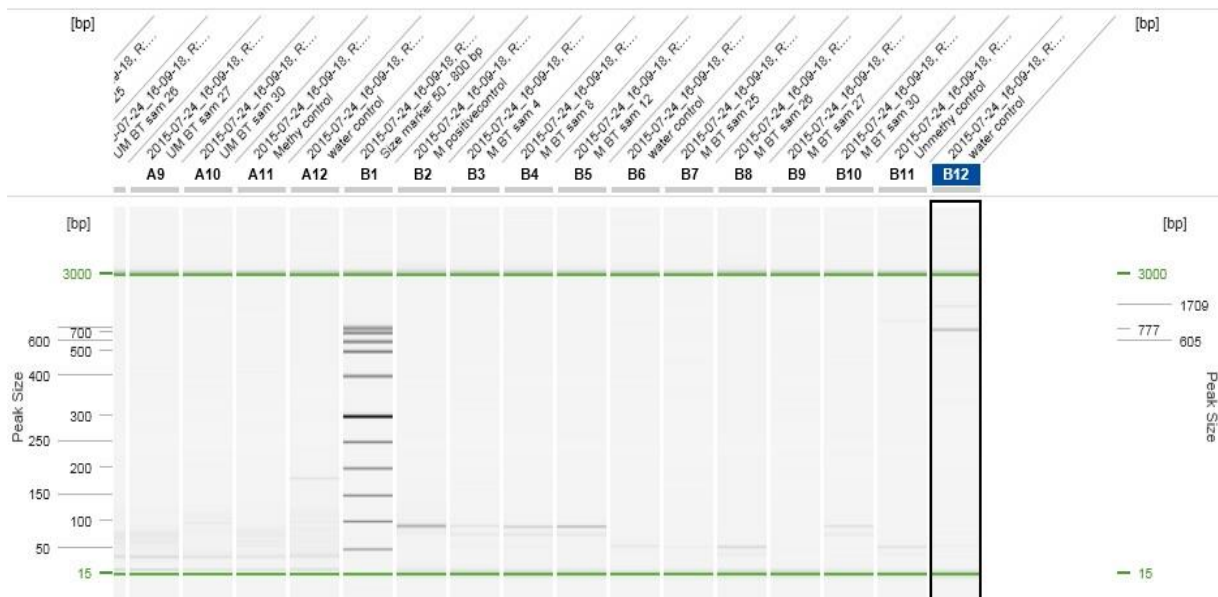


Figure 60: MSP results of MPM samples using primers 793 and 794. Positive control in B2 has a band around 100 bp. Sample 4 in B3, sample 8 in B4, sample 12 in B5, and sample 30 in B10 has a band at 100 bp along with an unspecific band at 80 bp. Water controls in B6 and B12 shows an unspecific band and contamination along with, sample 25 in B7, sample 26 in B8, sample 27 in B9 and negative control (named unmethy. control) in B11. Modified using QIAxcel ScreenGel 1.4.0 to manually adjust alignment markers.

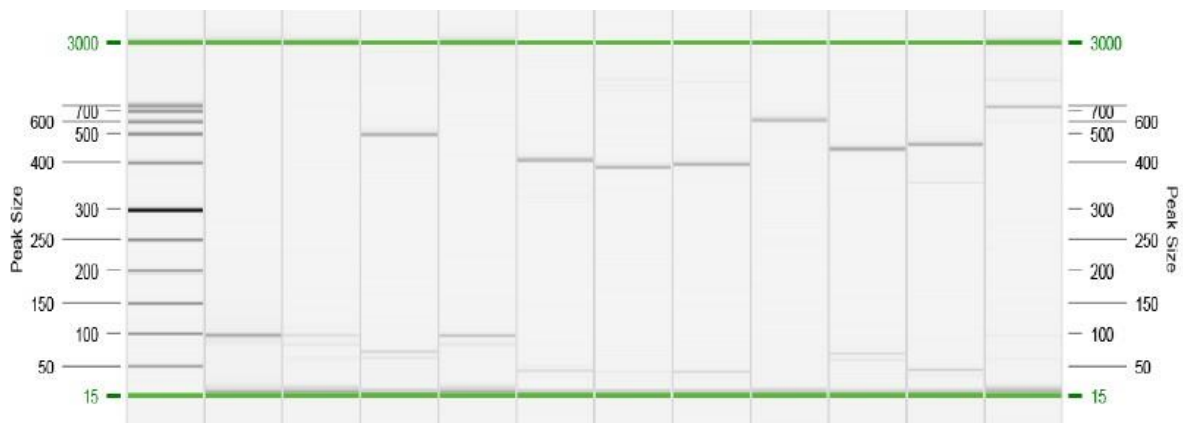


Figure 61: Unmodified version of figure 60 in close up. From left to right wells B1-B12. Shifted bands can be seen in the figure.

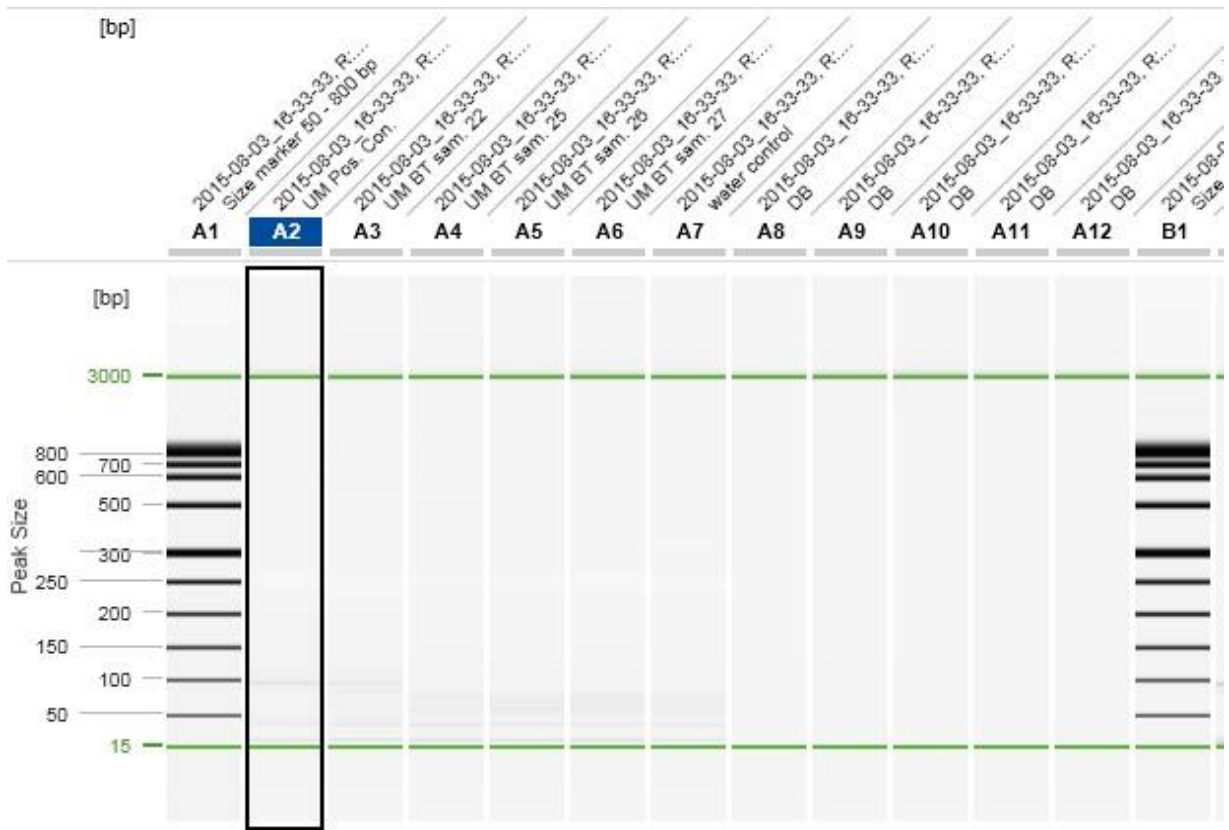


Figure 62: UMSP of MPM samples using primers 791 and 792. Positive control in A2 and sample 22 in A3 shows bands at 100 bp along with a contamination at 40 bp. Sample 25 in A4, sample 26 in A6, sample 27 in A7 and water control have a degraded DNA or contamination. Therefore their results are inconclusive. Modified using QIAxcel ScreenGel 1.4.0 to manually adjust alignment markers.



Figure 63: Unmodified version of figure 62 in close up. From left to right wells A1-A12. Shifted bands can be seen in the figure.

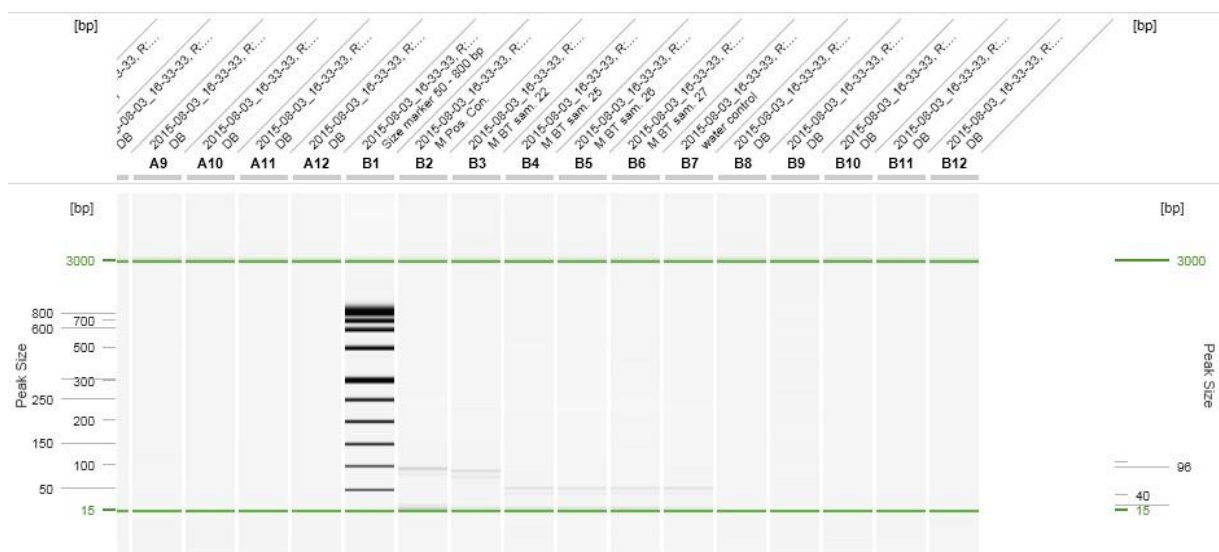


Figure 64: MSP results of MPM samples using primers 793 and 794. Positive control in B2 and sample 22 in B3 shows bands around 100 bp and an unspecific band around 80 bp. Sample 25 in B4, sample 26 in B5, sample 27 in B6 and water control have two unspecific bands around 50 bp. Modified using QIAxcel ScreenGel 1.4.0 to manually adjust alignment markers.



Figure 65: Unmodified version of figure 64 in close up. From left to right wells B1-B12. Shifted bands can be seen in the figure.



Figure 66: UMSP (A2-A5) using primers 791 & 792 and MSP (A5- A7) results using primers 793 & 794 of MPM sample 27. Positive control of UMSP shows a band at 100 bp and another one around 160 bp. Sample 27 in A3 shows no bands but has an unspecific band along with the water control. MSP positive control in A5 shows a band at 100 bp along with the sample 27 in A6. Water control in A7 shows also an unspecific band like A3 and A4.



Figure 67: Close up of figure 66. From left to right wells A1-A12.

## 5.2. Results of Pyrosequencing from DNA samples

In this part the Pyrosequencing results of the patient samples will be discussed. The promoter region of *pri-miR-145* has 2 DNA CpG islands. From CpG island 1s 3 methylation sites were analysed, whereas from island 2 five methylation sites were tested which were a small part of both islands. Each samples were BT treated and afterwards amplified using PCR with primers 808 & 809 or 811 & 812 depending on the island number. The PCR products were checked on the gel to make sure there was enough DNA to make Pyrosequencing, however these PCR pictures will not be discussed since they do not provide any data that is relevant for determining the methylation status of the promoter region of *pri-miR-145*.

Sam. Num.	Patient matched pair?	Type	Isl 1-1 (%)	Isl 1-2 (%)	Isl 1-3 (%)	Ava. meth.	Peak height. (SN)- Low ava.
#3	Yes	N	57,0	100,0	100,0	85,7	5,0
#4	Yes	T	24,0	42,0	40,0	35,3	40,0
#5	No	T	54,0	100,0	100,0	84,7	25,0
#6	Yes	T					
#7	Yes	N	61,0	100,0	100,0	87,0	15,0
#8	No	T	70,0	100,0	100,0	90,0	30,0
#9	No	T	38,0	57,0	67,0	54,0	15,0
#10	No	N	26,0	12,0	46,0	28,0	50,0
#11	Yes	T	51,0	100,0	100,0	83,7	25,0
#12	Yes	N	70,0	100,0	100,0	90,0	40,0
#13	No	T	52,0	100,0	100,0	84,0	30,0
#14	No	T	92,0	100,0	100,0	97,3	50,0
#15	No	T	50,0	100,0	100,0	83,3	20,0
#16	No	T	84,0	100,0	100,0	94,7	23,0
#17	No	T	3,0	94,0	100,0	65,7	25,0
#18	Yes	T	71,0	74,0	59,0	68,0	40,0
#19	Yes	N	97,0	100,0	100,0	99,0	50,0
#20	No	T					
#21	No	T	61,0	92,0	97,0	83,3	25,0
#22	Yes	T	79,0	100,0	100,0	93,0	22,0
#23	Yes	N	4,0	4,0	4,0	4,0	25,0
#24	No	N	98,0	99,0	100,0	99,0	100,0
#25	Same sample as above	N					
#26	Yes	T	88,0	100,0	100,0	96,0	22,0
#27	Yes	N	98,0	99,0	99,0	99,0	25,0
#28	Yes	T	28,0	79,0	83,0	63,3	25,0
#29	Yes	N	5,0	52,0	62,0	39,7	10,0

#30	No	T	44,0	79,0	75,0	66,0	40,0
#31	Yes	N	31,0	44,0	59,0	44,7	50,0
#32	Yes	T	69,0	100,0	100,0	89,7	20,0
#33	No	T	13,0	62,0	71,0	48,7	10,0
#34	No	T	24,0	49,0	58,0	43,7	10,0
#35	No	T	2,0	3,0	3,0	2,7	25,0
#36	No	T	45,0	74,0	97,0	72,0	11,0
#37	Yes	N	0,0	97,0	100,0	65,7	15,0
#38	Yes	T	44,0	58,0	72,0	58,0	10,0
#39	No	T	6,0	94,0	100,0	66,7	10,0
#40	No	T	47,0	75,0	95,0	72,3	10,0

Table 13: Methylation status of all 3 methylation sites from the CpG Island 1 of pri-miR-145 promoter region. Sam. Num. = sample number, Isl 1-1, -2, -3 (%) = methylation of CpG Island 1 site 1, 2 and 3 in percentage, Ava. meth. = average methylation of all sites, peak height. (SN)- Low ava. = Average lowest peak height for the single nucleotide, which shows the quality of Pyrosequencing. If the single nucleotide peak height is lower than 20 it shows a low quality Pyrosequencing.

Sam. Num.	Patient matched pair?	Type	Isl 2-1 (%)	Isl 2-2 (%)	Isl 2-3 (%)	Isl 2-4 (%)	Isl 2-5 (%)	Ava. Meth.	Peak height. (SN)- Low ava.
#3	Yes	N	75,0	90,0	82,0	100,0	78,0	85,0	10
#4	Yes	T	41,0	59,0	57,0	68,0	53,0	55,6	50
#5	No	T	75,0	90,0	88,0	100,0	72,0	85,0	15
#6	Yes	T							
#7	Yes	N	97,0	99,0	97,0	100,0	93,0	97,2	55
#8	No	T	87,0	94,0	94,0	100,0	88,0	92,6	25
#9	No	T	42,0	65,0	66,0	74,0	55,0	60,4	10
#10	No	N	42,0	65,0	61,0	73,0	46,0	57,4	22
#11	Yes	T	56,0	79,0	77,0	86,0	65,0	72,6	25
#12	Yes	N	44,0	72,0	74,0	90,0	58,0	67,6	50
#13	No	T	70,0	90,0	91,0	100,0	85,0	87,2	25
#14	No	T	67,0	87,0	89,0	100,0	81,0	84,8	10
#15	No	T	89,0	95,0	95,0	100,0	91,0	94,0	10
#16	No	T	84,0	94,0	96,0	100,0	90,0	92,8	10
#17	No	T	80,0	81,0	79,0	85,0	75,0	80,0	25
#18	Yes	T	66,0	89,0	87,0	94,0	72,0	81,6	25
#19	Yes	N	53,0	30,0	25,0	33,0	29,0	34,0	75
#20	No	T	1,0	2,0	93,0	100,0	8,0	40,8	25
#21	No	T	16,0	73,0	72,0	100,0	86,0	69,4	10
#22	Yes	T	73,0	83,0	85,0	100,0	75,0	83,2	22
#23	Yes	N	71,0	84,0	90,0	100,0	92,0	87,4	10
#24	No	N	92,0	88,0	94,0	100,0	93,0	93,4	9

#25	Same sam- ple as above	N							
#26	Yes	T	3,0	4,0	5,0	3,0	4,0	3,8	22
#27	Yes	N	2,0	92,0	97,0	100,0	88,0	75,8	20
#28	Yes	T	57,0	75,0	84,0	100,0	71,0	77,4	40
#29	Yes	N	60,0	80,0	77,0	100,0	61,0	75,6	22
#30	No	T	0,0	86,0	79,0	100,0	62,0	65,4	40
#31	Yes	N	72,0	86,0	73,0	100,0	85,0	83,2	10
#32	Yes	T	69,0	84,0	84,0	100,0	73,0	82,0	25
#33	No	T	80,0	96,0	92,0	100,0	88,0	91,2	15
#34	No	T	67,0	82,0	82,0	100,0	71,0	80,4	20
#35	No	T	46,0	47,0	45,0	45,0	40,0	44,6	40
#36	No	T	60,0	99,0	84,0	100,0	54,0	79,4	23
#37	Yes	N	60,0	64,0	81,0	100,0	90,0	79,0	15
#38	Yes	T	67,0	83,0	79,0	96,0	69,0	78,8	7
#39	No	T	83,0	82,0	78,0	85,0	72,0	80,0	22
#40	No	T	61,0	77,0	73,0	98,0	62,0	74,2	5

Table 14: Methylation status of all 5 methylation sites from the CpG Island 2 of pri-miR-145 promoter region. Sam. Num. = sample number, Isl 2-1, -2, -3, -4, -5 (%) = methylation of CpG Island 1 site 1, 2, 3, 4 and 5 in percentage, Ava. meth. = average methylation of all sites, peak height. (SN)- Low ava. = Average lowest peak height for the single nucleotide, which shows the quality of Pyrosequencing. If the single nucleotide peak height is lower than 20 it shows a low quality Pyrosequencing.

Sam. Num.	Patient matched pair?	Type	Isl 1 Ava. Meth. (%)	Isl 2 Ava. Meth. (%)	Both Isl. Ava. Meth. (%)
#3	Yes	N	85,7	85	85,3
#4	Yes	T	35,3	55,6	45,5
#5	No	T	84,7	85	84,8
#6	Yes	T			
#7	Yes	N	87,0	97,2	92,1
#8	No	T	90,0	92,6	91,3
#9	No	T	54,0	60,4	57,2
#10	No	N	28,0	57,4	42,7
#11	Yes	T	83,7	72,6	78,1
#12	Yes	N	90,0	67,6	78,8
#13	No	T	84,0	87,2	85,6
#14	No	T	97,3	84,8	91,1
#15	No	T	83,3	94	88,7
#16	No	T	94,7	92,8	93,7
#17	No	T	65,7	80	72,8
#18	Yes	T	68,0	81,6	74,8
#19	Yes	N	99,0	34	66,5

#20	No	T		40,8	40,8
#21	No	T	83,3	69,4	76,4
#22	Yes	T	93,0	83,2	88,1
#23	Yes	N	4,0	87,4	45,7
#24	No	N	99,0	93,4	96,2
#25	Same sam- ple as above	N			
#26	Yes	T	96,0	3,8	49,9
#27	Yes	N	99,0	75,8	87,4
#28	Yes	T	63,3	77,4	70,4
#29	Yes	N	39,7	75,6	57,6
#30	No	T	66,0	65,4	65,7
#31	Yes	N	44,7	83,2	63,9
#32	Yes	T	89,7	82	85,8
#33	No	T	48,7	91,2	69,9
#34	No	T	43,7	80,4	62,0
#35	No	T	2,7	44,6	23,6
#36	No	T	72,0	79,4	75,7
#37	Yes	N	65,7	79	72,3
#38	Yes	T	58,0	78,8	68,4
#39	No	T	66,7	80	73,3
#40	No	T	72,3	74,2	73,3

Table 15: Methylation status of all methylation sites from the CpG Island 1 and CpG Island 2 of pri-miR-145 promoter region. Sam. Num. = sample number, Isl 1 Ava. Meth. (%) = Average Methylation of CpG Island 1 of pri-miR-145 promoter region, Isl 2 Ava. Meth. (%) = Average Methylation of CpG Island 2 of pri-miR-145 promoter region, Both Isl. Ava. Meth. (%) = Average Methylation of CpG Island 1 and 2 of pri-miR-145 promoter region.

Now results of the each sample will be given with the graph taken from PyroMark Q24 software along with control samples. Water control gives no signal therefore it does not have a graph shown here.

**Positive Control for CpG Island 1 and Island 2 of pri-miR-145 promotor region:**

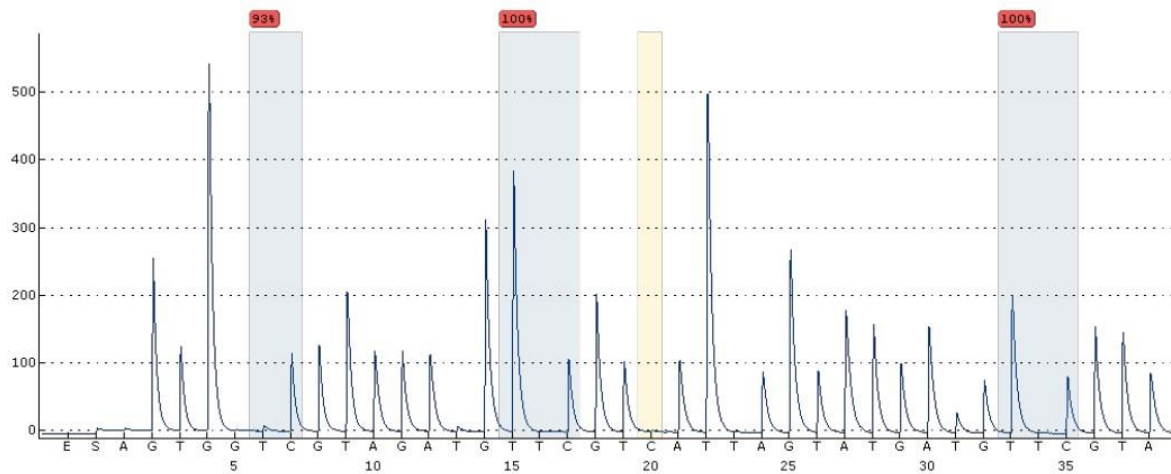


Figure 68: Pyrosequencing graph of CpG Island 1 from bisulfite converted fully methylated human DNA. Methylation sites are marked blue. The amount of methylation is indicated above each methylation site. At dispensation 20 the bisulfite conversion worked as expected that is marked in yellow. From left to right- Site 1: 93%, Site 2: 100%, Site 3: 100%, Average: 97,6% Methylation.

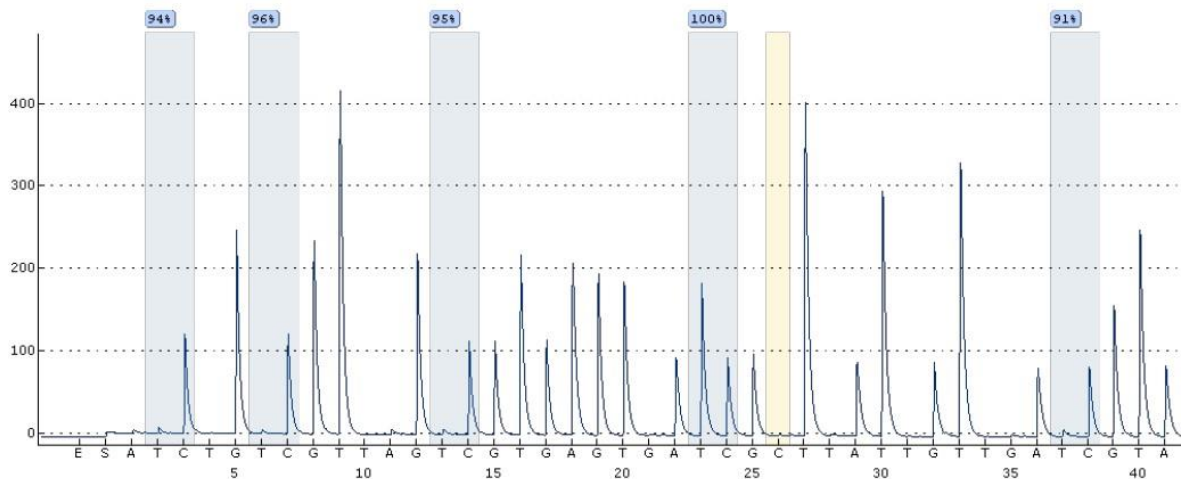


Figure 69: Pyrosequencing graph of CpG Island 2 from bisulfite converted fully methylated human DNA. Methylation sites are marked blue. The amount of methylation is indicated above each methylation site. At dispensation 26 the bisulfite conversion worked as expected that is marked in yellow. From left to right- Site 1: 94%, Site 2: 96%, Site 3: 95%, Site 4: 100%, Site 5: 91%, Average: 95,2% Methylation.

**Sample 3:**

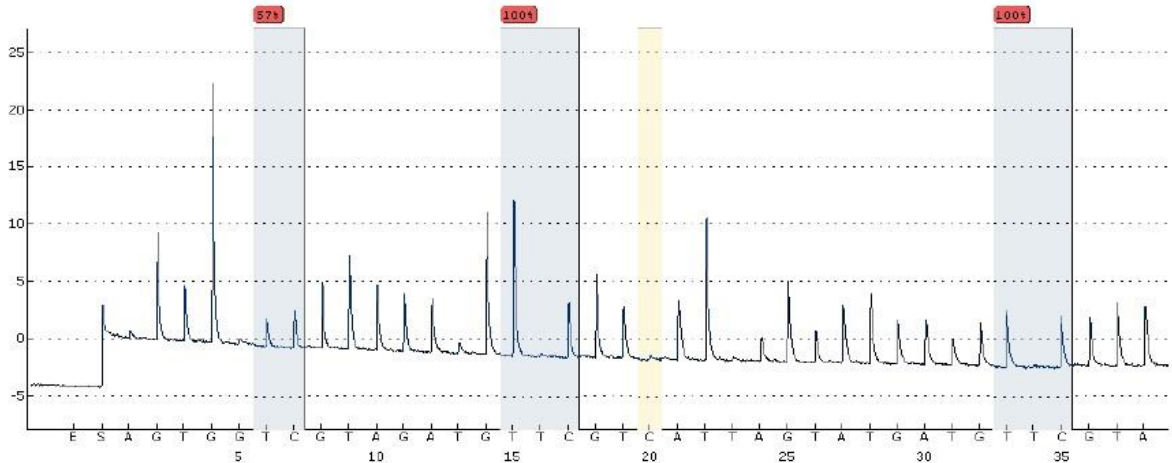


Figure 70: Pyrosequencing graph of CpG Island 1 from pri-miR-145 promoter region of MPM sample #3. Methylation sites are marked blue. The amount of methylation is indicated above each methylation site. At dispensation 20 the bisulfide conversion failed that is marked in yellow. The graph also shows a baseline drift along with low peak heights. This indicates that the quality of this pyrosequencing was poor. From left to right- Site 1: 57%, Site 2: 100%, Site 3: 100%, Average: 85,7% Methylation.

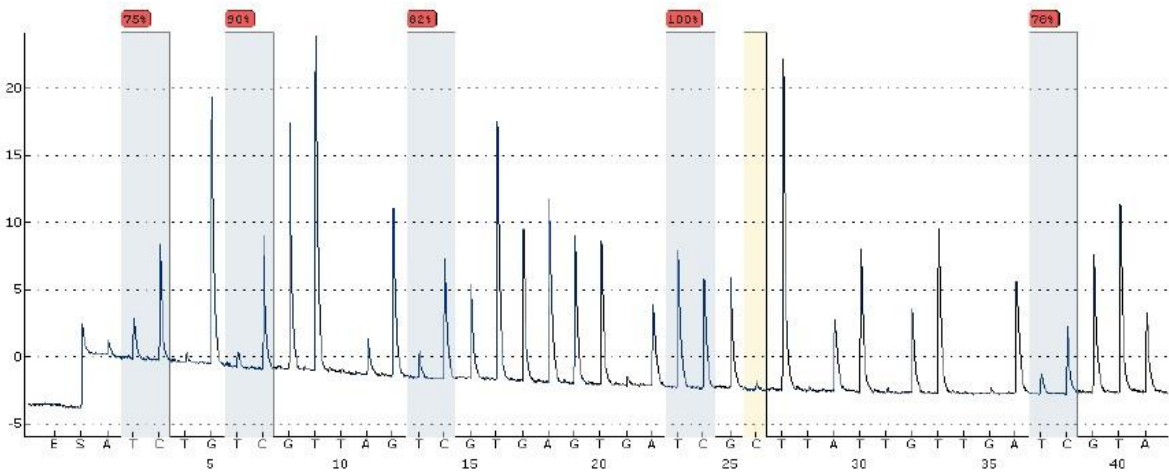
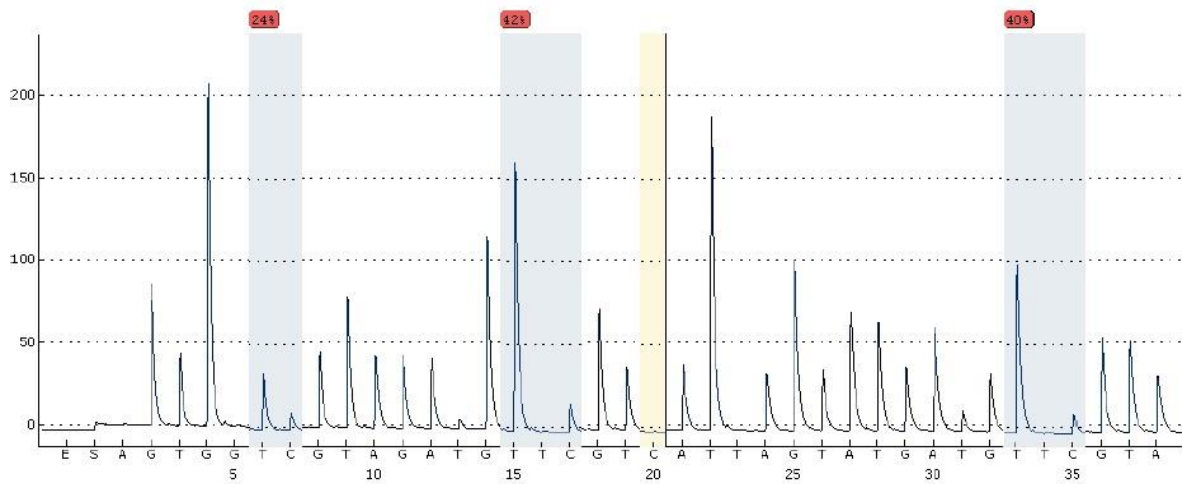
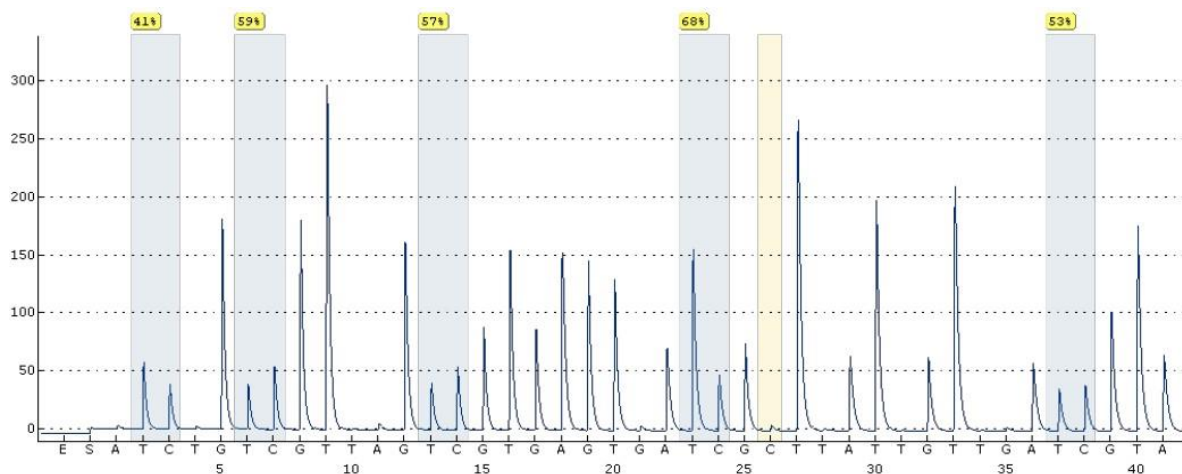


Figure 71: Pyrosequencing graph of CpG Island 2 from pri-miR-145 promoter region of MPM sample #3. Methylation sites are marked blue. The amount of methylation is indicated above each methylation site. At dispensation 26 the bisulfide conversion failed, which is marked in yellow. The graph also shows a baseline drift along with low peak heights. This indicates that the quality of this pyrosequencing was poor. From left to right- Site 1: 75%, Site 2: 90%, Site 3: 82 %, Site 4: 100%, Site 5: 78%, Average: 85% Methylation.

**Sample 4:**



*Figure 72: Pyrosequencing graph of CpG Island 1 from pri-miR-145 promoter region of MPM sample #4. Methylation sites are marked blue. The amount of methylation is indicated above each methylation site. At dispensation 20 the bisulfide conversion worked as expected that is marked in yellow. From left to right- Site 1: 24%, Site 2: 42%, Site 3: 40%, Average: 35,3% Methylation.*



*Figure 73: Pyrosequencing graph of CpG Island 2 from pri-miR-145 promoter region of MPM sample #4. Methylation sites are marked blue. The amount of methylation is indicated above each methylation site. At dispensation 26 the bisulfide conversion is uncertain that is marked in yellow. From left to right- Site 1: 41%, Site 2: 59%, Site 3: 57%, Site 4: 68%, Site 5: 53%, Average: 55,6% Methylation.*

**Sample 5:**

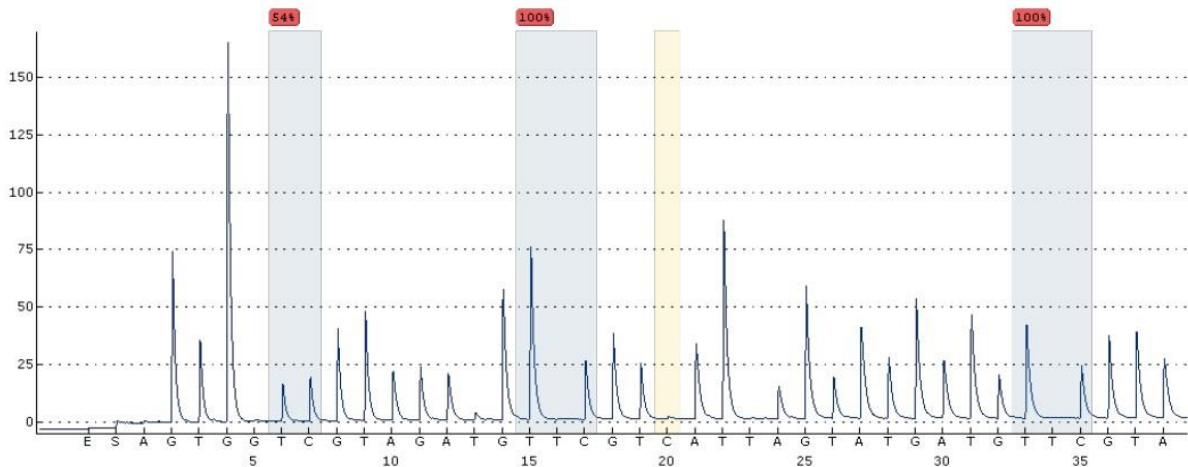


Figure 74: Pyrosequencing graph of CpG Island 1 from pri-miR-145 promoter region of MPM sample #5. Methylation sites are marked blue. The amount of methylation is indicated above each methylation site. At dispensation 20 the bisulfide conversion worked as expected that is marked in yellow. From left to right- Site 1: 54%, Site 2: 100%, Site 3: 100%, Average: 84,7% Methylation.

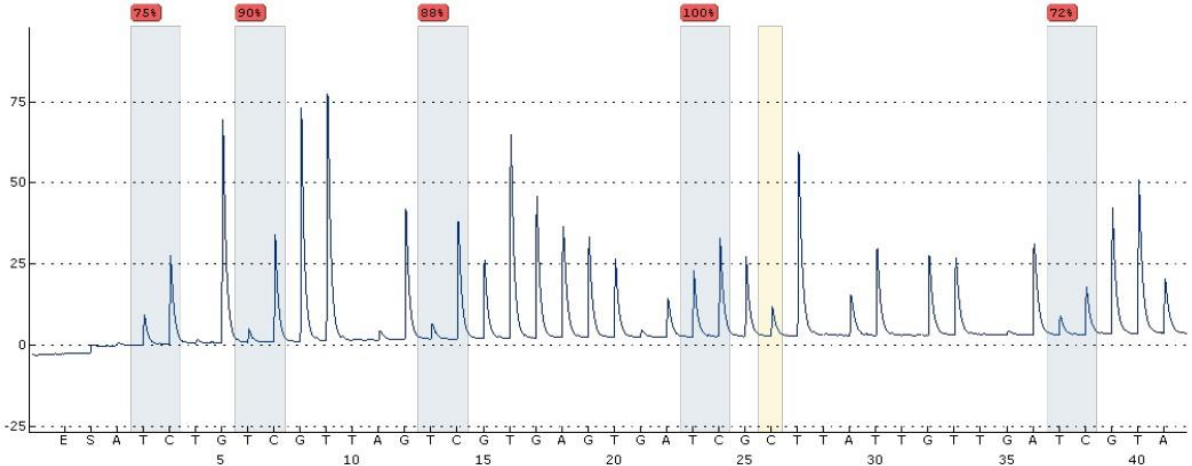


Figure 75: Pyrosequencing graph of CpG Island 2 from pri-miR-145 promoter region of MPM sample #5. Methylation sites are marked blue. The amount of methylation is indicated above each methylation site. At dispensation 26 the bisulfide conversion failed that is marked in yellow. From left to right- Site 1: 75%, Site 2: 90%, Site 3: 88%, Site 4: 100%, Site 5: 72%, Average: 85% Methylation.

## Sample 6: No DNA

## Sample 7:

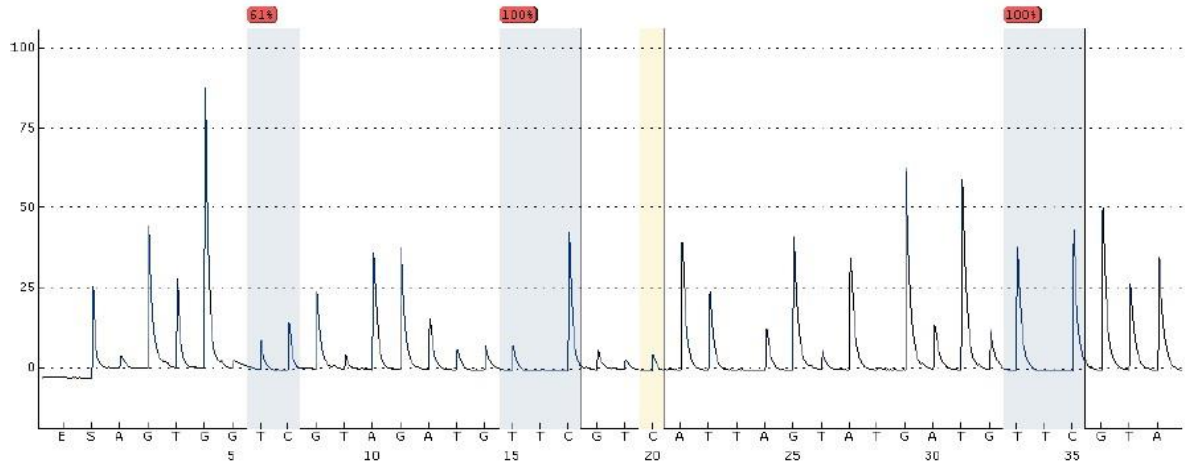


Figure 76: Pyrosequencing graph of CpG Island 1 from pri-miR-145 promoter region of MPM sample #7. Methylation sites are marked blue. The amount of methylation is indicated above each methylation site. At dispensation 20 the bisulfide conversion failed that is marked in yellow. The graph also shows low peak heights. This indicates that the quality of this pyrosequencing was poor. From left to right- Site 1: 61%, Site 2: 100%, Site 3: 100%, Average: 87% Methylation.

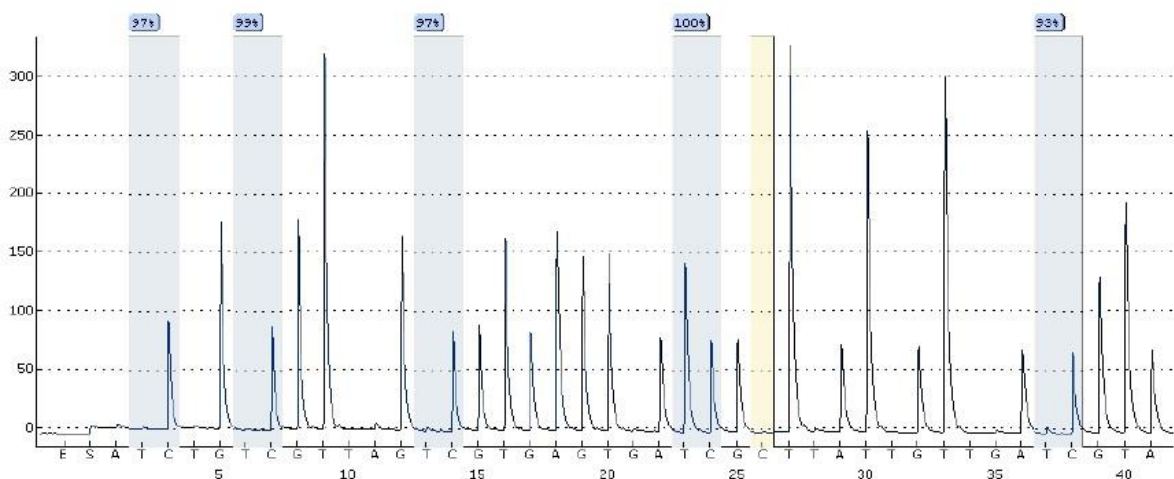


Figure 77: Pyrosequencing graph of CpG Island 2 from pri-miR-145 promoter region of MPM sample #7. Methylation sites are marked blue. The amount of methylation is indicated above each methylation site. At dispensation 26 the bisulfide conversion worked as expected that is marked in yellow. From left to right- Site 1: 97%, Site 2: 99%, Site 3: 97%, Site 4: 100%, Site 5: 93%, Average: 97,2% Methylation.

**Sample 8:**

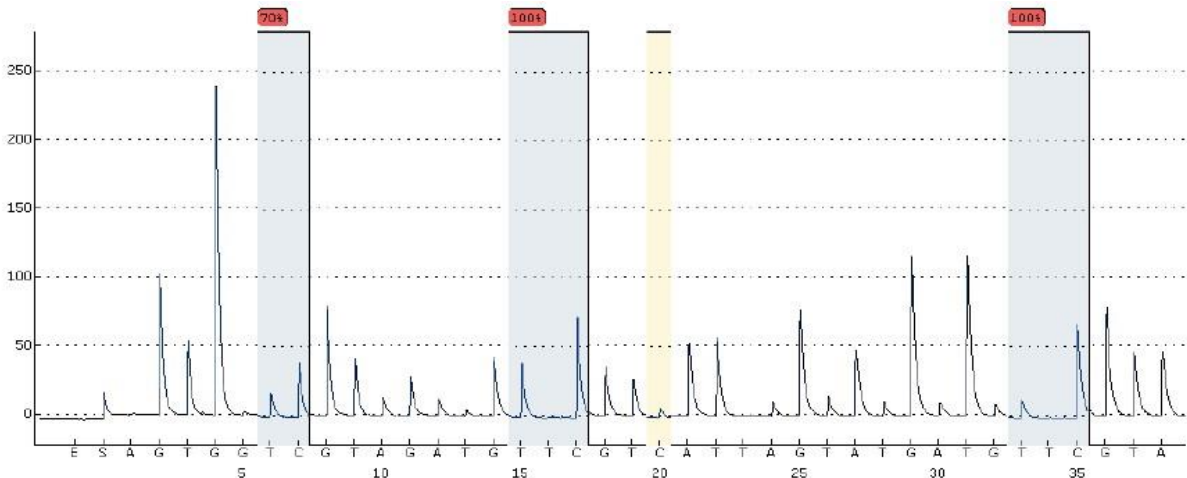


Figure 78: Pyrosequencing graph of CpG Island 1 from pri-miR-145 promoter region of MPM sample #8. Methylation sites are marked blue. The amount of methylation is indicated above each methylation site. At dispensation 20 the bisulfide conversion failed that is marked in yellow. From left to right- Site 1: 70%, Site 2: 100%, Site 3: 100%, Average: 90% Methylation.

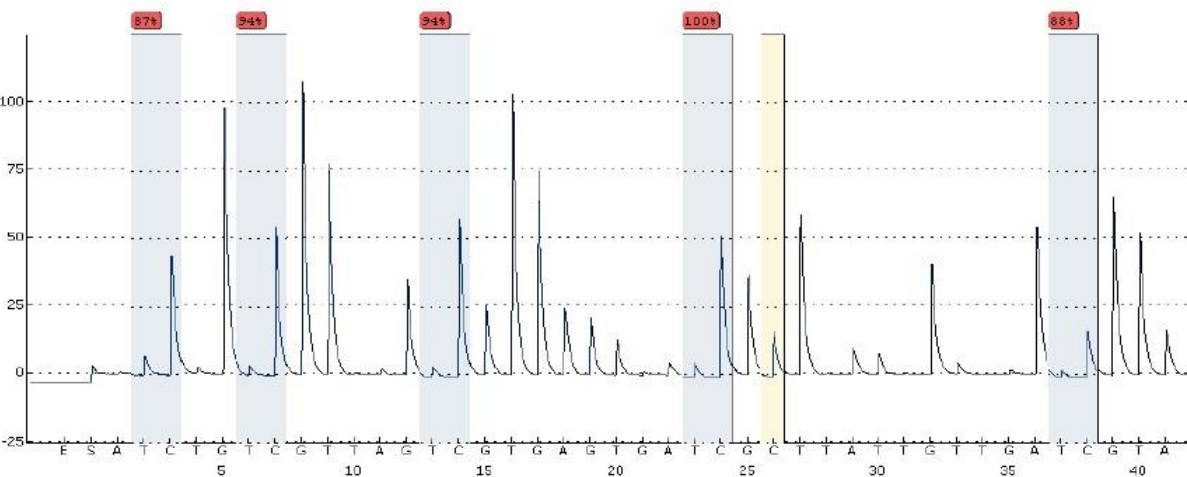


Figure 79: Pyrosequencing graph of CpG Island 2 from pri-miR-145 promoter region of MPM sample #8. Methylation sites are marked blue. The amount of methylation is indicated above each methylation site. At dispensation 26 the bisulfide conversion failed that is marked in yellow. From left to right- Site 1: 97%, Site 2: 99%, Site 3: 97%, Site 4: 100%, Site 5: 93%, Average: 92,6% Methylation.

## Sample 9:

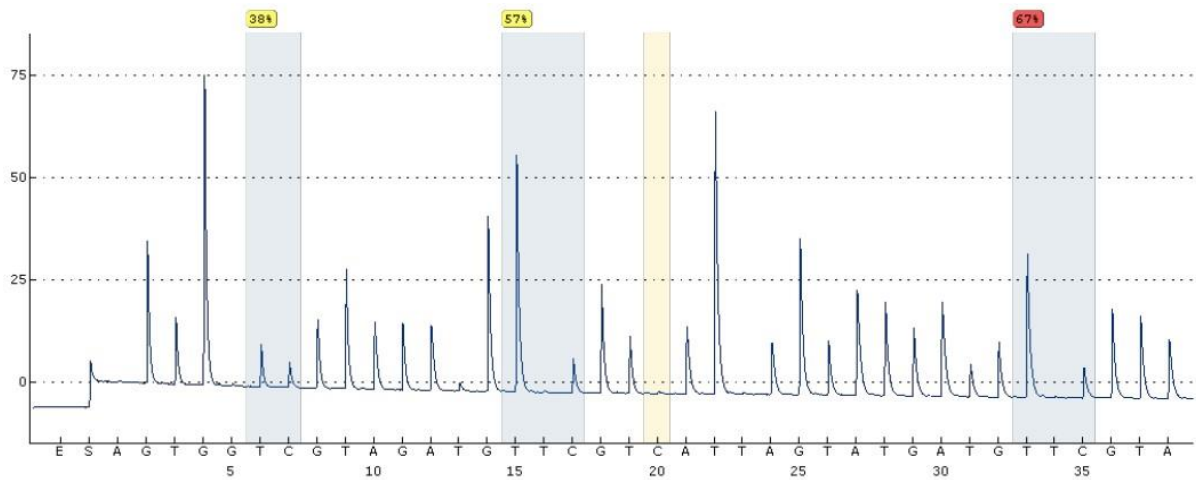


Figure 80: Pyrosequencing graph of CpG Island 1 from pri-miR-145 promoter region of MPM sample #9. Methylation sites are marked blue. The amount of methylation is indicated above each methylation site. At dispensation 20 the bisulfide conversion worked as expected that is marked in yellow. The graph also shows a baseline drift along with low peak heights. This indicates that the quality of this pyrosequencing was poor. From left to right- Site 1: 38%, Site 2: 57%, Site 3: 67%, Average: 54% Methylation.

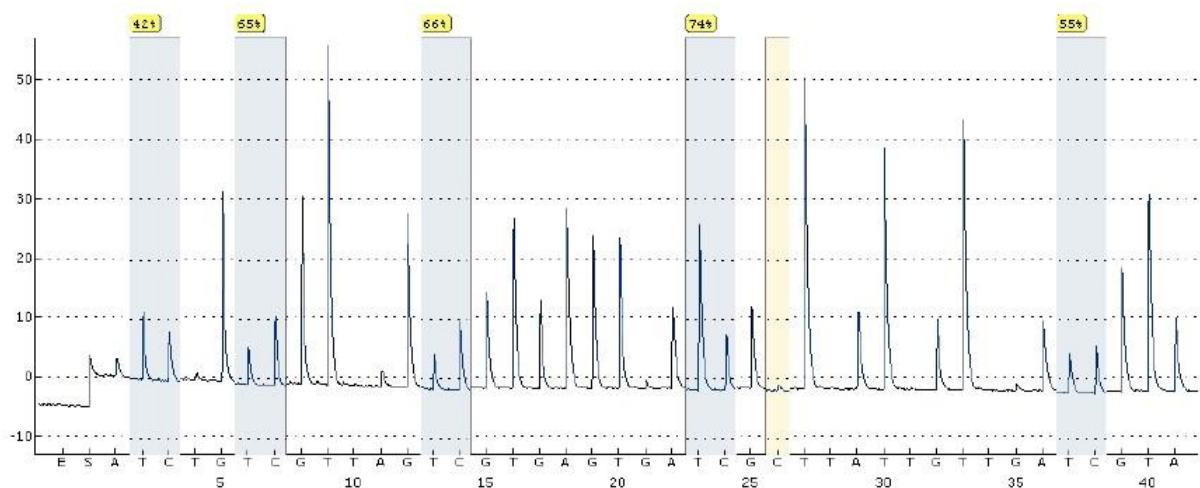


Figure 81: Pyrosequencing graph of CpG Island 2 from pri-miR-145 promoter region of MPM sample #9. Methylation sites are marked blue. The amount of methylation is indicated above each methylation site. At dispensation 26 the bisulfide conversion is uncertain that is marked in yellow. From left to right- Site 1: 42%, Site 2: 65%, Site 3: 66%, Site 4: 74%, Site 5: 55%, Average: 60,4% Methylation.

**Sample 10:**

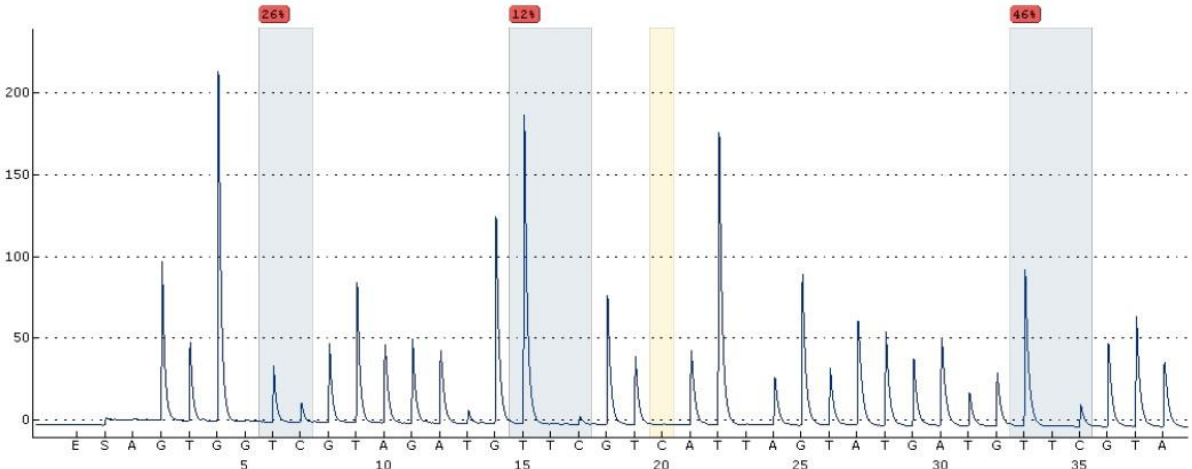


Figure 82: Pyrosequencing graph of CpG Island 1 from pri-miR-145 promoter region of MPM sample #10. Methylation sites are marked blue. The amount of methylation is indicated above each methylation site. At dispensation 20 the bisulfide conversion worked as expected that is marked in yellow. From left to right- Site 1: 26%, Site 2: 12%, Site 3: 46%, Average: 28% Methylation.

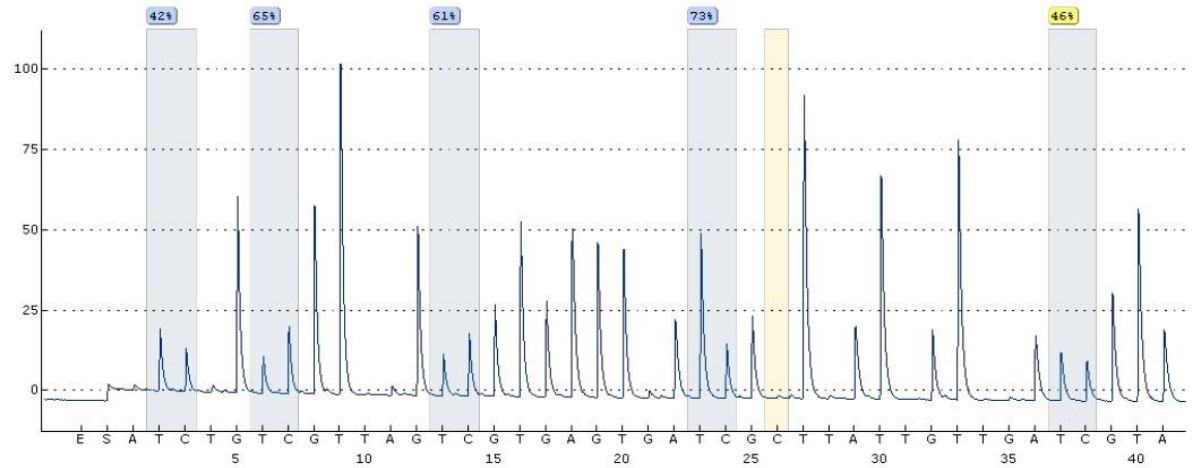
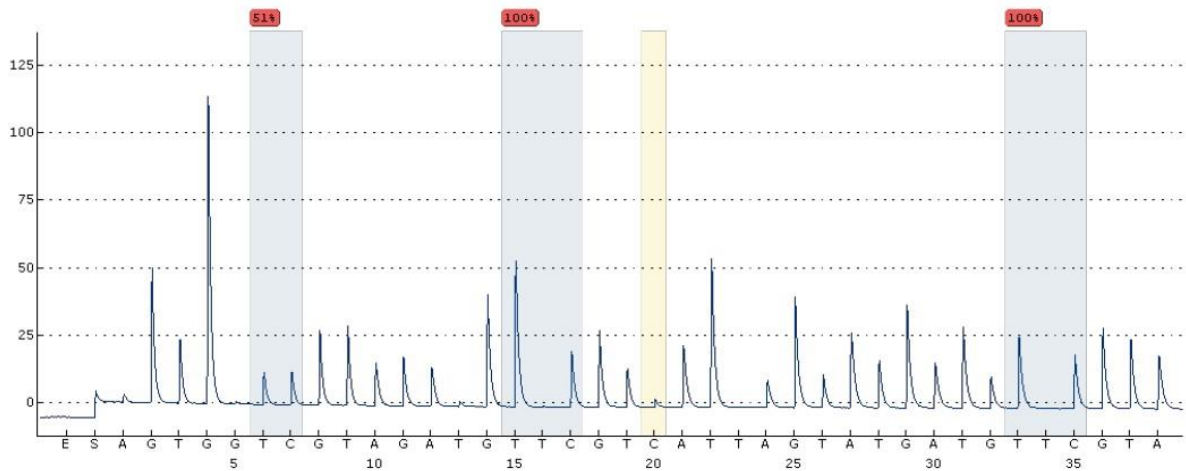
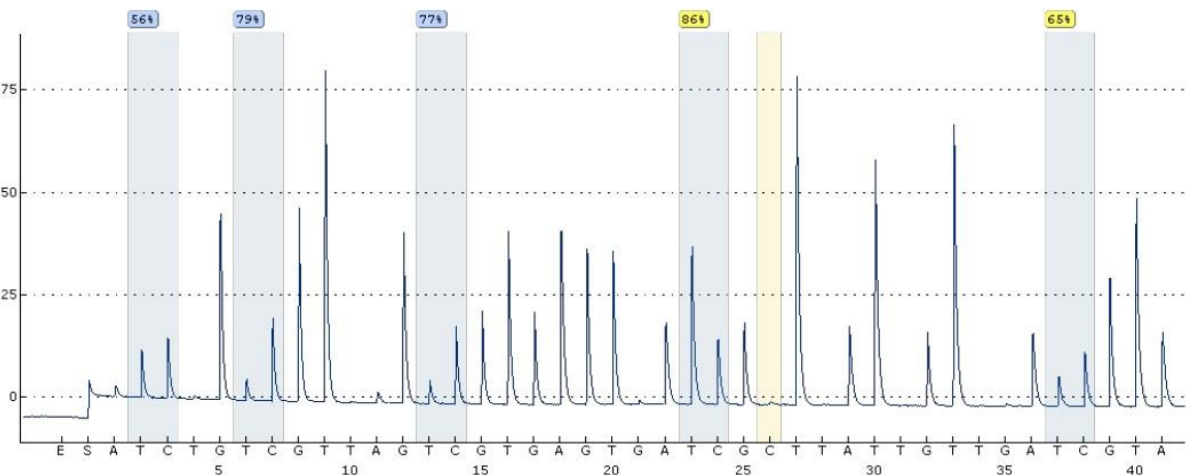


Figure 83: Pyrosequencing graph of CpG Island 2 from pri-miR-145 promoter region of MPM sample #10. Methylation sites are marked blue. The amount of methylation is indicated above each methylation site. At dispensation 26 the bisulfide conversion worked as expected that is marked in yellow. From left to right- Site 1: 42%, Site 2: 65%, Site 3: 61%, Site 4: 73%, Site 5: 46%, Average: 57,4% Methylation.

**Sample 11:**



*Figure 84: Pyrosequencing graph of CpG Island 1 from pri-miR-145 promoter region of MPM sample #11. Methylation sites are marked blue. The amount of methylation is indicated above each methylation site. At dispensation 20 the bisulfide conversion failed that is marked in yellow. From left to right- Site 1: 51%, Site 2: 100%, Site 3: 100%, Average: 83,7% Methylation.*



*Figure 85: Pyrosequencing graph of CpG Island 2 from pri-miR-145 promoter region of MPM sample #11. Methylation sites are marked blue. The amount of methylation is indicated above each methylation site. At dispensation 26 the bisulfide worked as expected that is marked in yellow. From left to right- Site 1: 56%, Site 2: 79%, Site 3: 77%, Site 4: 86%, Site 5: 65%, Average: 72,6% Methylation*

**Sample 12:**

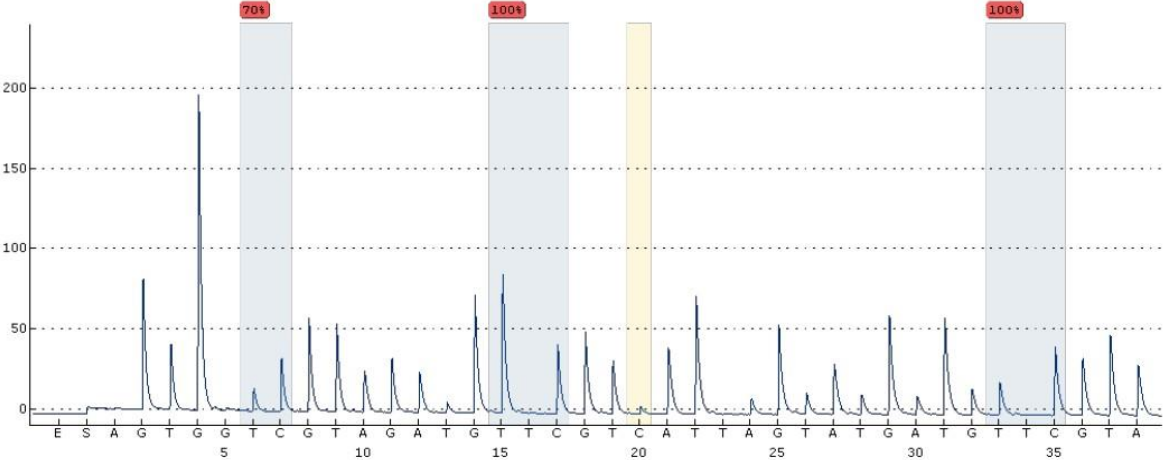


Figure 86: Pyrosequencing graph of CpG Island 1 from pri-miR-145 promoter region of MPM sample #12. Methylation sites are marked blue. The amount of methylation is indicated above each methylation site. At dispensation 20 the bisulfide conversion failed that is marked in yellow. From left to right- Site 1: 70%, Site 2: 100%, Site 3: 100 %, Average: 90% Methylation.

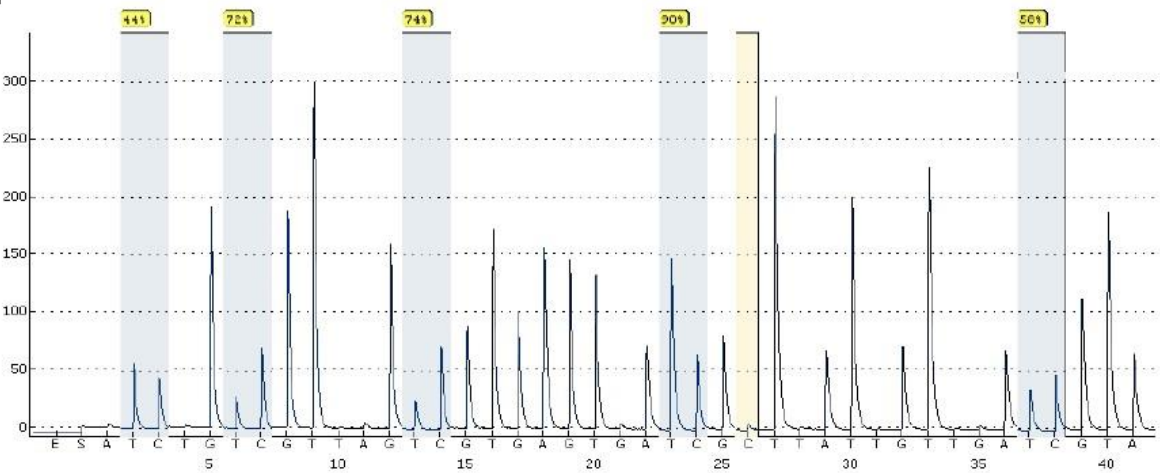


Figure 87: Pyrosequencing graph of CpG Island 2 from pri-miR-145 promoter region of MPM sample #12. Methylation sites are marked blue. The amount of methylation is indicated above each methylation site. At dispensation 26 the bisulfide conversion is uncertain that is marked in yellow. From left to right- Site 1: 44%, Site 2: 72%, Site 3: 74%, Site 4: 90%, Site 5: 58%, Average: 67,6% Methylation.

### Sample 13:

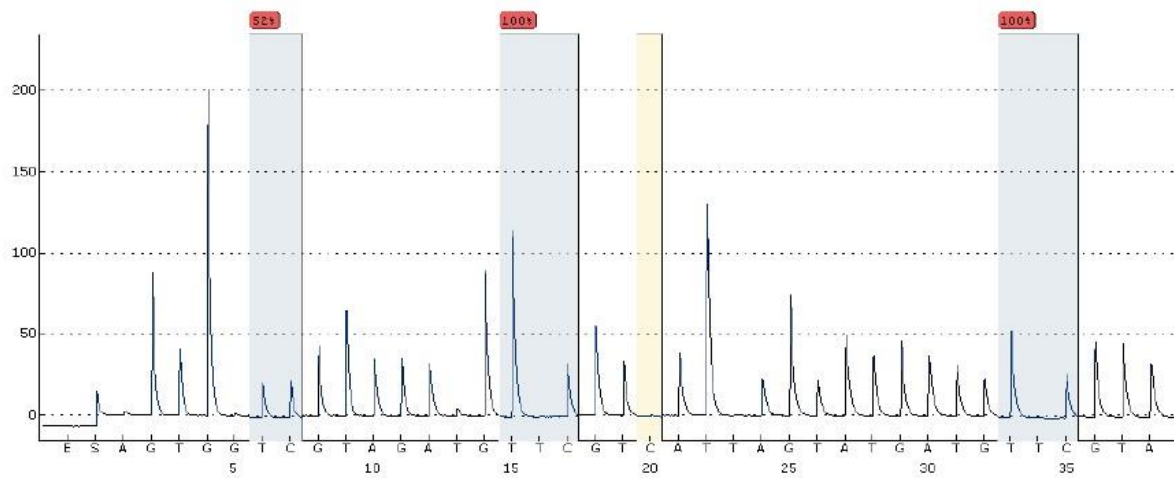


Figure 88: Pyrosequencing graph of CpG Island 1 from pri-miR-145 promoter region of MPM sample #13. Methylation sites are marked blue. The amount of methylation is indicated above each methylation site. At dispensation 20 the bisulfide conversion worked as expected that is marked in yellow. From left to right- Site 1: 52%, Site 2: 100%, Site 3: 100%, Average: 84% Methylation.

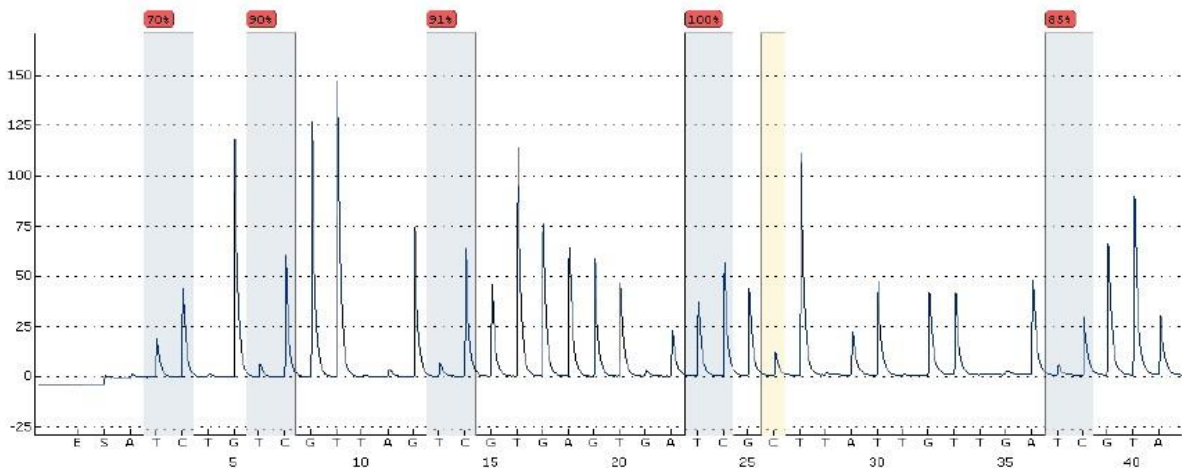


Figure 89: Pyrosequencing graph of CpG Island 2 from pri-miR-145 promoter region of MPM sample #13. Methylation sites are marked blue. The amount of methylation is indicated above each methylation site. At dispensation 26 the bisulfide conversion failed that is marked in yellow. From left to right- Site 1: 70%, Site 2: 90%, Site 3: 91%, Site 4: 100%, Site 5: 85%, Average: 87,2% Methylation.

**Sample 14:**

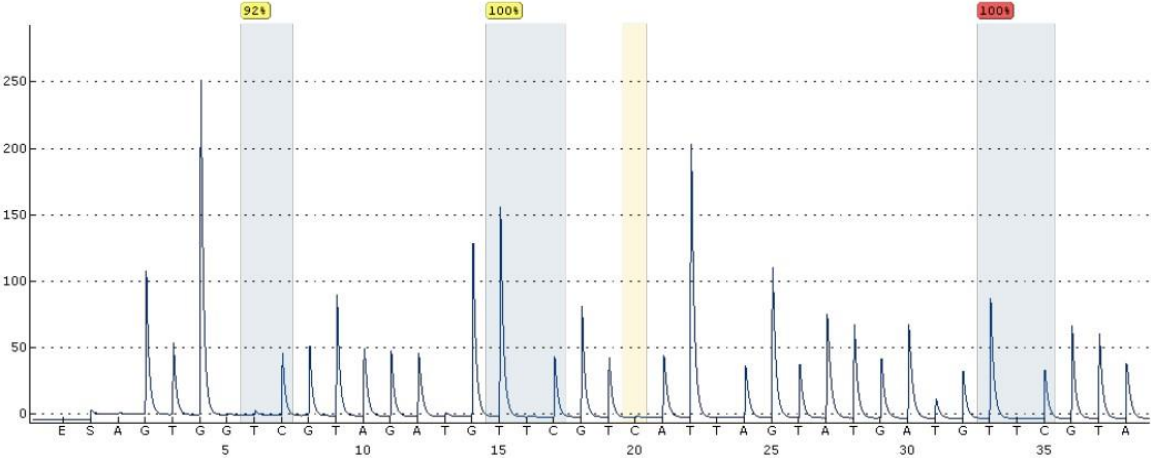


Figure 90: Pyrosequencing graph of CpG Island 1 from pri-miR-145 promoter region of MPM sample #14. Methylation sites are marked blue. The amount of methylation is indicated above each methylation site. At dispensation 20 the bisulfide conversion worked as expected that is marked in yellow. From left to right- Site 1: 92%, Site 2: 100%, Site 3: 100%, Average: 97,3% Methylation.

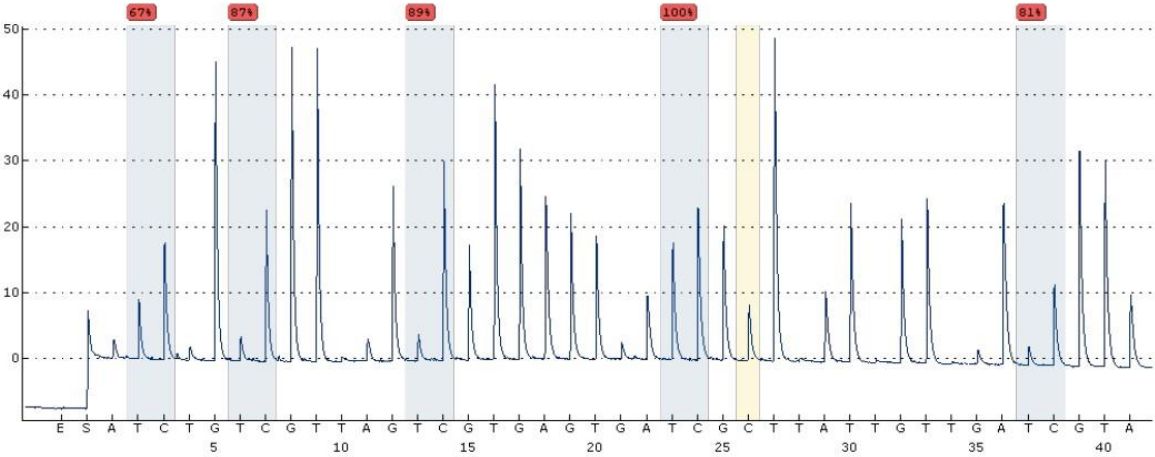
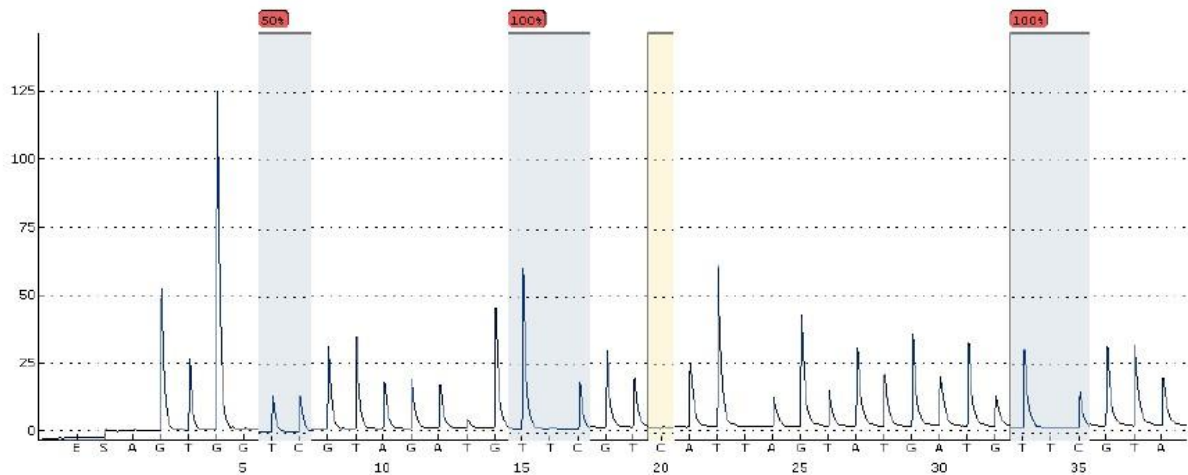
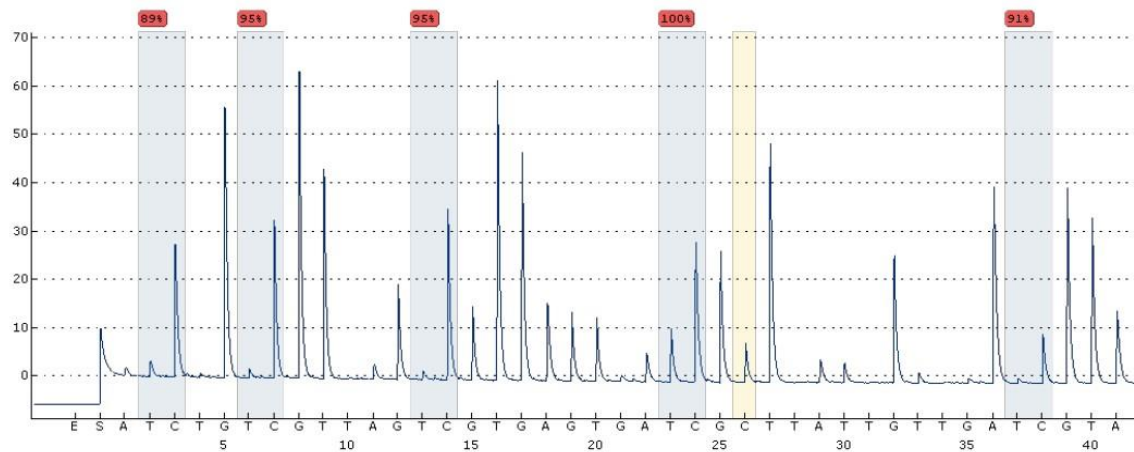


Figure 91: Pyrosequencing graph of CpG Island 2 from pri-miR-145 promoter region of MPM sample #14 Methylation sites are marked blue. The amount of methylation is indicated above each methylation site. At dispensation 26 the bisulfide conversion failed that it is marked in yellow. From left to right- Site 1: 67%, Site 2: 87%, Site 3: 89%, Site 4: 100%, Site 5: 81%, Average: 84,8% Methylation.

## Sample 15:



*Figure 92: Pyrosequencing graph of CpG Island 1 from pri-miR-145 promoter region of MPM sample #15. Methylation sites are marked blue. The amount of methylation is indicated above each methylation site. At dispensation 20 the bisulfide conversion is uncertain that is marked in yellow. From left to right- Site 1: 50%, Site 2: 100%, Site 3: 100%, Average: 83,3% Methylation.*



*Figure 93: Pyrosequencing graph of CpG Island 2 from pri-miR-145 promoter region of MPM sample #15. Methylation sites are marked blue. The amount of methylation is indicated above each methylation site. At dispensation 26 the bisulfide conversion failed that is marked in yellow. From left to right- Site 1: 89%, Site 2: 95%, Site 3: 95%, Site 4: 100%, Site 5: 91%, Average: 94% Methylation.*

**Sample 16:**

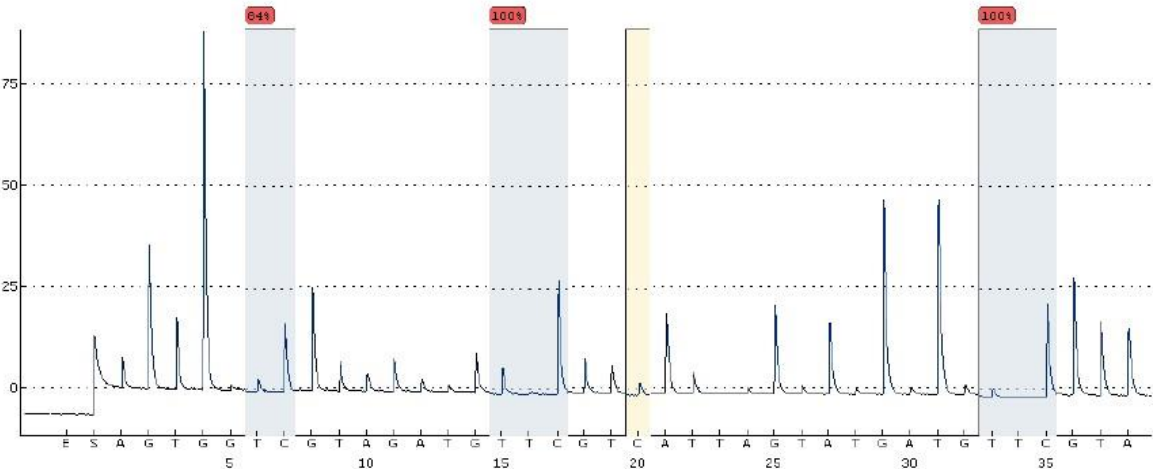


*Figure 94: Pyrosequencing graph of CpG Island 1 from pri-miR-145 promoter region of MPM sample #16. Methylation sites are marked blue. The amount of methylation is indicated above each methylation site. At dispensation 20 the bisulfide conversion failed that is marked in yellow. The graph also shows low peak heights. This indicates that the quality of this pyrosequencing was poor. From left to right- Site 1: 84%, Site 2: 100%, Site 3: 100%, Average: 94,7% Methylation.*

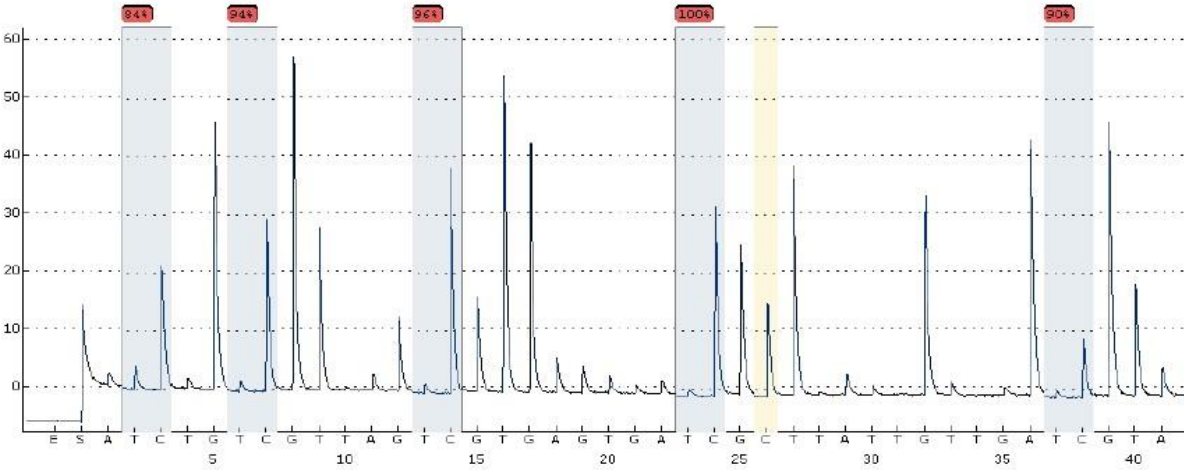


*Figure 95: Pyrosequencing graph of CpG Island 2 from pri-miR-145 promoter region of MPM sample #16. Methylation sites are marked blue. The amount of methylation is indicated above each methylation site. At dispensation 26 the bisulfide conversion failed that is marked in yellow. The graph also shows low peak heights. This indicates that the quality of this pyrosequencing was poor. From left to right- Site 1: 84%, Site 2: 94%, Site 3: 96%, Site 4: 100%, Site 5: 90%, Average: 92,8% Methylation.*

## Sample 17:

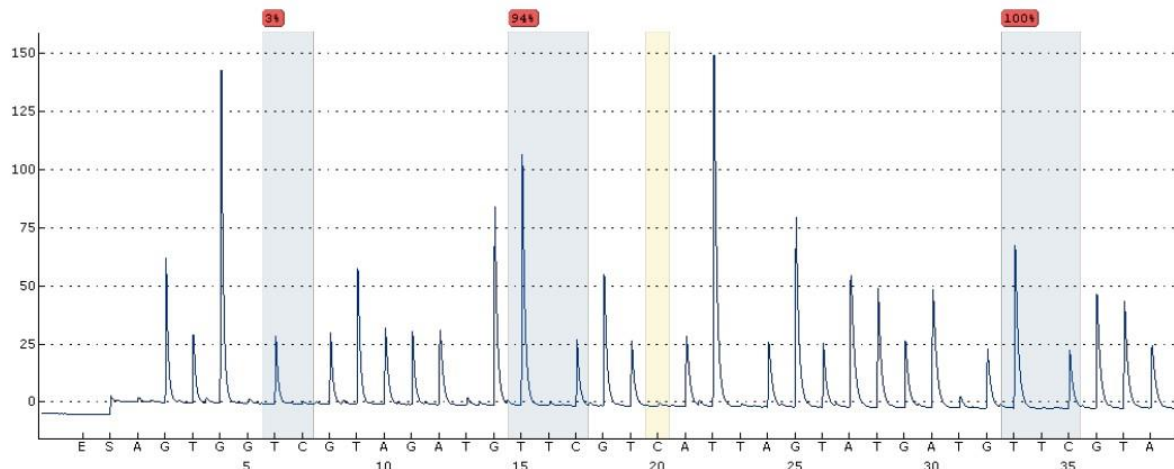


*Figure 96: Pyrosequencing graph of CpG Island 1 from pri-miR-145 promoter region of MPM sample #17. Methylation sites are marked blue. The amount of methylation is indicated above each methylation site. At dispensation 20 the bisulfide conversion worked as expected that is marked in yellow. From left to right- Site 1: 3%, Site 2: 94%, Site 3: 100%, Average: 65,7% Methylation.*

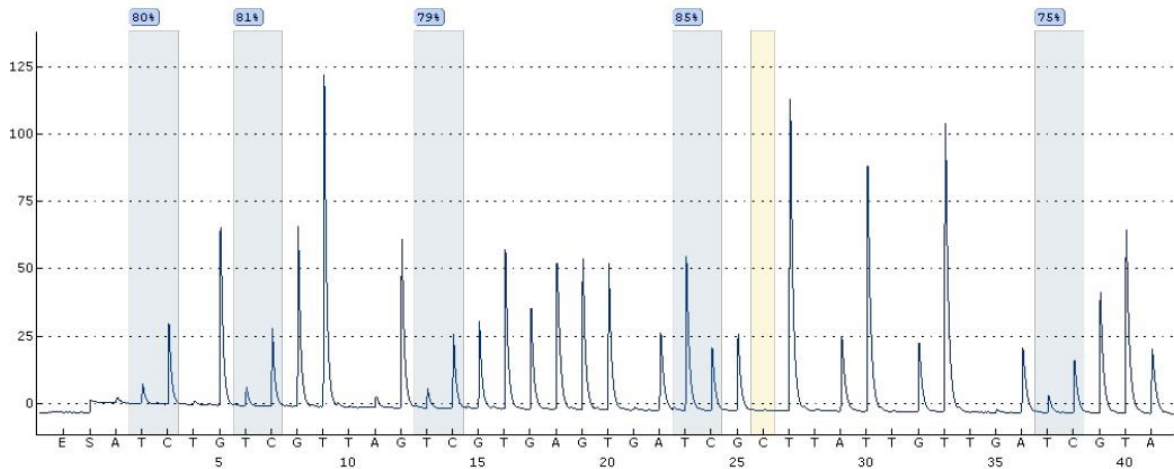


*Figure 97: Pyrosequencing graph of CpG Island 2 from pri-miR-145 promoter region of MPM sample #17. Methylation sites are marked blue. The amount of methylation is indicated above each methylation site. At dispensation 26 the bisulfide conversion worked as expected that is marked in yellow. From left to right- Site 1: 80%, Site 2: 81%, Site 3: 79%, Site 4: 85%, Site 5: 75%, Average: 80% Methylation.*

**Sample 18:**

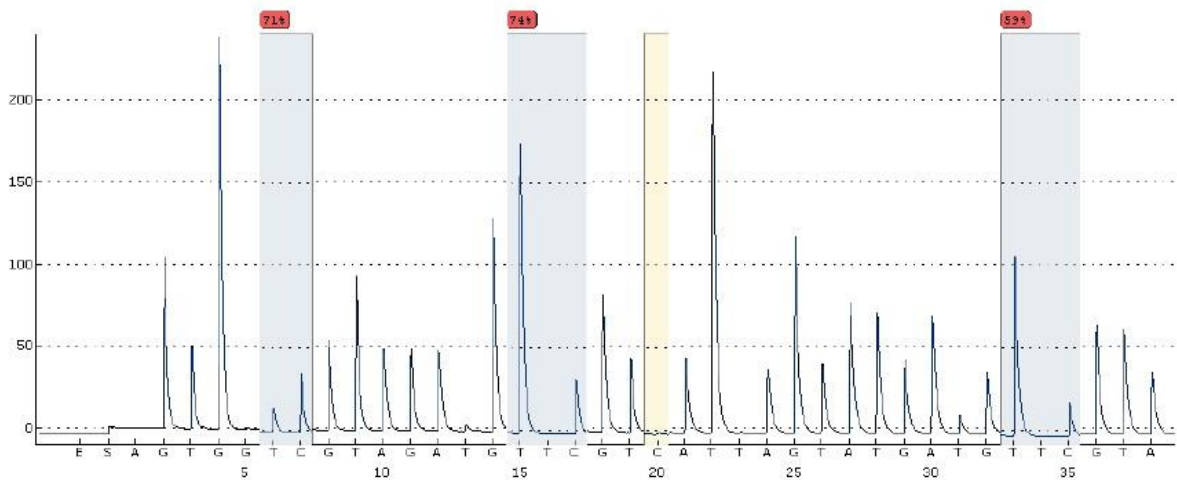


*Figure 98: Pyrosequencing graph of CpG Island 1 from pri-miR-145 promoter region of MPM sample #18. Methylation sites are marked blue. The amount of methylation is indicated above each methylation site. At dispensation 20 the bisulfide conversion worked as expected that is marked in yellow. From left to right- Site 1: 71%, Site 2: 74%, Site 3: 59%, Average: 68% Methylation.*

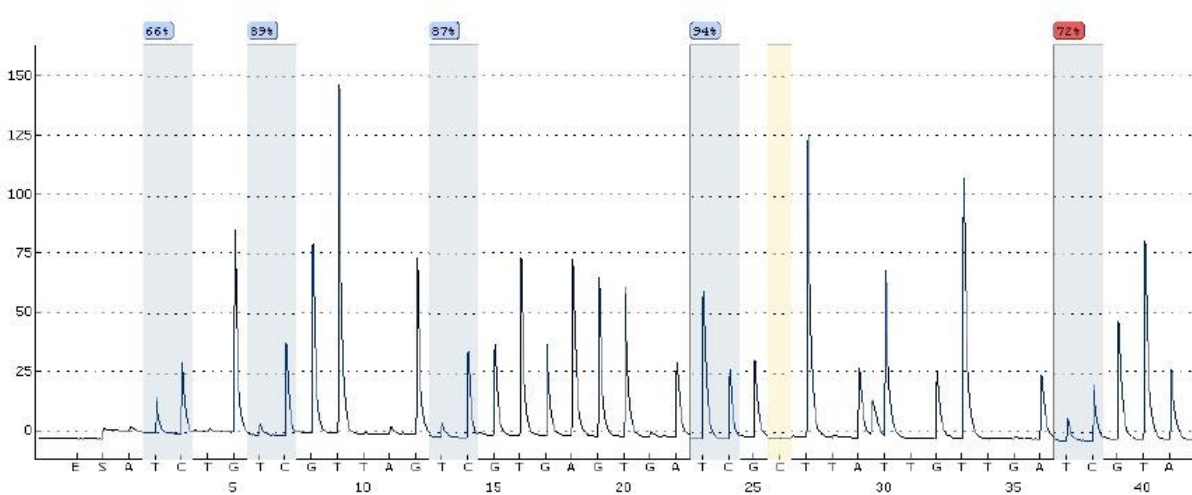


*Figure 99: Pyrosequencing graph of CpG Island 2 from pri-miR-145 promoter region of MPM sample #18. Methylation sites are marked blue. The amount of methylation is indicated above each methylation site. At dispensation 26 the bisulfite conversion worked as expected that is marked in yellow. From left to right- Site 1: 66%, Site 2: 89%, Site 3: 87%, Site 4: 94%, Site 5: 72%, Average: 81,6% Methylation.*

**Sample 19:**

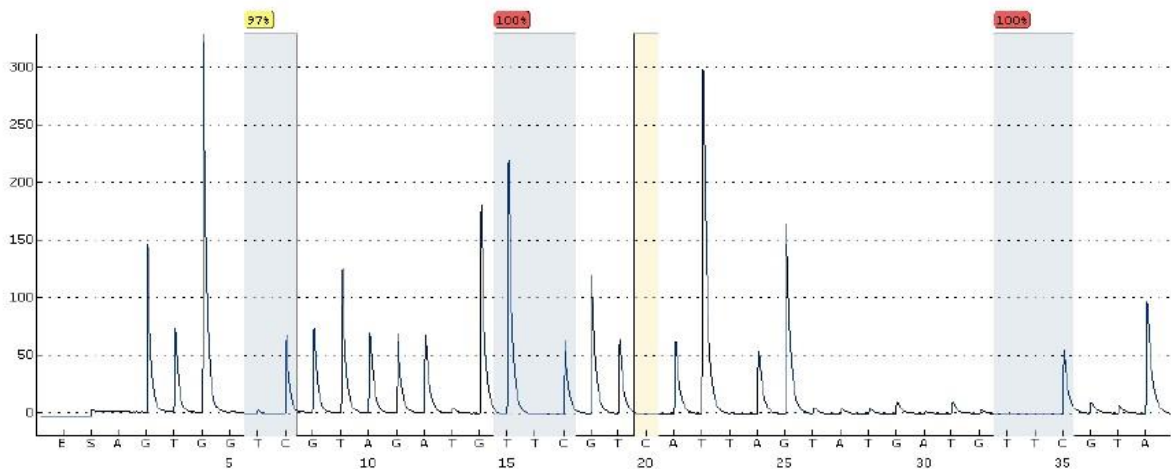


*Figure 100: Pyrosequencing graph of CpG Island 1 from pri-miR-145 promoter region of MPM sample #19. Methylation sites are marked blue. The amount of methylation is indicated above each methylation site. At dispensation 20 the bisulfide conversion worked as expected that is marked in yellow. Between nucleotides 25 – 35 there are no peaks visible, which indicates that the DNA sample was degraded or Pyrosequencing did not work. From left to right- Site 1: 97%, Site 2: 100%, Site 3: 100%, Average: 99% Methylation.*

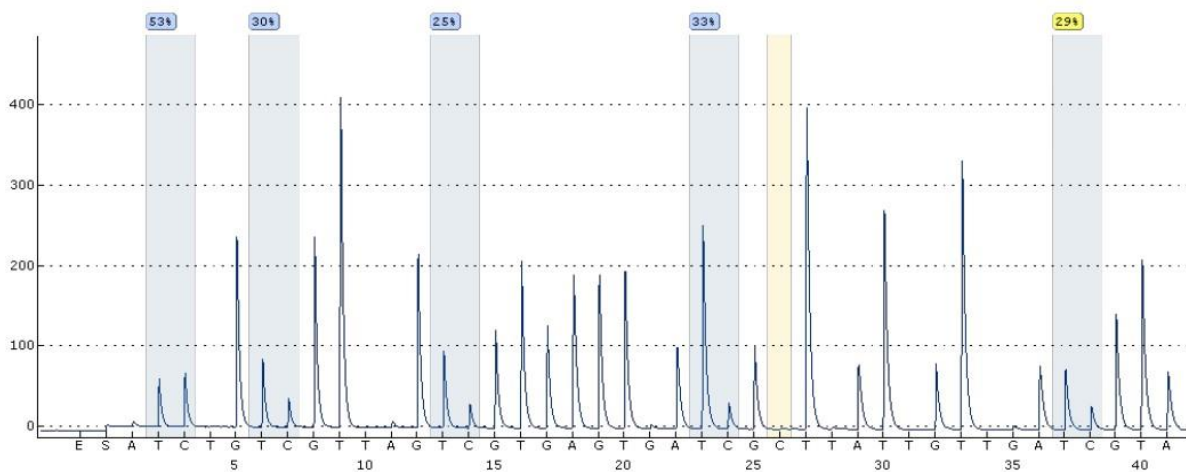


*Figure 101: Pyrosequencing graph of CpG Island 2 from pri-miR-145 promoter region of MPM sample #19. Methylation sites are marked blue. The amount of methylation is indicated above each methylation site. At dispensation 26 the bisulfide conversion worked as expected that is marked in yellow. From left to right- Site 1: 53%, Site 2: 30%, Site 3: 25%, Site 4: 33%, Site 5: 29%, Average: 34% Methylation.*

**Sample 20:**

**CpG Island 1 failed**

**CpG Island 2:**

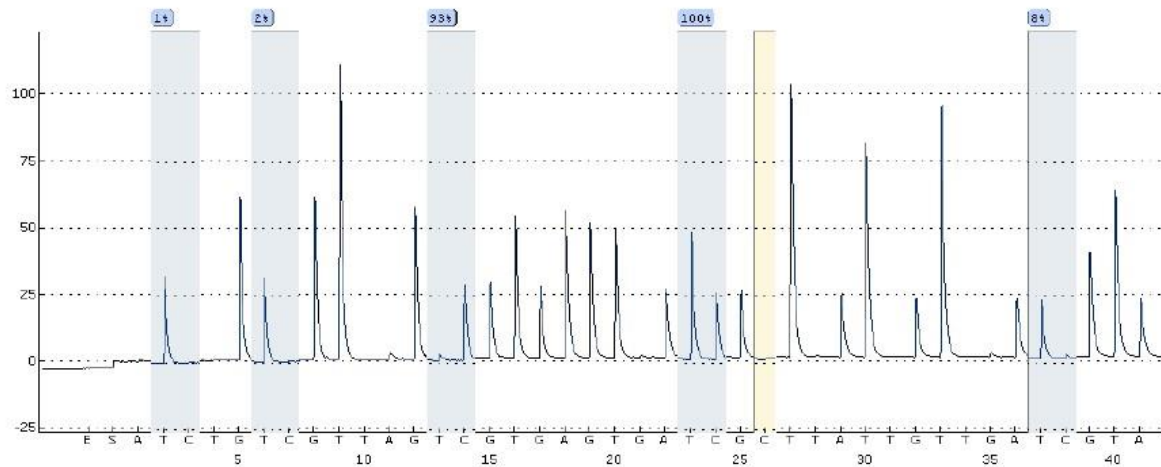


*Figure 102: Pyrosequencing graph of CpG Island 2 from pri-miR-145 promoter region of MPM sample #20. Methylation sites are marked blue. The amount of methylation is indicated above each methylation site. At dispensation 26 the bisulfite conversion worked as expected that is marked in yellow. From left to right- Site 1: 1%, Site 2: 2%, Site 3: 93%, Site 4: 100%, Site 5: 8%, Average: 40,8% Methylation.*

## Sample 21:

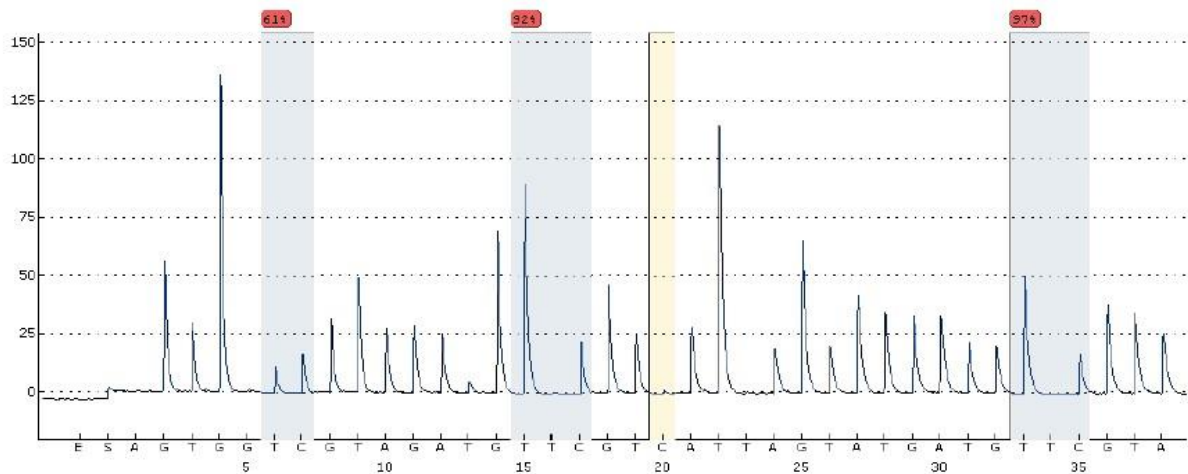


Figure 103: Pyrosequencing graph of CpG Island 1 from pri-miR-145 promoter region of MPM sample #21. Methylation sites are marked blue. The amount of methylation is indicated above each methylation site. At dispensation 20 the bisulfide conversion is uncertain that is marked in yellow. From left to right- Site 1: 61%, Site 2: 92%, Site 3: 97%, Average: 83,3% Methylation.

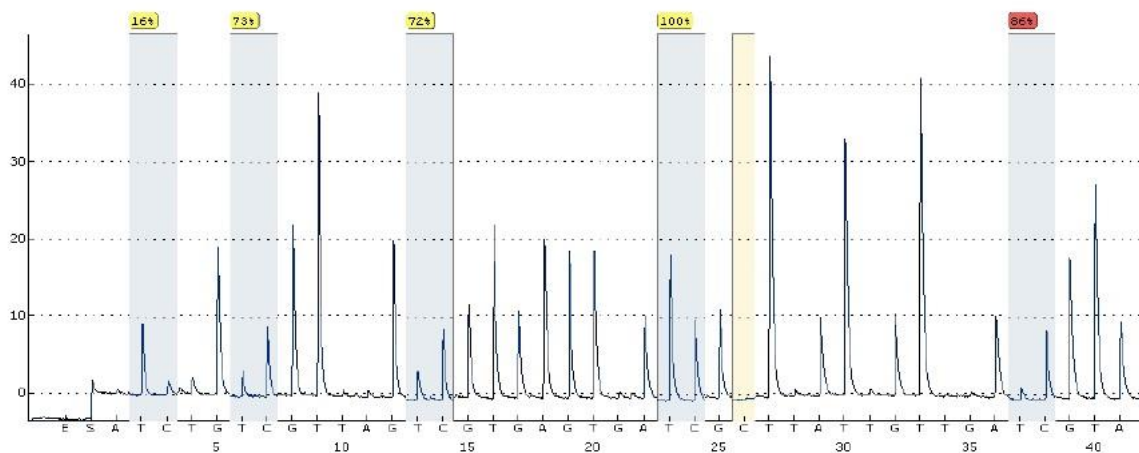


Figure 104: Pyrosequencing graph of CpG Island 2 from pri-miR-145 promoter region of MPM sample #21. Methylation sites are marked blue. The amount of methylation is indicated above each methylation site. At dispensation 26 the bisulfide conversion worked as expected that is marked in yellow. From left to right- Site 1: 16%, Site 2: 73%, Site 3: 72%, Site 4: 100%, Site 5: 86%, Average: 69,4% Methylation.

**Sample 22:**

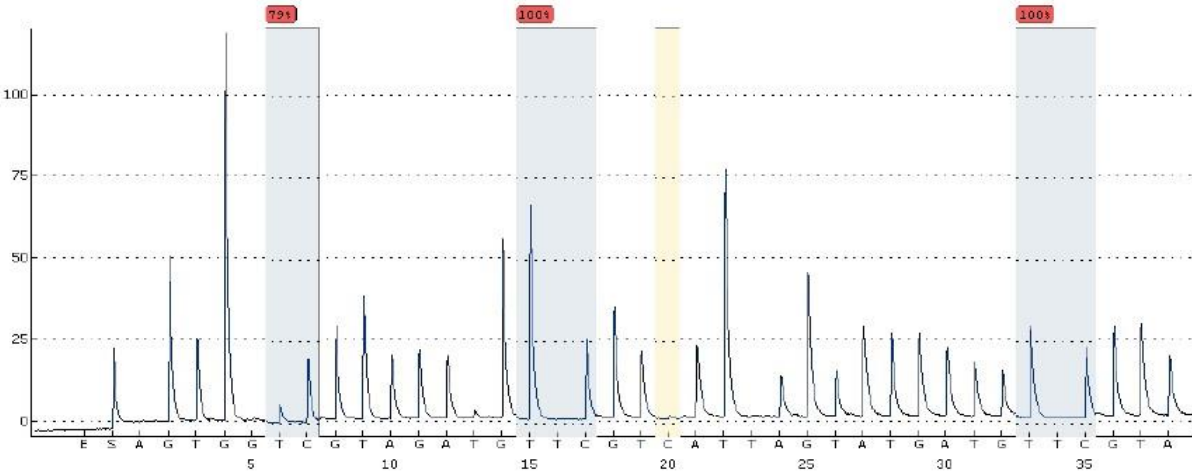


Figure 105: Pyrosequencing graph of CpG Island 1 from pri-miR-145 promoter region of MPM sample #22. Methylation sites are marked blue. The amount of methylation is indicated above each methylation site. At dispensation 20 the bisulfide conversion is uncertain that is marked in yellow. From left to right- Site 1: 79%, Site 2: 100%, Site 3: 100%, Average: 93% Methylation.

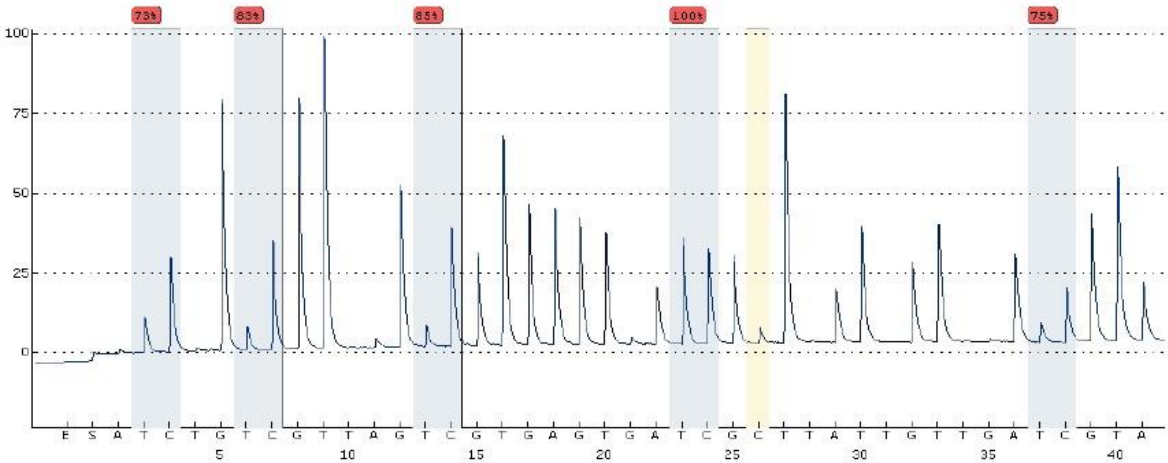


Figure 106: Pyrosequencing graph of CpG Island 2 from pri-miR-145 promoter region of MPM sample #22. Methylation sites are marked blue. The amount of methylation is indicated above each methylation site. At dispensation 26 the bisulfide conversion failed that is marked in yellow. From left to right- Site 1: 73%, Site 2: 83%, Site 3: 85%, Site 4: 100%, Site 5: 75%, Average: 83,2% Methylation.

## Sample 23:

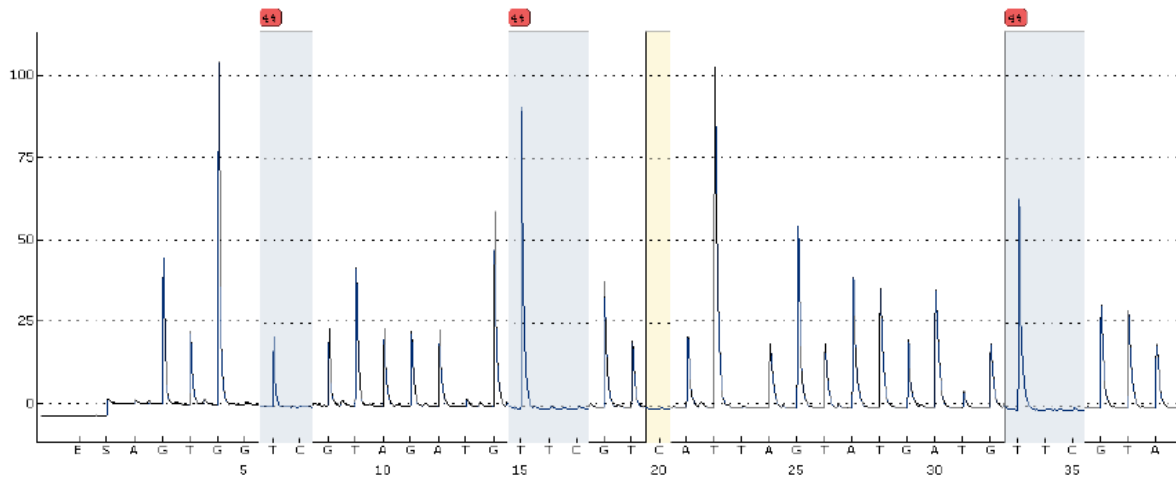


Figure 107: Pyrosequencing graph of CpG Island 1 from pri-miR-145 promoter region of MPM sample #23. Methylation sites are marked blue. The amount of methylation is indicated above each methylation site. At dispensation 20 the bisulfide conversion worked as expected that is marked in yellow. From left to right- Site 1: 4%, Site 2: 4%, Site 3: 4%, Average: 4% Methylation.

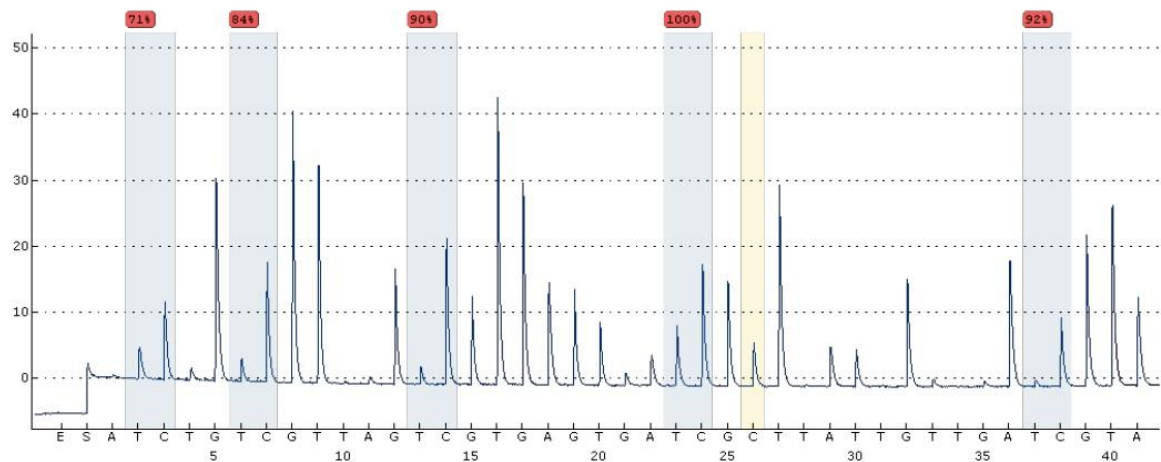


Figure 108: Pyrosequencing graph of CpG Island 2 from pri-miR-145 promoter region of MPM sample #23. Methylation sites are marked blue. The amount of methylation is indicated above each methylation site. At dispensation 26 the bisulfide conversion failed that is marked in yellow. Peak heights are low in general, which indicates a low quality Pyrosequencing. From left to right- Site 1: 71%, Site 2: 84%, Site 3: 90%, Site 4: 100%, Site 5: 92%, Average: 87,4% Methylation.

**Sample 24:**

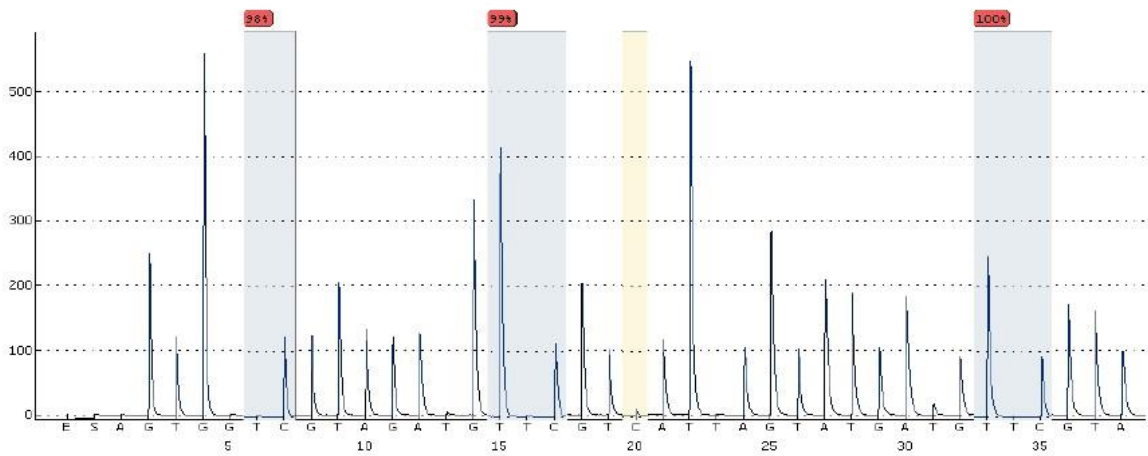


Figure 109: Pyrosequencing graph of CpG Island 1 from pri-miR-145 promoter region of MPM sample #24. Methylation sites are marked blue. The amount of methylation is indicated above each methylation site. At dispensation 20 the bisulfide conversion failed that is marked in yellow. From left to right- Site 1: 98%, Site 2: 99%, Site 3: 100%, Average: 99% Methylation.

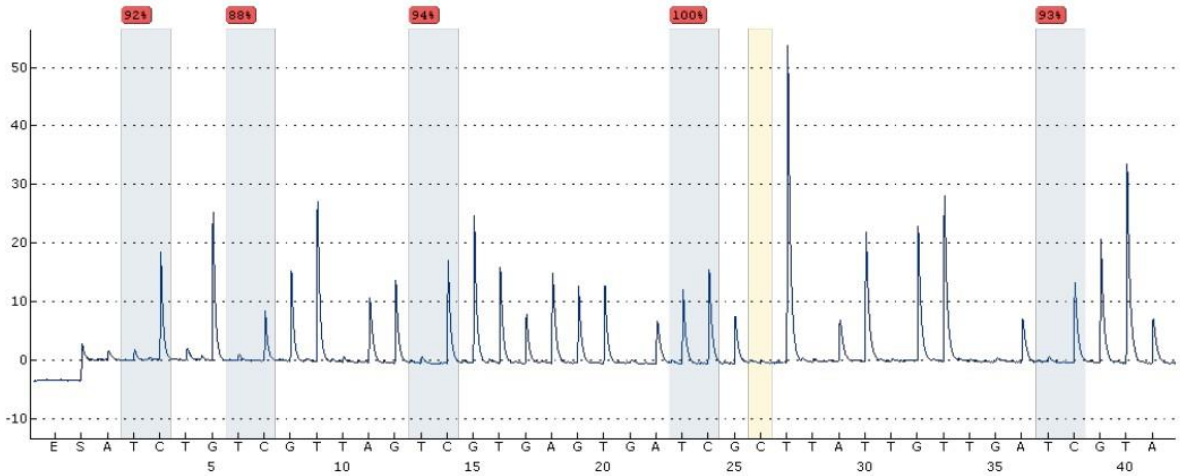


Figure 110: Pyrosequencing graph of CpG Island 2 from pri-miR-145 promoter region of MPM sample #24. Methylation sites are marked blue. The amount of methylation is indicated above each methylation site. At dispensation 26 the bisulfide conversion worked as expected that is marked in yellow. Peak heights are low in general, which indicates a low quality Pyrosequencing. From left to right- Site 1: 92%, Site 2: 88%, Site 3: 94%, Site 4: 100%, Site 5: 93%, Average: 93,4% Methylation.

## Sample 25 CpG Island 1 and CpG Island 2 failed.

### Sample 26:

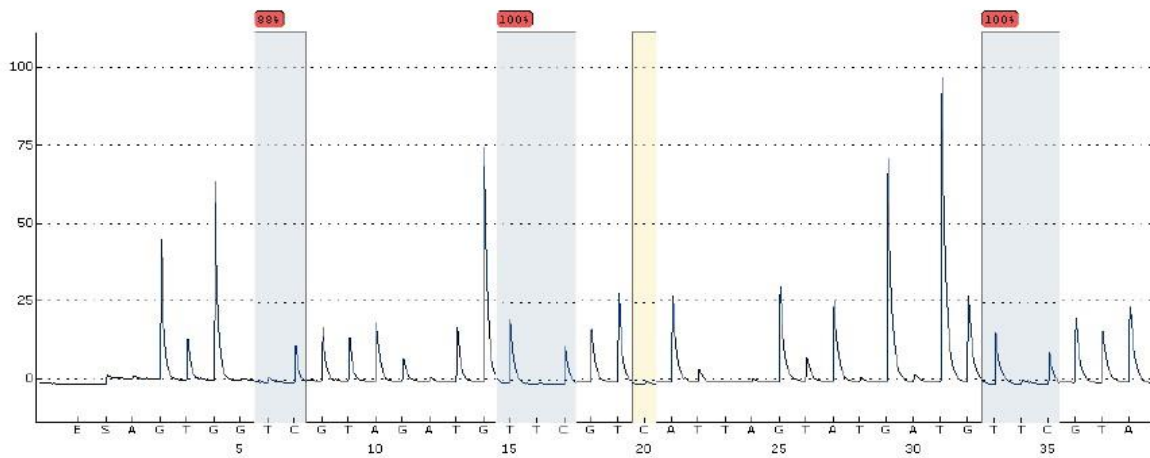


Figure 111: Pyrosequencing graph of CpG Island 1 from pri-miR-145 promoter region of MPM sample #26. Methylation sites are marked blue. The amount of methylation is indicated above each methylation site. At dispensation 20 the bisulfide conversion is uncertain that is marked in yellow. From left to right- Site 1: 88%, Site 2: 100%, Site 3: 100%, Average: 96% Methylation.

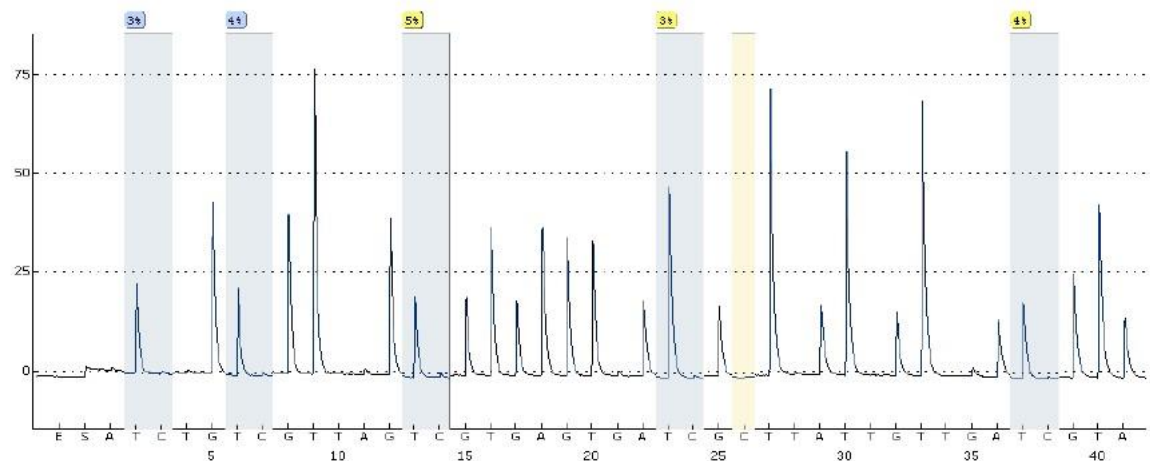


Figure 112: Pyrosequencing graph of CpG Island 2 from pri-miR-145 promoter region of MPM sample #26. Methylation sites are marked blue. The amount of methylation is indicated above each methylation site. At dispensation 26 the bisulfide conversion worked as expected that is marked in yellow. From left to right- Site 1: 3%, Site 2: 4%, Site 3: 5%, Site 4: 3%, Site 5: 4%, Average: 3,8% Methylation.

**Sample 27:**

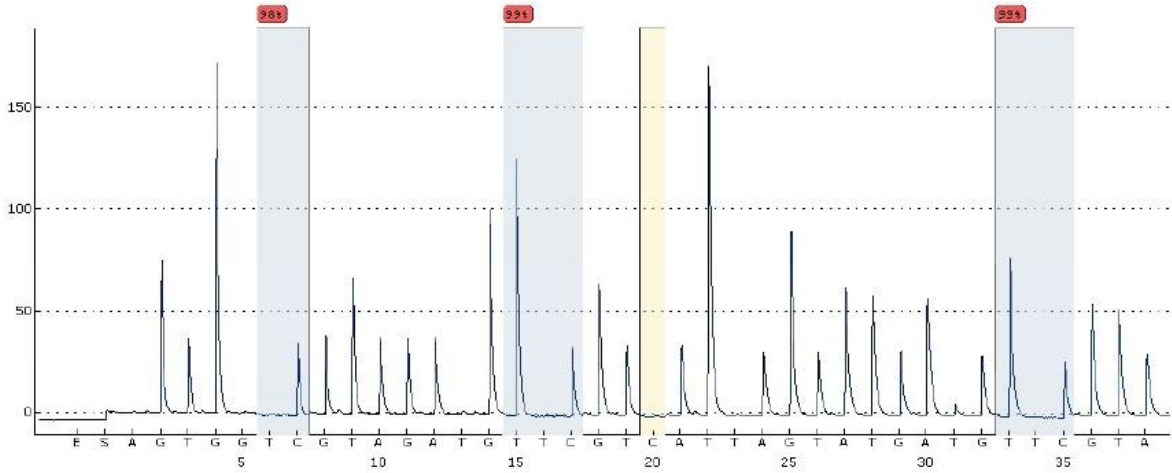


Figure 113: Pyrosequencing graph of CpG Island 1 from pri-miR-145 promoter region of MPM sample #27. Methylation sites are marked blue. The amount of methylation is indicated above each methylation site. At dispensation 20 the bisulfide conversion worked as expected that is marked in yellow. From left to right- Site 1: 98%, Site 2: 99%, Site 3: 99%, Average: 99% Methylation.

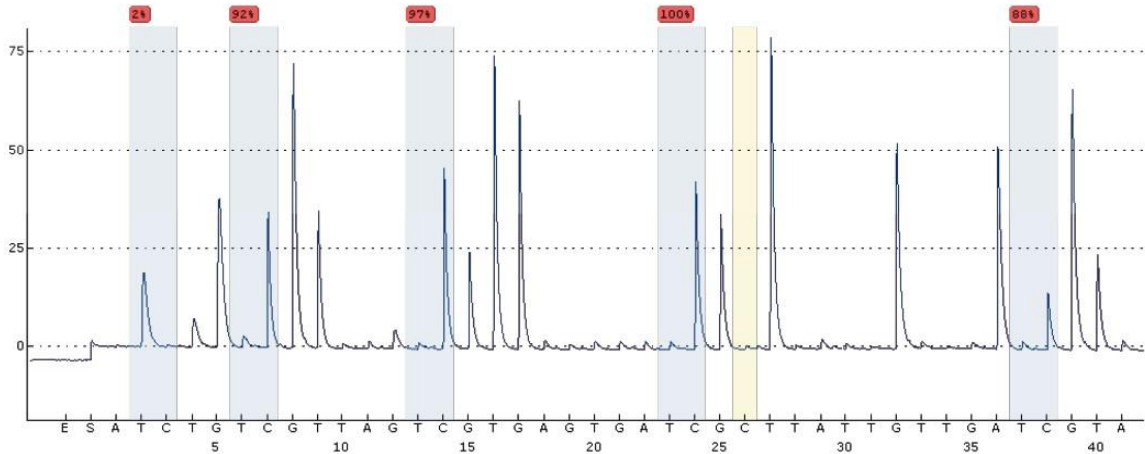


Figure 114: Pyrosequencing graph of CpG Island 2 from pri-miR-145 promoter region of MPM sample #27. Methylation sites are marked blue. The amount of methylation is indicated above each methylation site. At dispensation 26 the bisulfide conversion worked as expected that is marked in yellow. Though several peaks heights are very low or missing, which indicates a very low quality Pyrosequencing. From left to right- Site 1: 2%, Site 2: 92%, Site 3: 97%, Site 4: 100%, Site 5: 88%, Average: 75,8% Methylation.

## Sample 28:

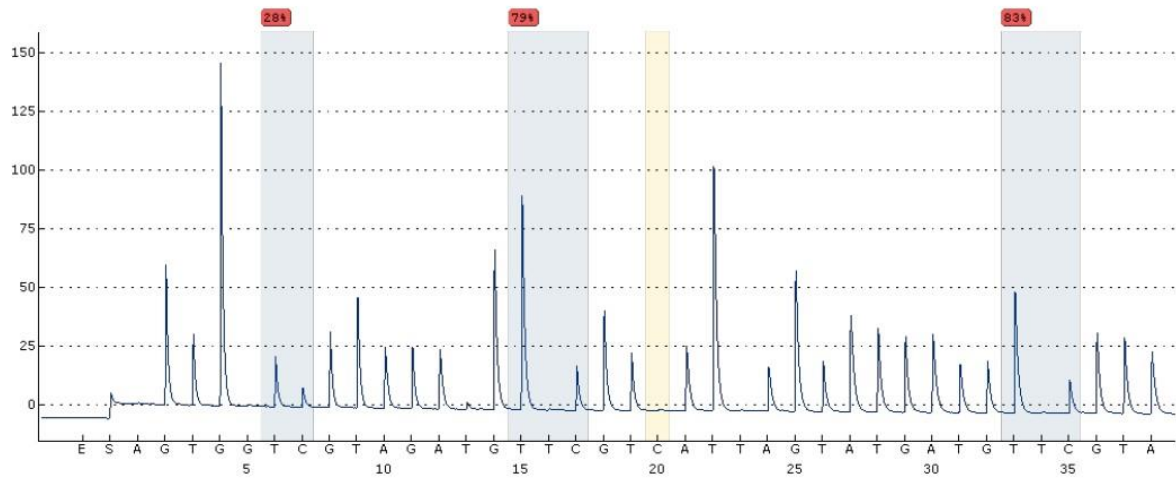


Figure 115: Pyrosequencing graph of CpG Island 1 from pri-miR-145 promoter region of MPM sample #28. Methylation sites are marked blue. The amount of methylation is indicated above each methylation site. At dispensation 20 the bisulfide conversion worked as expected that is marked in yellow. From left to right- Site 1: 28%, Site 2: 79%, Site 3: 83%, Average: 63,3% Methylation.

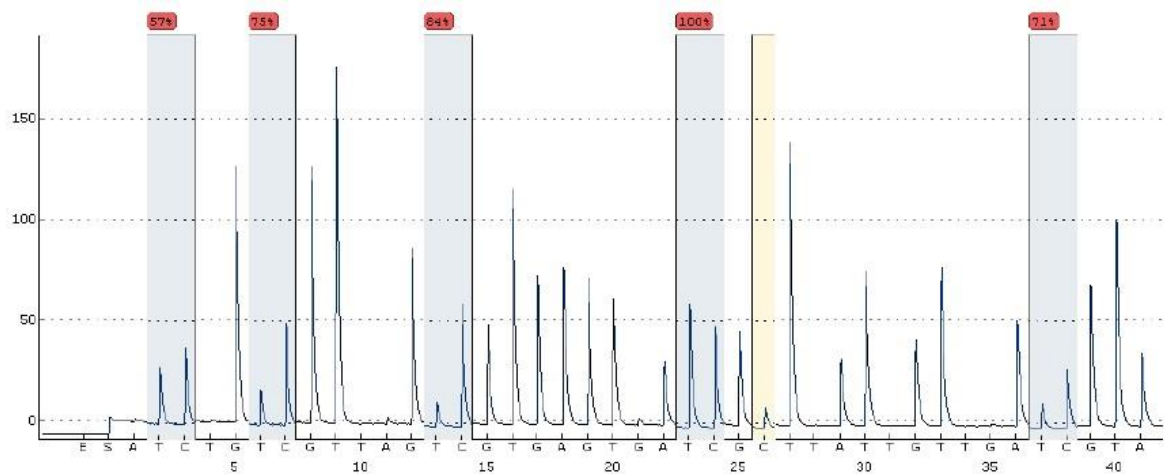


Figure 116: Pyrosequencing graph of CpG Island 2 from pri-miR-145 promoter region of MPM sample #28. Methylation sites are marked blue. The amount of methylation is indicated above each methylation site. At dispensation 26 the bisulfide conversion failed that is marked in yellow. From left to right- Site 1: 57%, Site 2: 75%, Site 3: 84%, Site 4: 100%, Site 5: 71%, Average: 77,4% Methylation.

**Sample 29:**

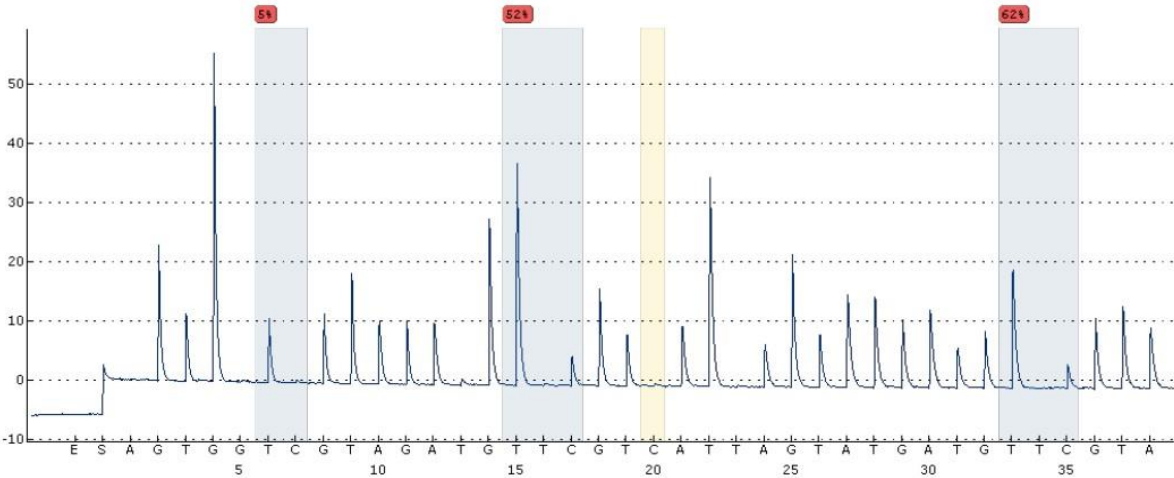


Figure 117: Pyrosequencing graph of CpG Island 1 from pri-miR-145 promoter region of MPM sample #29. Methylation sites are marked blue. The amount of methylation is indicated above each methylation site. At dispensation 20 the bisulfide conversion is uncertain that is marked in yellow. Also low peak heights (lower than 20) indicates a low quality pyrosequencing. From left to right- Site 1: 5%, Site 2: 52%, Site 3: 62%, Average: 39,7% Methylation.

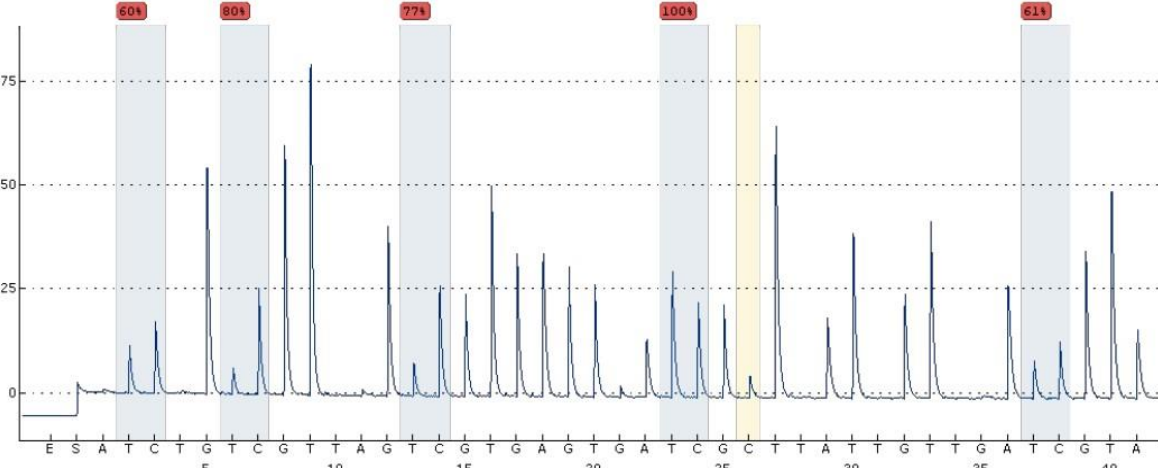
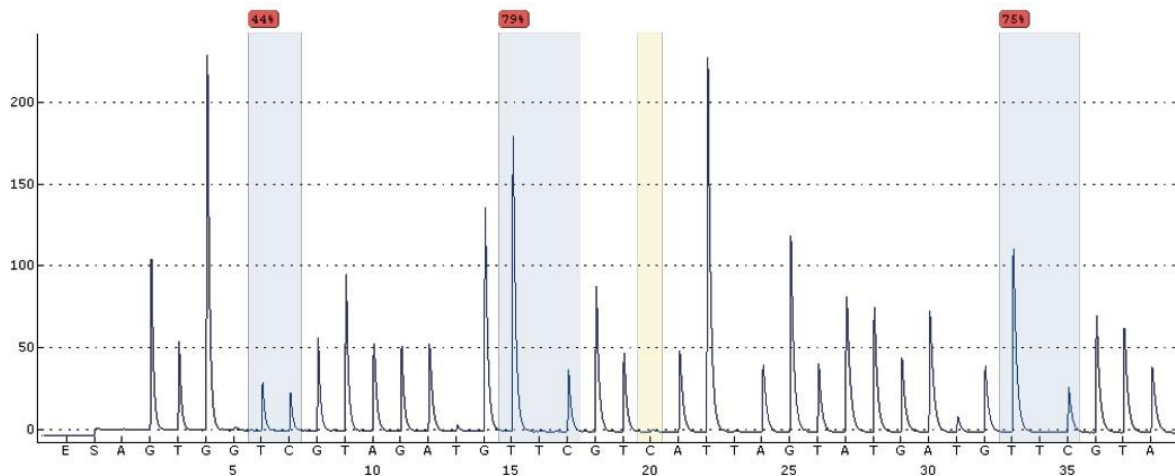
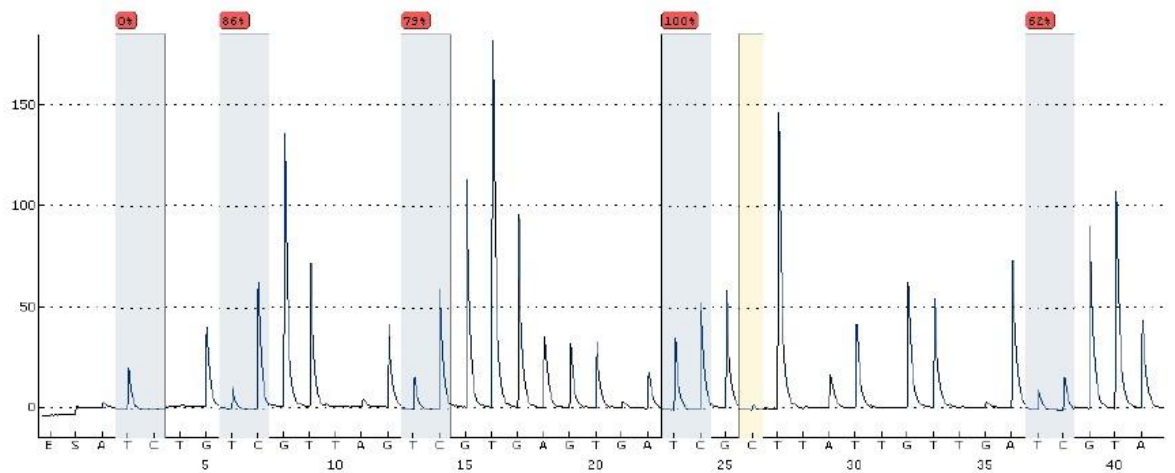


Figure 118: Pyrosequencing graph of CpG Island 2 from pri-miR-145 promoter region of MPM sample #29. Methylation sites are marked blue. The amount of methylation is indicated above each methylation site. At dispensation 26 the bisulfide conversion failed that is marked in yellow. From left to right- Site 1: 60%, Site 2: 80%, Site 3: 77%, Site 4: 100%, Site 5: 61%, Average: 75,6% Methylation.

**Sample 30:**



*Figure 119: Pyrosequencing graph of CpG Island 1 from pri-miR-145 promoter region of MPM sample #30. Methylation sites are marked blue. The amount of methylation is indicated above each methylation site. At dispensation 20 the bisulfite conversion worked as expected that is marked in yellow. From left to right- Site 1: 44%, Site 2: 79%, Site 3: 75%, Average: 66% Methylation.*



*Figure 120: Pyrosequencing graph of CpG Island 2 from pri-miR-145 promoter region of MPM sample #30. Methylation sites are marked blue. The amount of methylation is indicated above the each methylation site. At dispensation 26 the bisulfite conversion is uncertain that is marked in yellow. From left to right- Site 1: 0%, Site 2: 86%, Site 3: 79%, Site 4: 100%, Site 5: 62%, Average: 65,4% Methylation.*

**Sample 31:**

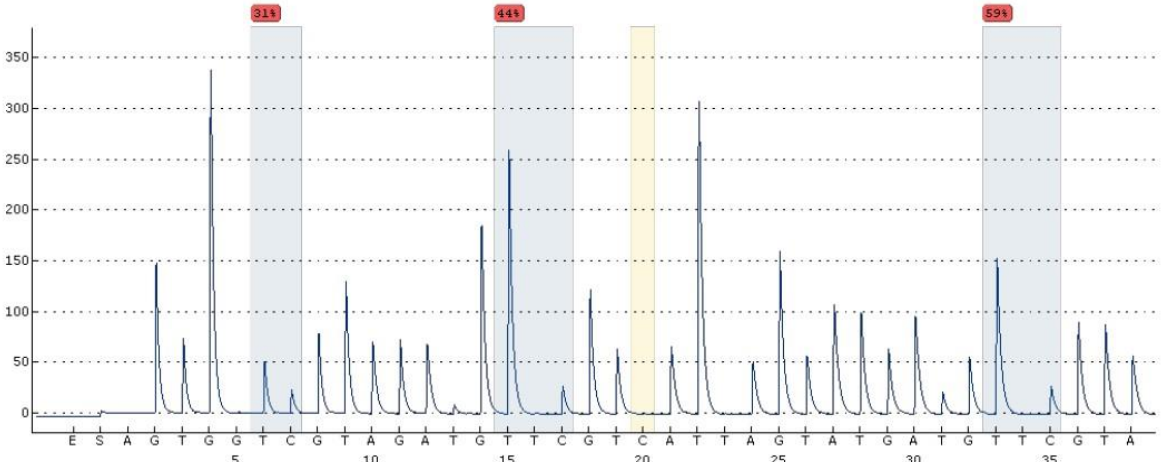


Figure 121: Pyrosequencing graph of CpG Island 1 from pri-miR-145 promoter region of MPM sample #31. Methylation sites are marked blue. The amount of methylation is indicated above each methylation site. At dispensation 20 the bisulfide conversion worked as expected that is marked in yellow. From left to right- Site 1: 31%, Site 2: 44%, Site 3: 59%, Average: 44,7% Methylation.

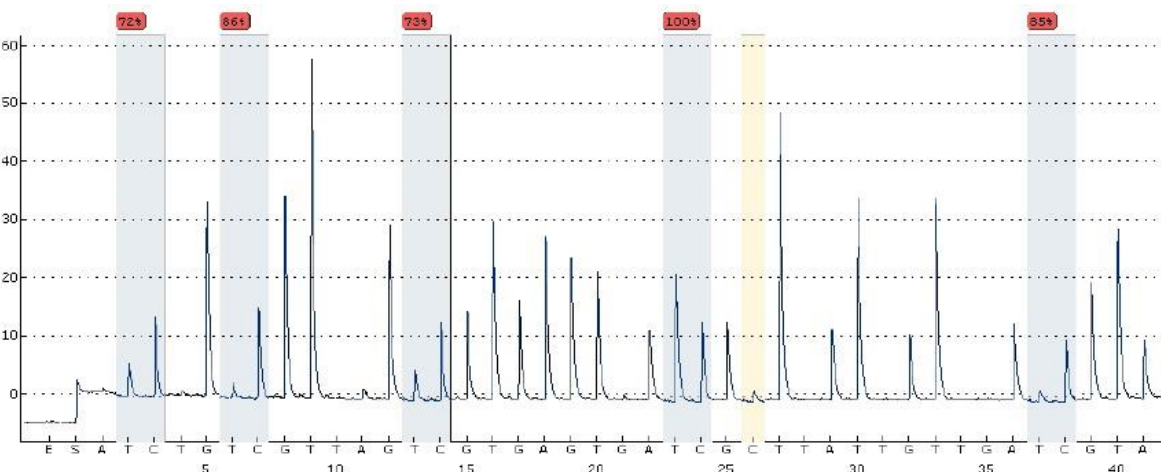


Figure 122: Pyrosequencing graph of CpG Island 2 from pri-miR-145 promoter region of MPM sample #31. Methylation sites are marked blue. The amount of methylation is indicated above each methylation site. At dispensation 26 the bisulfide conversion failed that is marked in yellow. Also low peak heights (lower than 20) indicates a low quality pyrosequencing. From left to right- Site 1: 72%, Site 2: 86%, Site 3: 73%, Site 4: 100%, Site 5: 85%, Average: 83,2% Methylation.

## Sample 32:

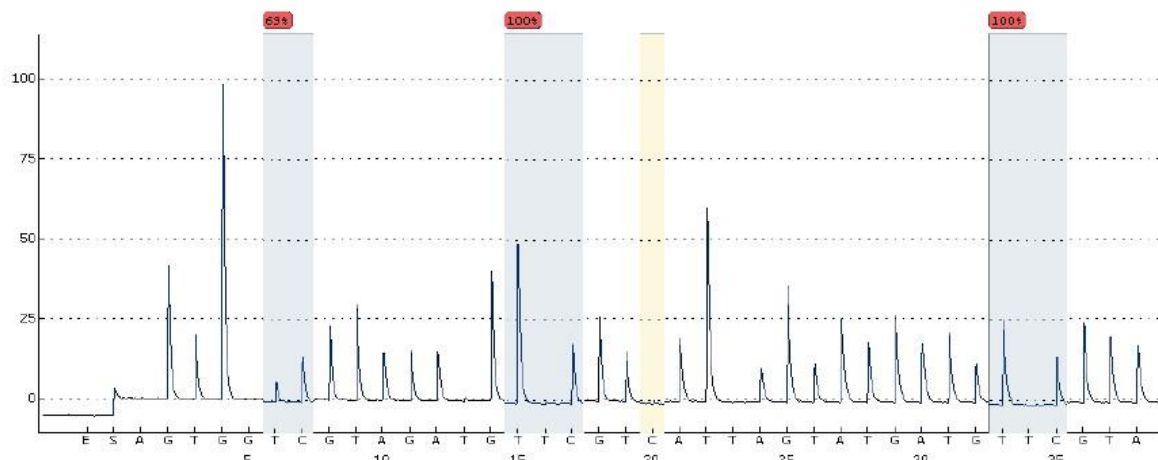


Figure 123: Pyrosequencing graph of CpG Island 1 from pri-miR-145 promoter region of MPM sample #32. Methylation sites are marked blue. The amount of methylation is indicated above each methylation site. At dispensation 20 the bisulfide conversion is uncertain that is marked in yellow. From left to right- Site 1: 69%, Site 2: 100%, Site 3: 100%, Average: 89,7% Methylation.

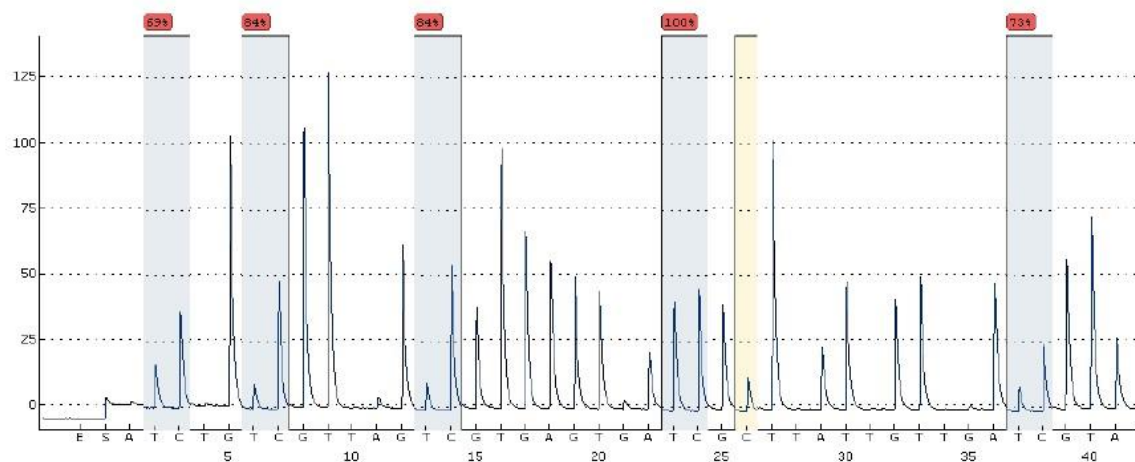


Figure 124: Pyrosequencing graph of CpG Island 2 from pri-miR-145 promoter region of MPM sample #32. Methylation sites are marked blue. The amount of methylation is indicated above each methylation site. At dispensation 26 the bisulfide conversion failed that is marked in yellow. From left to right- Site 1: 69%, Site 2: 84%, Site 3: 84%, Site 4: 100%, Site 5: 73%, Average: 82% Methylation.

**Sample 33:**

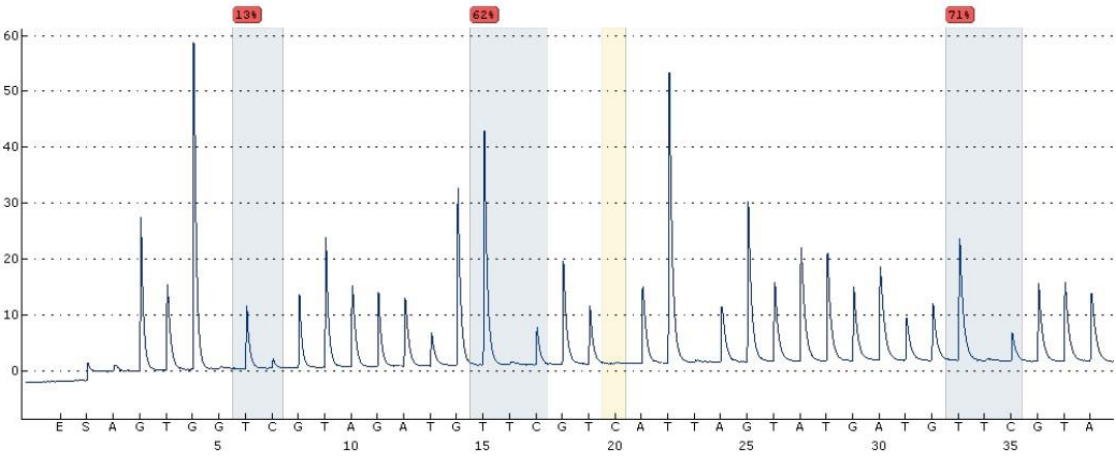


Figure 125: Pyrosequencing graph of CpG Island 1 from pri-miR-145 promoter region of MPM sample #33. Methylation sites are marked blue. The amount of methylation is indicated above each methylation site. At dispensation 20 the bisulfide conversion worked as expected that is marked in yellow. Also low peak heights (lower than 20) indicates a low quality pyrosequencing. From left to right- Site 1: 13%, Site 2: 62%, Site 3: 71%, Average: 48,7% Methylation.

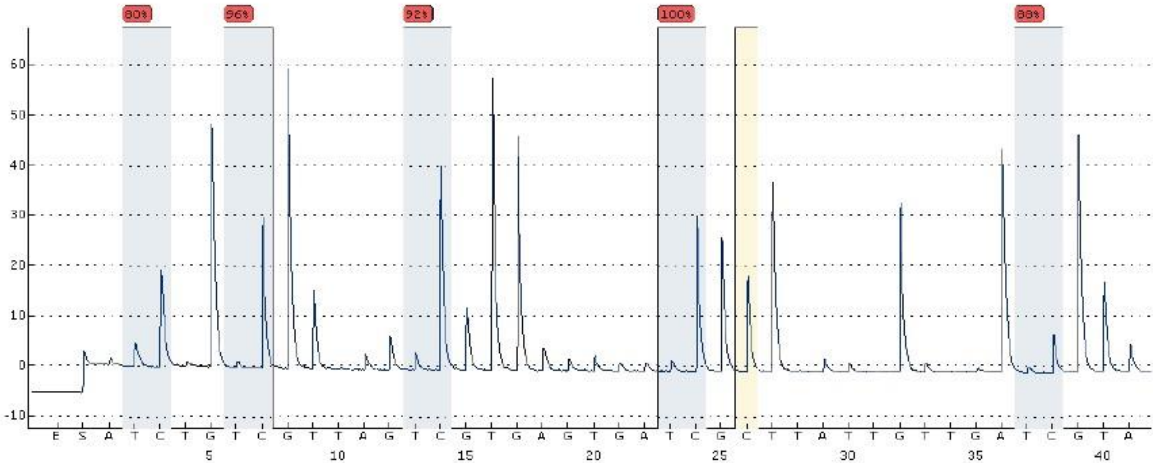
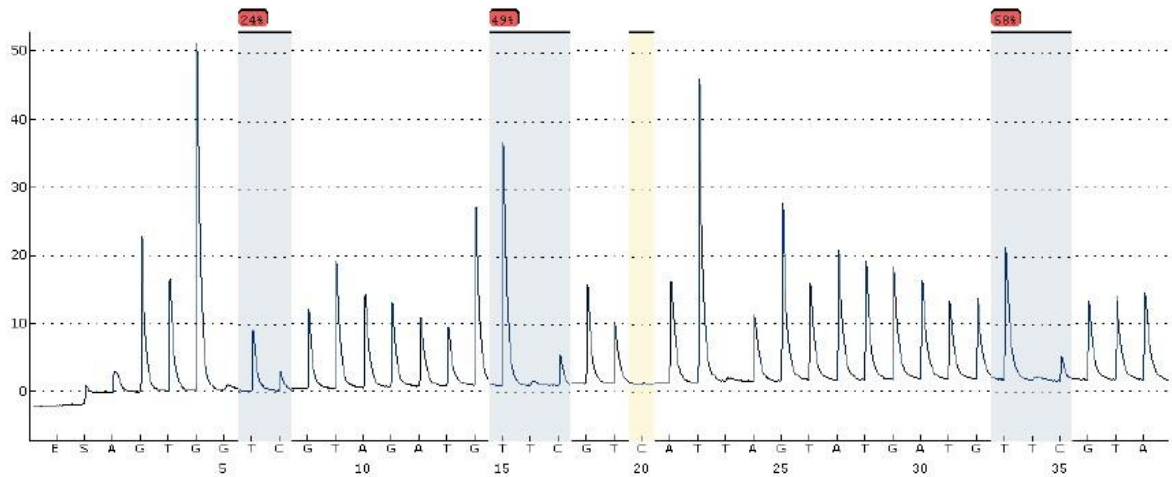
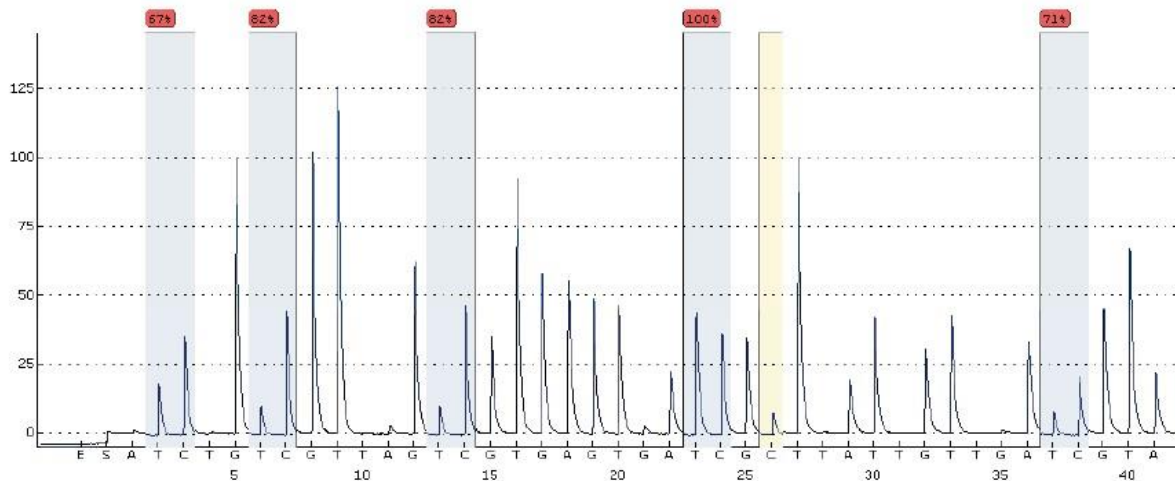


Figure 126: Pyrosequencing graph of CpG Island 2 from pri-miR-145 promoter region of MPM sample #33. Methylation sites are marked blue. The amount of methylation is indicated above each methylation site. At dispensation 26 the bisulfide conversion failed that is marked in yellow. Also very low peak heights (lower than 20) indicates a very low quality pyrosequencing. From left to right- Site 1: 80%, Site 2: 96%, Site 3: 92%, Site 4: 100%, Site 5: 88%, Average: 91,2% Methylation.

**Sample 34:**



*Figure 127: Pyrosequencing graph of CpG Island 1 from pri-miR-145 promoter region of MPM sample #34. Methylation sites are marked blue. The amount of methylation is indicated above each methylation site. At dispensation 20 the bisulfide conversion worked as expected that is marked in yellow. Also low peak heights (lower than 20) indicates a low quality pyrosequencing. From left to right- Site 1: 24%, Site 2: 49%, Site 3: 58%, Average: 43,7% Methylation*



*Figure 128: Pyrosequencing graph of CpG Island 2 from pri-miR-145 promoter region of MPM sample #34. Methylation sites are marked blue. The amount of methylation is indicated above each methylation site. At dispensation 26 the bisulfide conversion failed that is marked in yellow. Also very low peak heights (lower than 20) indicates a very low quality pyrosequencing. From left to right- Site 1: 67%, Site 2: 82%, Site 3: 82%, Site 4: 100%, Site 5: 71%, Average: 80,4% Methylation.*

**Sample 35:**

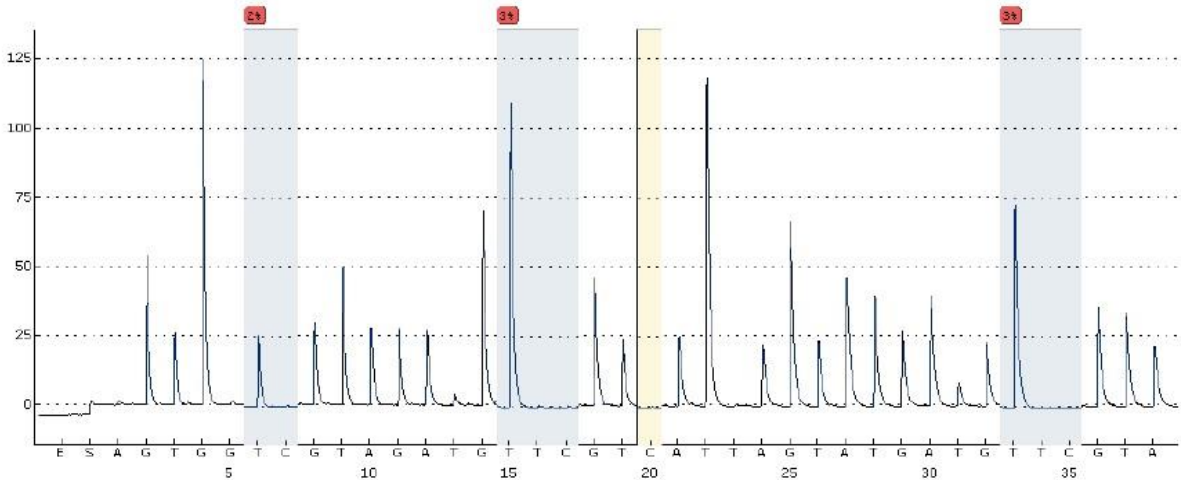


Figure 129: Pyrosequencing graph of CpG Island 1 from pri-miR-145 promoter region of MPM sample #35. Methylation sites are marked blue. The amount of methylation is indicated above each methylation site. At dispensation 20 the bisulfide conversion worked as expected that is marked in yellow. From left to right- Site 1: 2%, Site 2: 3%, Site 3: 3%, Average: 2,7% Methylation.

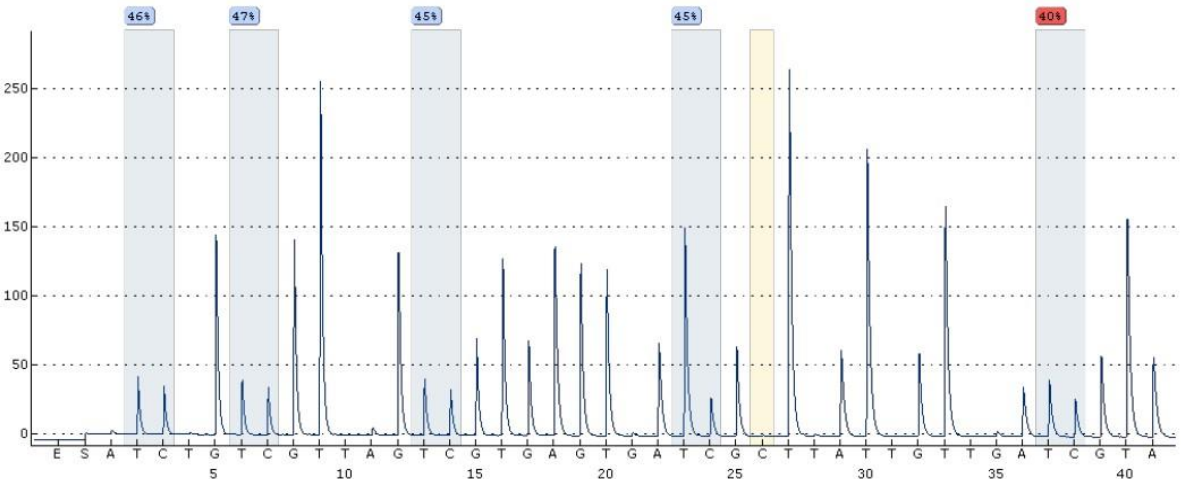
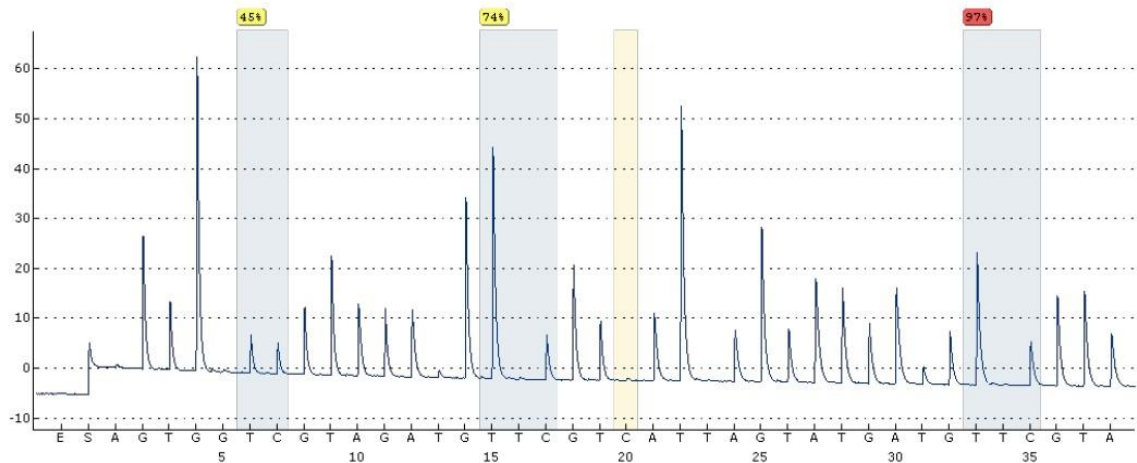
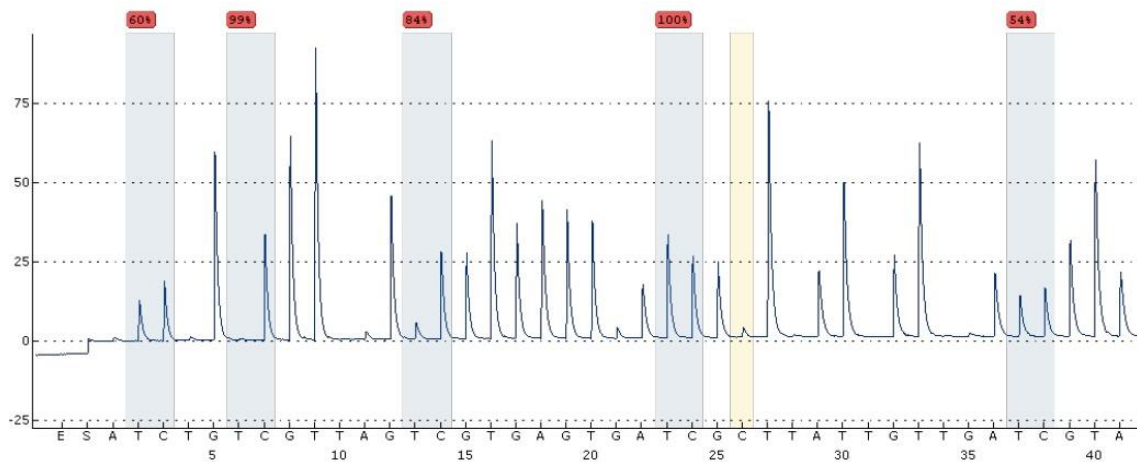


Figure 130: Pyrosequencing graph of CpG Island 2 from pri-miR-145 promoter region of MPM sample #35. Methylation sites are marked blue. The amount of methylation is indicated above each methylation site. At dispensation 26 the bisulfide conversion worked as expected that is marked in yellow. From left to right- Site 1: 46%, Site 2: 47%, Site 3: 45%, Site 4: 45%, Site 5: 40%, Average: 44,6% Methylation.

**Sample 36:**



*Figure 131: Pyrosequencing graph of CpG Island 1 from pri-miR-145 promoter region of MPM sample #36. Methylation sites are marked blue. The amount of methylation is indicated above each methylation site. At dispensation 20 the bisulfide conversion worked as expected that is marked in yellow. Also low peak heights (lower than 20) and baseline drift indicates a low quality pyrosequencing. From left to right- Site 1: 45%, Site 2: 74%, Site 3: 97%, Average: 72% Methylation.*



*Figure 132: Pyrosequencing graph of CpG Island 2 from pri-miR-145 promoter region of MPM sample #36. Methylation sites are marked blue. The amount of methylation is indicated above each methylation site. At dispensation 26 the bisulfide conversion failed that is marked in yellow. From left to right- Site 1: 60%, Site 2: 99%, Site 3: 84%, Site 4: 100%, Site 5: 54%, Average: 79,4% Methylation.*

### Sample 37:

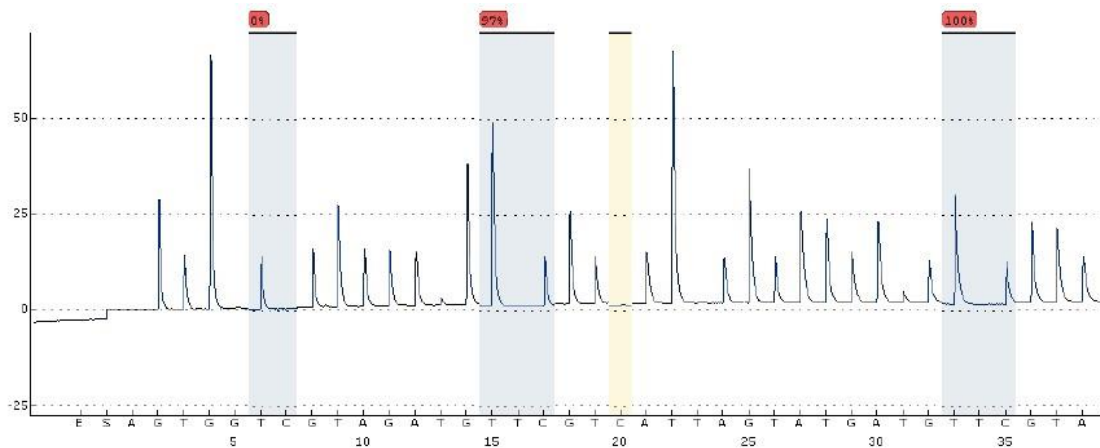


*Figure 133: Pyrosequencing graph of CpG Island 1 from pri-miR-145 promoter region of MPM sample #37. Methylation sites are marked blue. The amount of methylation is indicated above each methylation site. At dispensation 20 the bisulfite conversion worked as expected that is marked in yellow. Also low peak heights (lower than 20) and baseline drift indicates a low quality pyrosequencing. From left to right- Site 1: 0%, Site 2: 97%, Site 3: 100%, Average: 65% Methylation.*

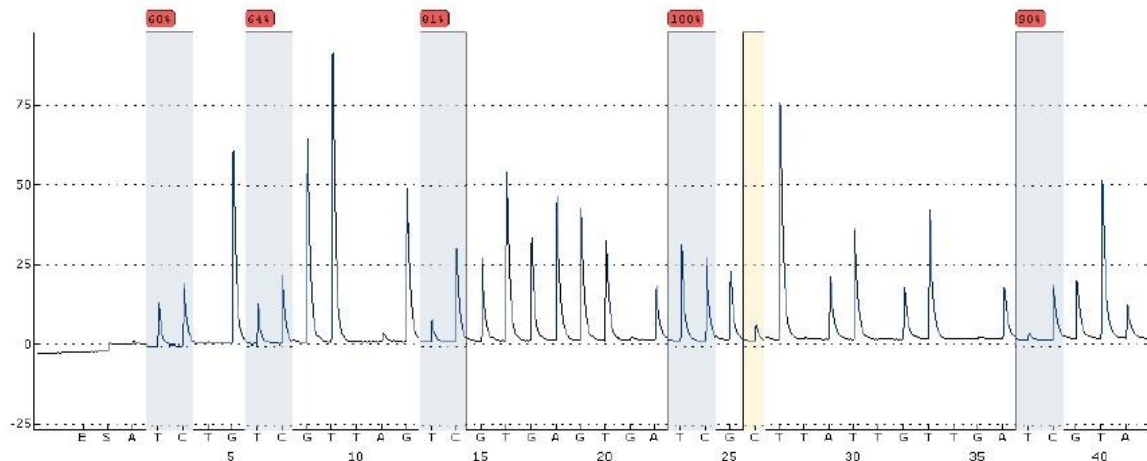


*Figure 134: Pyrosequencing graph of CpG Island 2 from pri-miR-145 promoter region of MPM sample #37. Methylation sites are marked blue. The amount of methylation is indicated above each methylation site. At dispensation 26 the bisulfite conversion failed that is marked in yellow. From left to right- Site 1: 60%, Site 2: 64%, Site 3: 81%, Site 4: 100%, Site 5: 90%, Average: 79% Methylation.*

**Sample 38:**

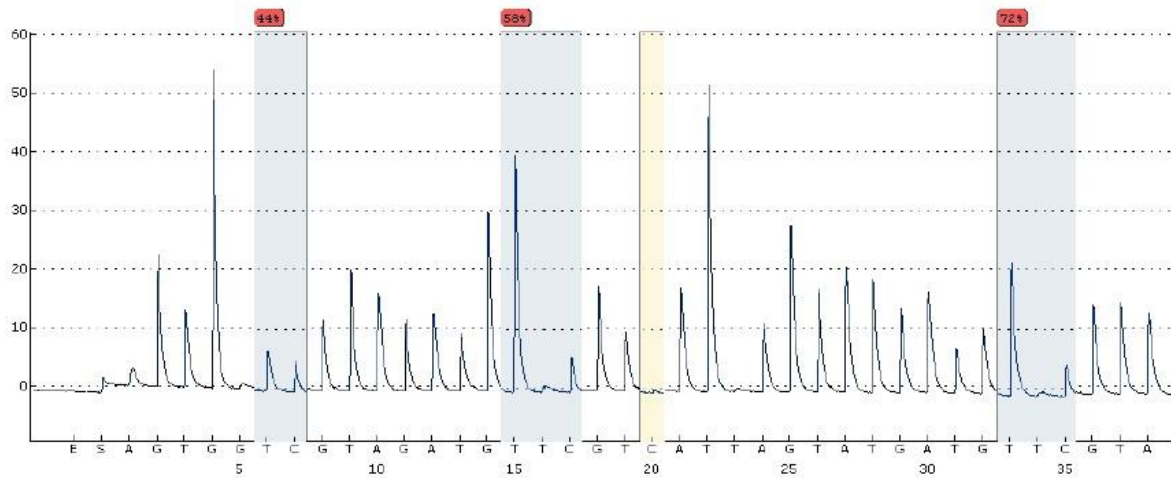


*Figure 135: Pyrosequencing graph of CpG Island 1 from pri-miR-145 promoter region of MPM sample #38. Methylation sites are marked blue. The amount of methylation is indicated above each methylation site. At dispensation 20 the bisulfide conversion worked as expected that is marked in yellow. Also low peak heights (lower than 20) indicates a low quality pyrosequencing. From left to right- Site 1: 44%, Site 2: 58%, Site 3: 72%, Average: 58% Methylation.*

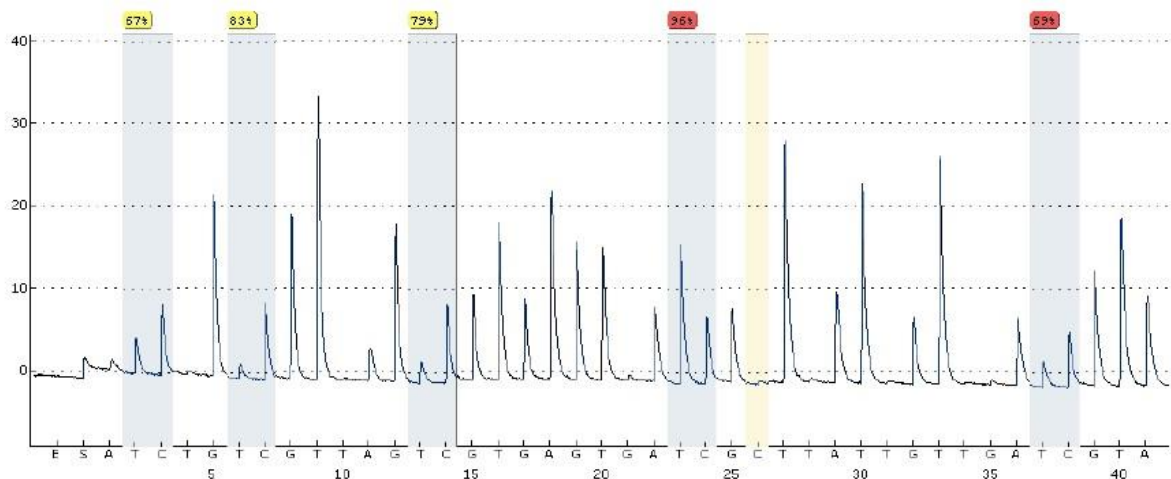


*Figure 136: Pyrosequencing graph of CpG Island 2 from pri-miR-145 promoter region of MPM sample #38. Methylation sites are marked blue. The amount of methylation is indicated above each methylation site. At dispensation 26 the bisulfide conversion worked as expected that is marked in yellow. Also low peak heights (lower than 20) indicates a low quality pyrosequencing. From left to right- Site 1: 67%, Site 2: 83%, Site 3: 79%, Site 4: 96%, Site 5: 69%, Average: 78,8% Methylation.*

**Sample 39:**

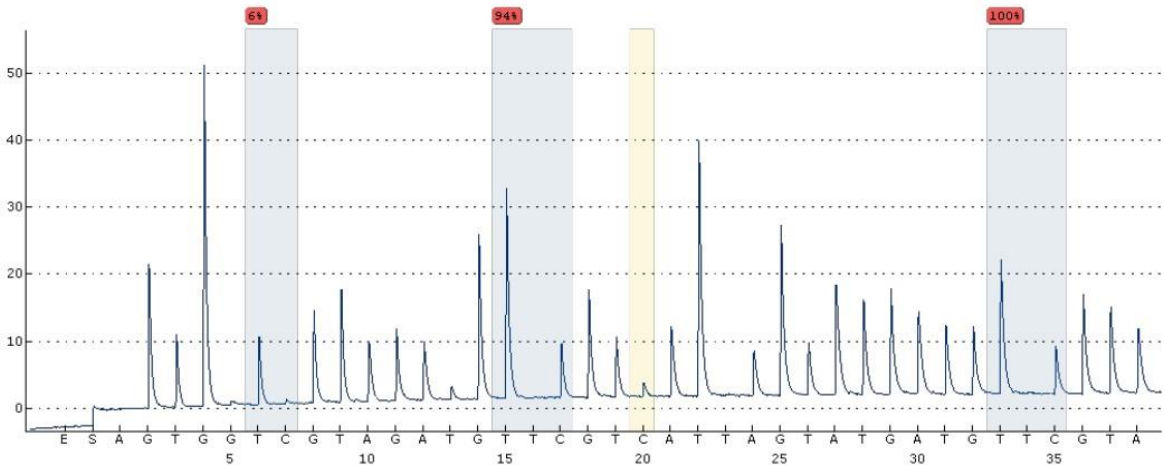


Figure 137: Pyrosequencing graph of CpG Island 1 from pri-miR-145 promoter region of MPM sample #39. Methylation sites are marked blue. The amount of methylation is indicated above each methylation site. At dispensation 20 the bisulfide conversion failed that is marked in yellow. Also low peak heights (lower than 20) and baseline drift indicates a low quality pyrosequencing. From left to right- Site 1: 6%, Site 2: 94%, Site 3: 100%, Average: 66,7% Methylation.

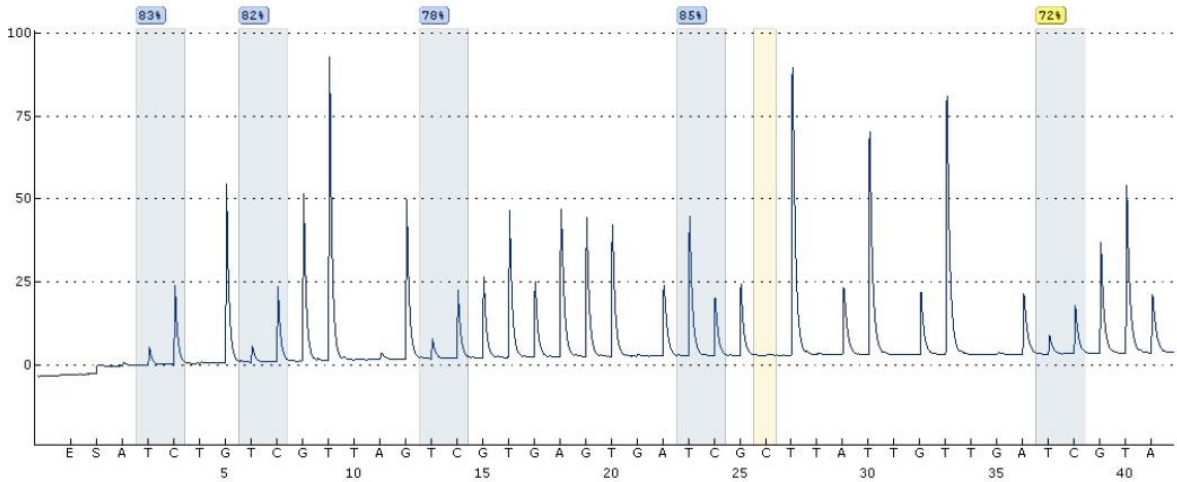


Figure 138: Pyrosequencing graph of CpG Island 2 from pri-miR-145 promoter region of MPM sample #39. Methylation sites are marked blue. The amount of methylation is indicated above each methylation site. At dispensation 26 the bisulfide conversion worked as expected that is marked in yellow. From left to right- Site 1: 83%, Site 2: 82%, Site 3: 78%, Site 4: 85%, Site 5: 72%, Average: 80% Methylation.

## Sample 40:

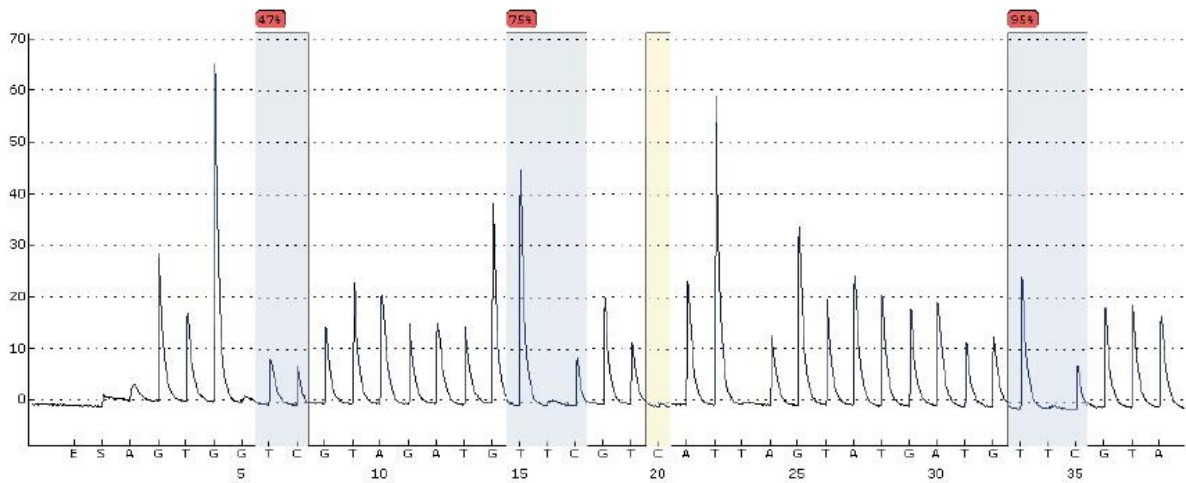


Figure 139: Pyrosequencing graph of CpG Island 1 from pri-miR-145 promoter region of MPM sample #40. Methylation sites are marked blue. The amount of methylation is indicated above each methylation site. At dispensation 20 the bisulfide conversion worked that is marked in yellow. Also the peak are too wide that indicates a low quality pyrosequencing and uncertain results. From left to right: Site 1: 47%, Site 2: 75%, Site 3: 95%, Average: 72,3% Methylation.

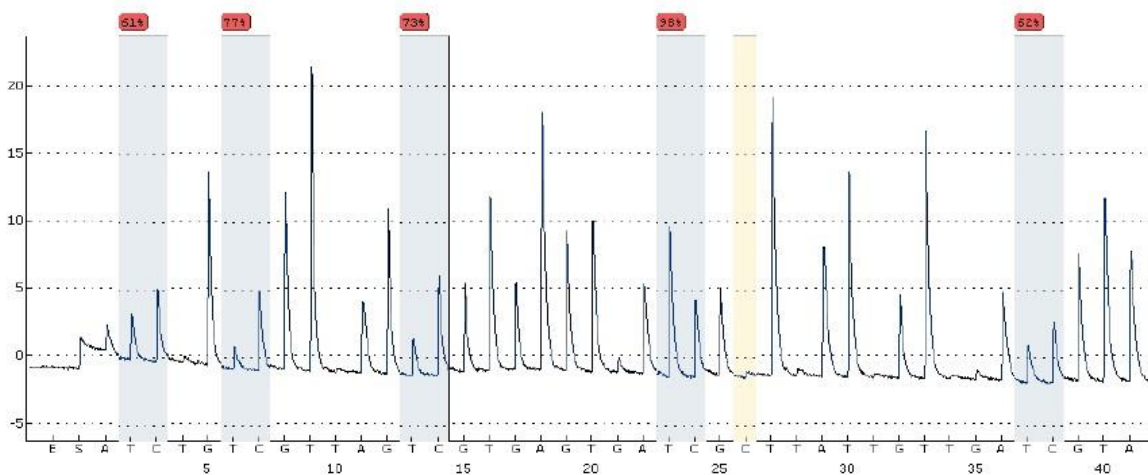


Figure 140: Pyrosequencing graph of CpG Island 2 from pri-miR-145 promoter region of MPM sample #40. Methylation sites are marked blue. The amount of methylation is indicated above each methylation site. At dispensation 26 the bisulfide conversion is uncertain that is marked in yellow. Also low peak heights (lower than 20) along with a baseline drift, which indicates a low quality pyrosequencing. From left to right- Site 1: 61%, Site 2: 77%, Site 3: 73%, Site 4: 98%, Site 5: 62%, Average: 74,2% Methylation.

### 5.3. Real time quantitative PCR (RT-qPCR) data

In table 16, the average methylation of both CpG islands in the *pri-miR-145* gene promoter is correlated with miR-145 expression assessed by quantitative PCR (TaqMan qPCR). The qPCR data were obtained from results previously published by the laboratory in Copenhagen.<sup>10</sup>

Tumour Samples			NNP Samples		
Sam. Nu.	Ava. Meth. (%)	miR-145 expression measured by qPCR	Sam. Nu.	Ava. Meth. (%)	miR-145 expression measured by qPCR
#04	45,5	4,7	#03	85,3	2,8
#08	91,3	2,8	#19	66,5	4,7
#09	57,2	4,4	#23	45,7	3,9
#11	78,1	4,2	#27	87,4	3,4
#18	74,8	3,2	#29	57,6	4,6
#22	88,1	1,2	#31	63,9	6,0
#30	65,7	0,6	#37	72,3	5,9
#33	69,9	1,7	Average:	68,4	4,5
#35	23,6	1,2			
#36	75,7	1,9		Control Sample	
#38	68,4	2,4	#10	42,7	5,13
#39	73,3	3,0			
#40	73,3	3,8			
Average:	68,1	2,7			

Table 16: Obtained QPCR data from Tumour samples, non-neoplastic pleura = NNP samples and control sample with reactive non-neoplastic mesothelial proliferation from a patient with Pneumothorax.

## 6. Discussion

This master thesis have aimed to analyse the methylation-status of miR-145 in MPM patients within tumour and NNP tissue samples, quantify methylation of the *pri-miR-145* promoter, correlate methylation data with the expression of miR-145 and finally correlate methylation data with clinic-pathological data, when possible.

Methylation specific PCR results as can be seen in Table 12 gave the following results: In total there were 11 samples that were fully methylated, 22 samples that were hemi-methylated and 1 sample that is unmethylated. Individual interpretations of the figures are given below each gel picture. However 2 bands, one around 40 bp and the sec one around 80 bp, appeared in the majority of the samples. The 40 bp band appears to be a primer dimer formation since it was seen in 17 gel pictures out of 25. The other band around 80 bp was observed in all 25 pictures in a different amount of samples. It is suspected that this is an unspecific band that was the caused by binding of primers to an unspecified location on the *pri-miR-145 gene*. Interestingly both UMSP primers and MSP primers are binding to this region. However no definitive conclusion can be drawn since the source paper for primers Cioce et al. did not mention a band at this height.<sup>47</sup>

According to MSP results the majority of the samples are hemimethylated, the results from pyrosequencing do not always correlate with the findings from MSP as it can be seen in Table 17. This can be due to the restrictions in MSP such as semi quantitative results, low quality DNA samples or false positive reads. It is striking that the samples that were labelled as hemimethylated can have up to 91.1 % methylation instead of something around 50% methylation according to the Pyrosequencing data of the same samples. These samples are #11 – 78.1 %, #13 – 85.6 %, #14 – 91.1 %, #15 – 88.7%, #22 – 88.1 %, #28 – 70.4 %, 32 – 85.8 %, #33 – 69.9 %, #36 – 75 %, 37 – 72.3%, #39 – 73.3 %, #40 – 73.3%. Moreover sample #07 which was unmethylated according to the MSP results shows 92.1 % methylation. Further analysis will be done according to the Pyrosequencing data.

Sam. Num.	MSP Results	Isl 1 Meth. (%)	Isl 2 Meth. (%)	Ava. Meth. (%)	qPCR data	Patient diagn.	Tissue Type
#03	Methylated	85,7	85	85,3	2,8	EMM	N
#04	Hemimethylated	35,3	55,6	45,5	4,74	"	T
#05	Methylated	84,7	85	84,8		BMM	T
#06	Hemimethylated					EMM	T
#07	Unmethylated	87,0	97,2	92,1		"	N
#08	Methylated	90,0	92,6	91,3	2,83	EMM	T
#09	Hemimethylated	54,0	60,4	57,2	4,4	BMM	T
#10	Hemimethylated	28,0	57,4	42,7	5,13	PNEU.	N (control)
#11	Hemimethylated	83,7	72,6	78,1	4,2	BMM	T
#12	Methylated	90,0	67,6	78,8		"	N
#13	Hemimethylated	84,0	87,2	85,6		EMM	T
#14	Hemimethylated	97,3	84,8	91,1		EMM	T
#15	Hemimethylated	83,3	94	88,7		EMM	T
#16	Methylated	94,7	92,8	93,7		EMM	T
#17	Methylated	65,7	80	72,8		EMM	T
#18	Methylated	68,0	81,6	74,8	3,16	BMM	T
#19	Methylated	99,0	34	66,5	4,69	"	N
#20	Hemimethylated		40,8	40,8		BMM	T
#21	Methylated	83,3	69,4	76,4		EMM	T
#22	Hemimethylated	93,0	83,2	88,1	1,22	EMM	T
#23	Hemimethylated	4,0	87,4	45,7	3,9	"	N
#24	No data	99,0	93,4	96,2		EMM	N
#25	No data					"	N
#26	No data	96,0	3,8	49,9		BMM	T
#27	No data	99,0	75,8	87,4	3,42	"	N
#28	Hemimethylated	63,3	77,4	70,4		EMM	T
#29	Hemimethylated	39,7	75,6	57,6	5,89	EMM	N
#30	Methylated	66,0	65,4	65,7	0,6	EMM	T
#31	Methylated	44,7	83,2	63,9	4,6	EMM	N
#32	Hemimethylated	89,7	82	85,8		"	T
#33	Hemimethylated	48,7	91,2	69,9	1,72	EMM	T
#34	Hemimethylated	43,7	80,4	62,0		BMM	T
#35	Hemimethylated	2,7	44,6	23,6	1,19	EMM	T
#36	Hemimethylated	72,0	79,4	75,7	1,89	"	T
#37	Hemimethylated	65,7	79	72,3	5,97	BMM	N
#38	Hemimethylated	58,0	78,8	68,4	2,38	"	T
#39	Hemimethylated	66,7	80	73,3	3	BMM	T
#40	Hemimethylated	72,3	74,2	73,3	3,8	BMM	T

Table 17: Overview of pyrosequencing data. Abbreviations and colours are according to the previous tables (Patient matched samples are marked in purple).

On average tumour tissue samples from MPM patients (n=25) had 72.6% methylation for *pri-miR-145 promoter region* and NNP tissue samples from MPM patients (n=10) had 74.6% methylation for the same region. These results indicate that both non-neoplastic pleural tissue and tumour tissue have similar amount of methylation on their *pri-miR-145 promoter region*. However when compared with control tissue from the patient with pneumothorax, which had only 42.7% methylation, there is a difference. Moreover, there was no significant difference detected between MPM patients with EMM diagnosis and MPM patients with BMM diagnosis, nor between tumour tissues and NNP tissues in either histological subtype. On average tumour tissue samples from MPM patient with EMM diagnosis (n= 15) had 75 % methylation in *pri-miR-145 promoter region* whereas NNP samples from MPM patients diagnosed with EMM (n= 6) had 73.5 % methylation for the same promoter region. Tumour tissue samples from MPM patients diagnosed with BMM (n=10) had on average 66.3 % whereas NNP samples from MPM patients diagnosed with BMM (n=3) had 75.4 % methylation. For BMM samples since the number of NNP samples is small thus it is presumably normal that there is difference of 10.9 % methylation.

Andersen et al. showed downregulation of miR-145 in tumour tissue samples from MPM patients vs NNP tissue samples from MPM patients.<sup>10</sup> The qPCR data, that I have received from the lab also correlates with these findings since average miR-145 expression rate of tumour tissue samples from MPM patients (n=13) was 2.7 compared to that of NNP tissue samples from MPM patients (n=7) that was 4.5. Furthermore, the miR-145 expression in the control tissue sample with non-neoplastic reactive mesothelial proliferation from the patient with pneumothorax was 5.13 as it can be seen in table 16. Moreover, tumour tissue samples from MPM patients diagnosed with EMM (n=7) showed on average expression rate of 2.0 compared to expression rate of NNP tissue samples from MPM patients diagnosed with EMM (n=4), which was 4.3. In addition to that, tumour tissue samples of MPM patients with BMM diagnosis (n=6) had an average expression rate for miR-145 of 3.5, while the average expression in NNP tissue samples of MPM patients with BMM diagnosis (n=3) was 4.7. This indicates that a higher amount of downregulation takes place in EMM patients compared to BMM patients.

Taken together the data suggest that, even though there is a downregulation of miR-145 in tumour tissue samples of MPM patients compared to NNP tissue samples from MPM patients, the mechanism of downregulation is not likely to be methylation of CpG islands in *pri-miR145* promoter. Thus, alternative mechanisms of miR-145 downregulation may occur in MPM. However, the data should be taken with caution, as they have been generated in a small cohort of samples. In this respect, Ciocce et al. recently observed, in a similarly small cohort of FFPE and frozen MPM tissue samples, prevalently of the EMM subtype, and in MPM cell lines, that miR-145 was downregulated in large part by promoter hypermethylation.<sup>46</sup> The reasons for the discrepancy between Ciocce et al.'s data and our results is not clear, but differences in experimental and methodological setups and types of specimens may at least in part explain it. In any case, studies of miR-145 expression's regulation in larger cohorts are warranted to assess whether methylation plays a role in this process.

Considering alternative mechanisms for miR-145 downregulation in MPM, it is worth mentioning that as previously discussed the deletion of 9p21 containing the tumour suppressor gene *CDKN2A* is the most common genetic event described so far in MPMs.<sup>27</sup> *CDKN2A/ARF* encodes the tumour suppressors p16 (INK4a), a cyclin-dependent kinase inhibitor suppressing cyclin D-CDK4/6 activities, and p14 (ARF), a component of the p53 cell cycle checkpoint. Therefore, homozygous deletions of the *CDKN2A/ARF* locus in MPM might simultaneously impair both the retinoblastoma (Rb) and p53 pathways.<sup>16,34</sup> Since p53 regulates miR-143/miR-145,<sup>68</sup> any impairment in this pathway (for instance by loss of p14ARF expression) could explain the downregulation of expression of miR-143/145 in the tumour tissue samples of MPM patients that I have investigated compared to the NNP tissue samples from MPM patients. Furthermore, miR-143/145 targets MDM2 that can also inhibit p53 activity. Therefore, a reduced amount of expression in miR-143/miR-145 can lead to further inhibition of p53 by upregulated MDM2, thus creating an autoregulatory loop.<sup>68</sup>

Another possible explanation could be the direct and prolonged physical interaction between asbestos fibers and the epidermal growth factor receptor (EGFR) on the surface of mesothelial cells, which can induce continuous auto-phosphorylation and activation of EGFR and its downstream signalling cascades. Guo et al. postulated that EGFR modulates the downregulation of miR-145 through activation of ERK1/2 in lung cancer cells.<sup>61</sup> Therefore, the same mechanism

could be in place in these tumour tissue sample of MPM patients compared to the NNP tissue samples.

For the future, projects inspecting the p53-MDM2 autoregulatory loop and EGFR pathway in MPM can clarify the downregulation mechanism of miR-145 in MPM. Moreover, it will be interesting to investigate the regulation mechanisms of other possible diagnostic microRNAs as postulated by Andersen et al.<sup>10</sup>

## **7 Acknowledgements**

This project was conducted at the Laboratory of Molecular Pathology of the department of Pathology of Rigshospitalet, Copenhagen University Hospital between 01.09.2014 – 30.09.2015. Research related costs were covered by the Laboratory of Molecular Pathology. I was supported by a Danish government scholarship under the cultural agreements between Austria and Denmark, which was given by the Danish Ministry of Higher Education and Science, and by an Erasmus+ Internship scholarship given by the Austrian Agency for International Mobility and Cooperation in Education, Science and Research under the framework of EU Erasmus+ Programme, as well as by financial support from my family. I would like to thank you all of my supervisors: Eric Santoni-Rugiu, Morten Grauslund and Franz Michael Jantsch and for all their support and help during the project, along with main technician in the project Pia Rovsing Sandholm.

## 8. References

- 1 Charalampidis, C. *et al.* Physiology of the pleural space. *J Thorac Dis* **7**, S33-37, doi:10.3978/j.issn.2072-1439.2014.12.48 (2015).
- 2 Cagle, P. T. & Allen, T. C. Pathology of the pleura: what the pulmonologists need to know. *Respirology* **16**, 430-438, doi:10.1111/j.1440-1843.2011.01957.x (2011).
- 3 Suzuki, Y. Pathology of human malignant mesothelioma--preliminary analysis of 1,517 mesothelioma cases. *Ind Health* **39**, 183-185 (2001).
- 4 Chen, S. E. & Pace, M. B. Malignant pleural mesothelioma. *Am J Health Syst Pharm* **69**, 377-385, doi:10.2146/ajhp110281 (2012).
- 5 Robinson, B. W., Musk, A. W. & Lake, R. A. Malignant mesothelioma. *Lancet* **366**, 397-408, doi:10.1016/S0140-6736(05)67025-0 (2005).
- 6 Kao, S. C. *et al.* Malignant mesothelioma. *Intern Med J* **40**, 742-750, doi:10.1111/j.1445-5994.2010.02223.x (2010).
- 7 Safe\_Work\_Australia. Mesothelioma in Australia: Incidence (1982 to 2013) and Mortality (1997 to 2012). (2015).
- 8 Surveillance\_Research\_Program\_of\_the\_USA\_National\_Cancer\_Institute. Cancer Statistics Review 1975-2009 (Vintage 2009 Populations).
- 9 Marinaccio, A. *et al.* Pleural malignant mesothelioma epidemic: incidence, modalities of asbestos exposure and occupations involved from the Italian National Register. *Int J Cancer* **130**, 2146-2154, doi:10.1002/ijc.26229 (2012).
- 10 Andersen, M. *et al.* Diagnostic potential of miR-126, miR-143, miR-145, and miR-652 in malignant pleural mesothelioma. *The Journal of molecular diagnostics : JMD* **16**, 418-430, doi:10.1016/j.jmoldx.2014.03.002 (2014).
- 11 Trapani, D. *Epigenetical regulation of microRNA-126 in malignant pleural mesothelioma* Biology Applied to Biomedicine thesis, University of Pisa, Italy, (2014).
- 12 Dr E. R. A. Merewether, C. W. P. The effects of asbestos dust on the lungs and dust suppression in the asbestos industry. Part I. Occurrence of pulmonary fibrosis and other pulmonary affections in asbestos workers. Part II. Processes giving rise to dust and methods for its suppression. (1930).
- 13 Wagner, J. C., Sleggs, C. A. & Marchand, P. Diffuse pleural mesothelioma and asbestos exposure in the North Western Cape Province. *Br J Ind Med* **17**, 260-271 (1960).
- 14 Selikoff, I. J., Churg, J. & Hammond, E. C. Relation between Exposure to Asbestos and Mesothelioma. *N Engl J Med* **272**, 560-565, doi:10.1056/NEJM196503182721104 (1965).
- 15 Carbone, M. & Yang, H. Molecular pathways: targeting mechanisms of asbestos and erionite carcinogenesis in mesothelioma. *Clinical cancer research : an official journal of the American Association for Cancer Research* **18**, 598-604, doi:10.1158/1078-0432.CCR-11-2259 (2012).
- 16 Yang, H., Testa, J. R. & Carbone, M. Mesothelioma epidemiology, carcinogenesis, and pathogenesis. *Curr Treat Options Oncol* **9**, 147-157, doi:10.1007/s11864-008-0067-z (2008).
- 17 Kaufman, A. J. & Pass, H. I. Current concepts in malignant pleural mesothelioma. *Expert Rev Anticancer Ther* **8**, 293-303, doi:10.1586/14737140.8.2.293 (2008).

- 18 BURKE, B. Shipyards, a Crucible for Tragedy  
Part 1: How the war created a monster. *Asbestos News* (2001).
- 19 Joshi, T. K. & Gupta, R. K. Asbestos-related morbidity in India. *Int J Occup Environ Health* **9**, 249-253, doi:10.1179/oeh.2003.9.3.249 (2003).
- 20 de Assis, L. V., Locatelli, J. & Isoldi, M. C. The role of key genes and pathways involved in the tumorigenesis of Malignant Mesothelioma. *Biochimica et biophysica acta* **1845**, 232-247, doi:10.1016/j.bbcan.2014.01.008 (2014).
- 21 Cutrone, R. *et al.* Some oral poliovirus vaccines were contaminated with infectious SV40 after 1961. *Cancer research* **65**, 10273-10279, doi:10.1158/0008-5472.CAN-05-2028 (2005).
- 22 Kroczyńska, B. *et al.* Crocidolite asbestos and SV40 are cocarcinogens in human mesothelial cells and in causing mesothelioma in hamsters. *Proceedings of the National Academy of Sciences of the United States of America* **103**, 14128-14133, doi:10.1073/pnas.0604544103 (2006).
- 23 Lopez-Rios, F., Illei, P. B., Rusch, V. & Ladanyi, M. Evidence against a role for SV40 infection in human mesotheliomas and high risk of false-positive PCR results owing to presence of SV40 sequences in common laboratory plasmids. *Lancet* **364**, 1157-1166, doi:10.1016/S0140-6736(04)17102-X (2004).
- 24 Shivapurkar, N. *et al.* Presence of simian virus 40 sequences in malignant mesotheliomas and mesothelial cell proliferations. *J Cell Biochem* **76**, 181-188 (1999).
- 25 Gee, G. V. *et al.* SV40 associated miRNAs are not detectable in mesotheliomas. *British journal of cancer* **103**, 885-888, doi:10.1038/sj.bjc.6605848 (2010).
- 26 Carbone, M. *et al.* A mesothelioma epidemic in Cappadocia: scientific developments and unexpected social outcomes. *Nat Rev Cancer* **7**, 147-154, doi:10.1038/nrc2068 (2007).
- 27 Guo, G. *et al.* Whole-exome sequencing reveals frequent genetic alterations in BAP1, NF2, CDKN2A, and CUL1 in malignant pleural mesothelioma. *Cancer research* **75**, 264-269, doi:10.1158/0008-5472.CAN-14-1008 (2015).
- 28 Bott, M. *et al.* The nuclear deubiquitinase BAP1 is commonly inactivated by somatic mutations and 3p21.1 losses in malignant pleural mesothelioma. *Nat Genet* **43**, 668-672, doi:10.1038/ng.855 (2011).
- 29 Yoshikawa, Y. *et al.* Frequent inactivation of the BAP1 gene in epithelioid-type malignant mesothelioma. *Cancer science* **103**, 868-874, doi:10.1111/j.1349-7006.2012.02223.x (2012).
- 30 Testa, J. R. *et al.* Germline BAP1 mutations predispose to malignant mesothelioma. *Nat Genet* **43**, 1022-1025, doi:10.1038/ng.912 (2011).
- 31 Sekido, Y. *et al.* Neurofibromatosis type 2 (NF2) gene is somatically mutated in mesothelioma but not in lung cancer. *Cancer research* **55**, 1227-1231 (1995).
- 32 Bianchi, A. B. *et al.* High frequency of inactivating mutations in the neurofibromatosis type 2 gene (NF2) in primary malignant mesotheliomas. *Proceedings of the National Academy of Sciences of the United States of America* **92**, 10854-10858 (1995).
- 33 Murakami, H. *et al.* LATS2 is a tumor suppressor gene of malignant mesothelioma. *Cancer research* **71**, 873-883, doi:10.1158/0008-5472.CAN-10-2164 (2011).
- 34 Testa, J. R. & Giordano, A. SV40 and cell cycle perturbations in malignant mesothelioma. *Semin Cancer Biol* **11**, 31-38, doi:10.1006/scbi.2000.0344 (2001).

- 35 Travis, W. D., Brambilla, E., Burke, A.P., Marx, A., Nicholson, A. G. *WHO Classification of Tumours of the Lung, Pleura, Thymus and Heart*. 4th Edition edn, Vol. 7th Volume (2015).
- 36 Zimling, Z. G., Jørgensen, A. & Santoni-Rugiu, E. The diagnostic value of immunohistochemically detected methylthioadenosine phosphorylase deficiency in malignant pleural mesotheliomas. *Histopathology* **60**, E96-105, doi:10.1111/j.1365-2559.2012.04196.x (2012).
- 37 Kortsik, C. S. *et al.* Immunocytochemical characterization of malignant mesothelioma and carcinoma metastatic to the pleura: IOB3--a new tumor marker. *Lung* **173**, 79-87 (1995).
- 38 Abutaily, A. S., Addis, B. J. & Roche, W. R. Immunohistochemistry in the distinction between malignant mesothelioma and pulmonary adenocarcinoma: a critical evaluation of new antibodies. *J Clin Pathol* **55**, 662-668 (2002).
- 39 King, J. E. & Hasleton, P. S. Immunohistochemistry and the diagnosis of malignant mesothelioma. *Histopathology* **38**, 471-476 (2001).
- 40 Scherpereel, A. *et al.* Guidelines of the European Respiratory Society and the European Society of Thoracic Surgeons for the management of malignant pleural mesothelioma. *Eur Respir J* **35**, 479-495, doi:10.1183/09031936.00063109 (2010).
- 41 Baas, P. *et al.* Malignant pleural mesothelioma: ESMO Clinical Practice Guidelines for diagnosis, treatment and follow-up. *Ann Oncol* **26 Suppl 5**, v31-39, doi:10.1093/annonc/mdv199 (2015).
- 42 Vogelzang, N. J. *et al.* Phase III study of pemetrexed in combination with cisplatin versus cisplatin alone in patients with malignant pleural mesothelioma. *J Clin Oncol* **21**, 2636-2644, doi:10.1200/JCO.2003.11.136 (2003).
- 43 Kotova, S., Wong, R. M. & Cameron, R. B. New and emerging therapeutic options for malignant pleural mesothelioma: review of early clinical trials. *Cancer Manag Res* **7**, 51-63, doi:10.2147/CMAR.S72814 (2015).
- 44 Garzon, R., Calin, G. A. & Croce, C. M. MicroRNAs in Cancer. *Annu Rev Med* **60**, 167-179, doi:10.1146/annurev.med.59.053006.104707 (2009).
- 45 Chan, S. H. & Wang, L. H. Regulation of cancer metastasis by microRNAs. *J Biomed Sci* **22**, 9, doi:10.1186/s12929-015-0113-7 (2015).
- 46 Jansson, M. D. & Lund, A. H. MicroRNA and cancer. *Mol Oncol* **6**, 590-610, doi:10.1016/j.molonc.2012.09.006 (2012).
- 47 Ciocce, M. *et al.* Protumorigenic effects of mir-145 loss in malignant pleural mesothelioma. *Oncogene*, doi:10.1038/onc.2013.476 (2013).
- 48 Cimmino, A. *et al.* miR-15 and miR-16 induce apoptosis by targeting BCL2. *Proceedings of the National Academy of Sciences of the United States of America* **102**, 13944-13949, doi:10.1073/pnas.0506654102 (2005).
- 49 Siebolts, U. *et al.* Tissues from routine pathology archives are suitable for microRNA analyses by quantitative PCR. *J Clin Pathol* **62**, 84-88, doi:10.1136/jcp.2008.058339 (2009).
- 50 Guled, M. *et al.* CDKN2A, NF2, and JUN are dysregulated among other genes by miRNAs in malignant mesothelioma -A miRNA microarray analysis. *Genes Chromosomes Cancer* **48**, 615-623, doi:10.1002/gcc.20669 (2009).
- 51 Busacca, S. *et al.* MicroRNA signature of malignant mesothelioma with potential diagnostic and prognostic implications. *Am J Respir Cell Mol Biol* **42**, 312-319, doi:10.1165/rcmb.2009-0060OC (2010).

- 52 Balatti, V. *et al.* MicroRNAs dysregulation in human malignant pleural mesothelioma. *J Thorac Oncol* **6**, 844-851, doi:10.1097/JTO.0b013e31820db125 (2011).
- 53 Benjamin, H. *et al.* A diagnostic assay based on microRNA expression accurately identifies malignant pleural mesothelioma. *The Journal of molecular diagnostics : JMD* **12**, 771-779, doi:10.2353/jmoldx.2010.090169 (2010).
- 54 Gee, G. V. *et al.* Downregulated microRNAs in the differential diagnosis of malignant pleural mesothelioma. *Int J Cancer* **127**, 2859-2869, doi:10.1002/ijc.25285 (2010).
- 55 Andersen, M. *et al.* Are differentially expressed microRNAs useful in the diagnostics of malignant pleural mesothelioma? *APMIS* **120**, 767-769, doi:10.1111/j.1600-0463.2012.02891.x (2012).
- 56 Santarelli, L. *et al.* Association of MiR-126 with soluble mesothelin-related peptides, a marker for malignant mesothelioma. *PloS one* **6**, e18232, doi:10.1371/journal.pone.0018232 (2011).
- 57 Tomasetti, M. *et al.* Clinical significance of circulating miR-126 quantification in malignant mesothelioma patients. *Clin Biochem* **45**, 575-581, doi:10.1016/j.clinbiochem.2012.02.009 (2012).
- 58 Reid, G. *et al.* Restoring expression of miR-16: a novel approach to therapy for malignant pleural mesothelioma. *Ann Oncol* **24**, 3128-3135, doi:10.1093/annonc/mdt412 (2013).
- 59 Kubo, T. *et al.* Epigenetic silencing of microRNA-34b/c plays an important role in the pathogenesis of malignant pleural mesothelioma. *Clinical cancer research : an official journal of the American Association for Cancer Research* **17**, 4965-4974, doi:10.1158/1078-0432.CCR-10-3040 (2011).
- 60 He, L. *et al.* A microRNA component of the p53 tumour suppressor network. *Nature* **447**, 1130-1134, doi:10.1038/nature05939 (2007).
- 61 Ak, G. *et al.* MicroRNA and mRNA features of malignant pleural mesothelioma and benign asbestos-related pleural effusion. *Biomed Res Int* **2015**, 635748, doi:10.1155/2015/635748 (2015).
- 62 Guo, Y. H. *et al.* Abnormal activation of the EGFR signaling pathway mediates the downregulation of miR145 through the ERK1/2 in non-small cell lung cancer. *Oncology reports* **31**, 1940-1946, doi:10.3892/or.2014.3021 (2014).
- 63 Kojima, S. *et al.* The tumor-suppressive microRNA-143/145 cluster inhibits cell migration and invasion by targeting GOLM1 in prostate cancer. *Journal of human genetics* **59**, 78-87, doi:10.1038/jhg.2013.121 (2014).
- 64 Lu, R. *et al.* miR-145 functions as tumor suppressor and targets two oncogenes, ANGPT2 and NEDD9, in renal cell carcinoma. *J Cancer Res Clin Oncol* **140**, 387-397, doi:10.1007/s00432-013-1577-z (2014).
- 65 Kent, O. A., McCall, M. N., Cornish, T. C. & Halushka, M. K. Lessons from miR-143/145: the importance of cell-type localization of miRNAs. *Nucleic acids research* **42**, 7528-7538, doi:10.1093/nar/gku461 (2014).
- 66 Lagos-Quintana, M. *et al.* Identification of tissue-specific microRNAs from mouse. *Curr Biol* **12**, 735-739 (2002).
- 67 Landgraf, P. *et al.* A mammalian microRNA expression atlas based on small RNA library sequencing. *Cell* **129**, 1401-1414, doi:10.1016/j.cell.2007.04.040 (2007).
- 68 Zhang, J. *et al.* Loss of microRNA-143/145 disturbs cellular growth and apoptosis of human epithelial cancers by impairing the MDM2-p53 feedback loop. *Oncogene* **32**, 61-69, doi:10.1038/onc.2012.28 (2013).

- 69 Kent, O. A. *et al.* Repression of the miR-143/145 cluster by oncogenic Ras initiates a tumor-promoting feed-forward pathway. *Genes Dev* **24**, 2754-2759, doi:10.1101/gad.1950610 (2010).
- 70 Chen, Z. *et al.* miRNA-145 inhibits non-small cell lung cancer cell proliferation by targeting c-Myc. *J Exp Clin Cancer Res* **29**, 151, doi:10.1186/1756-9966-29-151 (2010).
- 71 miRbase. *Stem-loop sequence hsa-mir-145* <[http://www.mirbase.org/cgi-bin/mirna\\_entry.pl?acc=MI0000461](http://www.mirbase.org/cgi-bin/mirna_entry.pl?acc=MI0000461)> (
- 72 Zimling, Z. G. *et al.* Low ERCC1 expression in malignant pleural mesotheliomas treated with cisplatin and vinorelbine predicts prolonged progression-free survival. *J Thorac Oncol* **7**, 249-256, doi:10.1097/JTO.0b013e318233d6a9 (2012).
- 73 Zimling, Z. G. *et al.* A biomarker profile for predicting efficacy of cisplatin-vinorelbine therapy in malignant pleural mesothelioma. *Cancer chemotherapy and pharmacology* **70**, 743-754, doi:10.1007/s00280-012-1965-0 (2012).
- 74 Bartel, D. P. MicroRNAs: target recognition and regulatory functions. *Cell* **136**, 215-233, doi:10.1016/j.cell.2009.01.002 (2009).
- 75 Andersen, M. *et al.* Methylation-associated Silencing of microRNA-126 and its Host Gene EGFL7 in Malignant Pleural Mesothelioma. *Anticancer research* **35**, 6223-6229 (2015).
- 76 Krueger, F., Kreck, B., Franke, A. & Andrews, S. R. DNA methylome analysis using short bisulfite sequencing data. *Nat Methods* **9**, 145-151, doi:10.1038/nmeth.1828 (2012).
- 77 ZymoResearch. Protocol for EZ DNA Gold Methylation Kit.
- 78 NatureJournal. Glossary.
- 79 Pompilii, J. DensityDesign Integrated Course Final Synthesis Studio.

## 9. Attachments

### 9.1. Abstract in German

**Zweck:** Bestimmung der epigenetischen Herunterregulierung Mechanismus der microRNA-145 beim malignen Pleuramesotheliom (MPM) und mögliche Verwendung von miR-145 als diagnostischer Biomarker in MPM.

**Experimentelles Design:** Die Korrelation der Methylierungsstatus und Expression-Muster der miR-145 und durch die Untersuchung Mechanismen der Ko-Regulierung mit seinen "möglichen Host-Gene. Analyse der DNA-Methylierung ob epigenetischen Mechanismus in Herunterregulierung von miR-145 in MPM beteiligt ist, wurde unter Verwendung methylierungsspezifischer PCR (MSP) an Formalin-fixierten Paraffinblöcken eingebetteten (FFPE) chirurgischen Proben nach Bisulfit-Behandlung durchgeführt. Die Methylierung von miRs wurde durch Pyrosequenzierung quantifiziert und miR Expression durch quantitative RT-PCR (qRT-PCR) nachgewiesen.

**Ergebnisse:** Die Methylierung spezifischer PCR-Ergebnisse, wie in Tabelle 12 zu sehen ist, ergab die folgenden Ergebnisse: Insgesamt sind 11 Proben voll methyliert, 22 Proben sind Hemi-methyliert und eine Probe ist nicht methyliert. Im Durchschnitt Tumorgewebeproben von MPM-Patienten (n = 25) hatten 72,6% Methylierung für pri-miR-145-Promotor-Region und NNP Gewebe Proben von MPM Patienten hatten 74,6% (n = 10) Methylierung. Diese Ergebnisse zeigen, daß sowohl nicht-neoplastischen pleuralen Gewebe und als auch Tumorgewebe hat die gleiche Menge Methylierung an ihrer pri-miR-145-Promotorregion. Darüber hinaus gab es keine signifikanten Unterschied zwischen MPM Patienten mit epitheloiden malignen Mesotheliom (EMM) Diagnose und MPM Patienten mit biphasischen malignes Mesotheliom (BMM) Diagnose, NNP Gewebe EMM - BMM Diagnose.

QPCR Daten, die ich aus dem Labor bekommen habe, zeigt auch Herunterregulation der miR-145 in Tumorgewebeproben im Vergleich zu NNP Gewebeproben von Patienten mit MPM. Im Durchschnitt miR-145 Expressionsrate von Tumorgewebeproben von MPM-Patienten (n = 13)

2,7 im Vergleich zu NNP Gewebeproben von MPM-Patienten (n = 7) ist 4,5 und Kontrollgewebeprobe aus dem Patienten mit Pneumothorax hat 5,13. Dies zeigt an, daß eine höhere Menge der Herunterregulierung erfolgt im EMM-Patienten im Vergleich zu BMM Patienten. Zusammen, auch wenn es eine Herunterregulierung miR-145 in Tumorgewebeproben von Patienten MPM im Vergleich zu NNP Gewebeproben von MPM Patienten gibt, der Mechanismus der Herunterregulierung ist nicht Methylierung als bisher angenommen.

## 9.2. Scientific CV in English

### Personal Details

Address: Dominikanerbastei 21/ 33, 1010, Vienna, Austria

Mobile: +43 677 617 798 67

Email: [aslan.mustafa90@gmail.com](mailto:aslan.mustafa90@gmail.com)

LinkedIn: [at.linkedin.com/in/mustafathescientist](https://at.linkedin.com/in/mustafathescientist)

Birthday: 24.03.1990



### Profile

I merge neurology and molecular biology knowledge in my personality, which together with my research experience gives me the ability to work in a wide variety of tasks. Working and studying in multiple countries gave me intercultural communication skills, whereas my volunteering experience increased my teamwork skills. I am fluent in German & English, have Austrian High School Diploma and received IELTS Academic Diploma with an overall score of 7.5 / 9.

### Work Experience

#### **Research Assistant, University of Copenhagen Hospital - Rigshospitalet, Denmark**

Sept.2014 – Oct. 2015

I was investigating the potential use of microRNAs as diagnostic biomarkers for malignant pleural mesothelioma, which would provide the opportunity to diagnose this cancer type in early stages. I focused on miR-145 and its' methylation-mediated regulation of expression. During this project, I gained problem solving skills and learned to work independently in a systematic way to find the root cause of problems while proving my hypothesis. I have been awarded with two scholarships by Danish Ministry of Science and Austrian Agency for Cooperation in Science for my project.

*Acquired techniques: DNA isolation, bisulfite conversion of DNA, methylation specific polymerase chain reaction, pyrosequencing, high resolution capillary electrophoresis, real-time polymerase chain reaction*

**Research Assistant, Raible Group, Max F. Perutz Laboratories, Austria**

Mar. 2014 - May 2014

I have worked on inducing mutations through specific transcription activator-like effector nucleases (TALENs) to *Platynereis dumerili* vasotocin-neurophysin coding region in embryos in order to make knock out mutants. In addition I also worked on re-engineering of TALEN expression vectors to include a germline 3'UTR and an endogenous promoter, so that they could be delivered as plasmids instead of as mRNAs and also have enhanced expression in the germline. Since the group was multidisciplinary and multinational, I have increased my communication skills to be successful in such working environment.

*Acquired techniques: Restriction Digestion, Cloning, PCR, Microinjection, Genetic Screening, Fluorescence Microscopy, Gel Electrophoresis and Handling of Platynereis Dumerilii*

**Research Assistant, Firat University, Turkey**

July 2012 – Aug. 2012

I was investigating the roles of different proteins in Type 2 Diabetes and attending patient visits with my supervisor, who was a physician in the Firat University Hospital. Therefore I increased my knowledge about diabetes, its causes and effects on people.

*Acquired techniques: Enzyme-Linked Immunosorbent Assay (Elisa)*

**Education**

**Genetics and Developmental Biology, MSc, University of Vienna, Austria**

Nov. 2013 – Dec. 2015

I gained knowledge in neurobiology, developmental biology and genetics, while following and presenting latest publications in these fields. Current GPA: 1,64 / 5 according to the Austrian five point grading scheme: 1 - excellent, 5 – insufficient.

*Acquired techniques: Combined Bisulfite Restriction Analysis (COBRA), RT-PCR, Western Blot, RNA Isolation, Antibody Staining, Immunofluorescence Microscopy*

**Medicine, One Year Exchange Programme, University of Copenhagen, Denmark**

Sept. 2014 – Oct. 2015

I gained cultural adaptability skills by challenging myself in a foreign environment, while learning about Scandinavian work culture. I also increased my theoretical knowledge & practical experience in oncology and pathology.

**Global Advancement Programme (GAP), Diploma Course, Academic Forum for Foreign Affairs (AFA) - United Nations Association of Austria**

Sept. 2013 – June 2014

I gained entrepreneurship and negotiation skills through discussions & trainings with the leading economists & politicians of Austria and been awarded with three scholarships by AFA, E-fellows.net and Careerloft.de Career Network.

**Biology/Microbiology & Genetics, BSc, University of Vienna, Austria**

Sept. 2009 – Nov. 2013

I gained an analytical mind-set and learned to be a problem solver, through living in a foreign country for many years and taking care of unforeseen problems. Acquired GPA: 2,29 / 5 according to the Austrian five point grading scheme.

*Acquired techniques: Titration, Distillation, IR spectrometry, UV/VIS photometry, HPLC-MS- HPLC-UV/VIS, Fluorescence Correlation Spectroscopy, SDS Page, Cloning, Transformation, Northern Blot, Southern Blot, Hybrid2yeast, Reporter Gene Assay*

## **Volunteer and International Experience**

### **Youth Goodwill Ambassador of Denmark (YGA), Copenhagen Capacity, Denmark**

Sept. 2014 – Sept. 2015

I worked voluntarily as an ambassador and joined global network of international students from 60+ countries for promoting Denmark as an attractive study and work destination, where I increased my teamwork and marketing skills. For this aim we developed videos using Hyperlapse technology in Instagram to be used by University of Copenhagen.

### **Project Manager, Junior Chamber International (JCI), Denmark**

Nov. 2014 – Sept. 2015

I volunteered and became a part of an international network of active citizens, which aims to empower young people to create positive change. There I took my passion about ballroom dances to the next level and created a dance academy in Copenhagen using my entrepreneurship skills, where I taught our members ballroom dances.

### **Project Manager & Moderator, European Youth Parliament (EYP), Austria**

Jan. 2010 – Dec. 2011

I volunteered and was a part of the international network of young people, which aims to shape young people to responsible citizens by involving them in political discussions. I brought a new idea to life and created one day parliamentary simulations. The first three of them, which were in Vienna, Graz and Linz were organized by me. I led a team of 15 organizers and gained leadership skills.

## **Publication**

Role of Social Media in Communication, Mustafa Aslan

GAP-Journal 2013/14 - Academic Forum for Foreign Affairs - Vienna (AFA),

pp. 23-32; ISBN: 978-3-902923-34-9

## Languages

**Turkish** - Native proficiency

**Danish** - Elementary proficiency

**English** - Full professional proficiency

**German** - Full professional proficiency